Diss. ETH No. 18923

Noble gases as tracers for transport of solutes and fluids in lake and ocean sediments

A dissertation submitted to the
SWISS FEDERAL INSTITUTE OF TECHNOLOGY ZURICH

for the degree of
DOCTOR OF SCIENCES

presented by
YAMA TOMONAGA
Dipl. Umwelt-Natw. ETH
born 6 May 1978
citizen of Rueyres-Les-Prés/Léchelles (FR)

accepted on the recommendation of
Prof. Dr. Rolf Kipfer, examiner
Prof. Dr. Bernhard Wehrli, co-examiner
Prof. Dr. Bernard Bourdon, co-examiner

2010

Chapter 3 has been submitted as:
Tomonaga, Y., Brennwald, M. S., and Kipfer, R. (in review). An improved method for the analysis of dissolved noble gases in the pore water of unconsolidated sediments. *Limnol. Oceanogr.: Methods*.

Chapter 4 has been submitted as:
Tomonaga, Y., Brennwald, M. S., and Kipfer, R. (in review). Attenuation of noble-gas transport in laminated sediments of the Stockholm Archipelago? *Earth Planet. Sci. Lett.*.

Chapter 5 has been submitted as:
Tomonaga, Y., Brennwald, M. S., and Kipfer, R. (in review). Spatial distribution of helium in the sediments of Lake Van (Turkey). *Geochim. Cosmochim. Acta*.

Acknowledgements

I would like to thank the referees of my dissertation *Rolf Kipfer* aka. *RoKi*, *Bernhard Wehrli* and *Bernard Bourdon*. Their comments and suggestions helped to improve the work considerably.

Thanks are due to the present and former members of the Environmental Isotopes Group at Eawag for their great support during the last few years: *Matthias Brennwald*, *Eduhard Hoehn*, *David Livingstone* (who thoroughly checked and corrected the English of the submitted chapters), *Yvonne Scheidegger*, *Lars Mächler*, *Stephan Huxol*, *Ryan North* (who also had the courage to review the language of my drafts), *Markus Hofer*, *Stephan Klump*, *Helena Amaral*, *Christian Holzner*, *Nora Denecke*, and *Thomas Jankowski*.

Special thanks are owed to the people of the Sedimentology Group at Eawag, in particular: *Thomas Kulbe*, *Mike Sturm*, *Flavio Anselmetti*, and *Mona Stockhecke*. Although my knowledge pertaining to this muddy research field was quite limited, they never gave up trying to introduce me to its concepts and methods.

Furthermore, I am grateful to the members of the noble-gas laboratory at ETH Zurich. In particular, I thank *Urs Menet* and *Heiri Baur* for their valuable technical support during the development of the new analytical method in the "cellar".

Thanks are also due to *Per Jonsson* at the Stockholm University for the pleasant fieldwork in the Stockholm Archipelago. The vast quantity of clamps used for the acquisition of the sediment samples of the high-resolution profile gave me a strong motivation to look for an easier (and healthier) way to close the sampling containers.

I would also like to express my thanks to *Aysegül Feray Meydan* and *Ismet Meydan*, *Münip Kanan*, *Mete Orhan*, *Mehmet Sahin*, *Mustafa Karabiyikoğlu* and *Sefer Örçen* at the Yüzüncü Yıl University in Van and *Frank Peeters*, *Andrea Huber* and *Heike Kaden* at the University of Constance for their indispensable support and great company during the expeditions on Lake Van. I really appreciated the uncountable cups of çay enjoyed on the shores of Lake Van.

Further thanks go to the SONNE cruise crew at IFM-GEOMAR, and in particular *Matthias Haeckel*, for giving me the chance to work on the sediment samples taken off shore from New Zealand.

Finally, I want to thank *my family*, *Alessandra* and *all the friends* I did not explicitly mention, for giving me the chance to escape from the academic environment.

Contents

Summary

This work focuses on the use of noble gases as tracers for the transport of solutes and fluids in unconsolidated sediments of lakes and oceans. Atmospheric noble gases enter the water body of lakes and oceans by gas exchange at the air/water interface according to the local pressure, temperature and salinity conditions. During the deposition of sediment particles at the bottom of water bodies a part of the water (and the noble-gas species dissolved in it) overlying the sediment/water boundary is "trapped" in the pore space of the growing sediment column. As noble gases are in general not affected by any biogeochemical processes, deviations from the expected atmospheric equilibrium concentrations can be used to identify the relevant physical processes that affect the abundance of solutes in the sediment column. The characterization of the solute transport in the sediment column is necessary to understand the temporal evolution of concentration signals generated by, for example, climate forcing or fluids emanating from geochemical reservoirs located below the sediments.

Recent analytical progress allowed for the first time to determine noble-gas concentrations and isotope ratios in lacustrine sediments in a robust and reliable manner. The previously developed standard method was applied in the largest noble-gas study ever accomplished in unconsolidated sediments from *Lake Van* in order to determine the spatial variability of the He release from solid earth. The results show that the He release is highly heterogeneous in space. However, the He liberated into the water body of Lake Van originates from the same single geochemical source which seems to be a mixture of He from a depleted mantle source combined with radiogenic He produced in the sediment column. The effective diffusivity of He in the pore space was determined to be about four times lower than the diffusivity in bulk water and the maximal He flux to be five times smaller than the continental He flux estimated by global He budget studies.

An even stronger attenuation of diffusive transport processes was observed in a sediment core from the *Stockholm Archipelago* where an approximately 100 year old mass movement included a large amount of atmospheric gases in the sediment column. The modeling of the gas excess indicates that the effective diffusivity in the pore space must be at least three orders of magnitude smaller than diffusivity in free water in order to explain the sharp concentration increase of atmospheric noble gases observed at a sediment depth of about 40 cm (i.e. the upper boundary of the mass movement).

The two case studies of Lake Van and the Stockholm Archipelago show that the effective diffusion in sediments is clearly limited by the geometry of the pore space and under particular circumstances diffusive processes may become practically negligible even at shallow depths.

Although the quality of the results for Lake Van and the Stockholm Archipelago matches the pre-set experimental precision, the standard method to determine noble-gas

abundances in lacustrine sediments still needs experienced personnel to be successfully carried out. For instance, the texture of the sediments sometimes severely limits the complete noble-gas extraction. Moreover, as the sediment samples are heated during extraction, the uncontrolled release of radiogenic He from the sediment grains can sometimes affect the results. In light of these experimental challenges, a new analytical approach was developed within the framework of this thesis. The new method is based on the separation of the pore water and the sediment matrix phases by centrifugation of the bulk sediment samples. After the centrifugation process the "pure" pore water phase is separated from the rest of the sample and analyzed as a common free water sample. Compared to the previous standard method, the new centrifugation method is much simpler to handle, less operator-sensitive, has a constant high extraction efficiency and does not foster the release of He from the sediment minerals.

The newly developed analytical method was further adapted in order to determine noble-gas abundances in ocean sediments taken off shore from *New Zealand* with the aim to characterize the origin of a cold methane seepage by using its He isotope signature. From the collected data it was concluded that ^{3}He-rich fluids emanate preferentially in the vicinity of the Pacific-Australian subduction zone. However, while the major terrigenic He component is identified to be of crustal origin, methane seems to be predominantly biologically produced in the upper part of the sediment column. The occurrence of ^{3}He from the Earth's mantle also suggests that traces of thermogenic/abiogenic methane are present which were not identified by the more "conventional" analysis of carbon isotopes of dissolved CH_4 in the water column.

In conclusion, noble gases in unconsolidated sediments of lakes (and oceans) are ideal tracers to characterize the solute transport within the pore water space at very local scales. Moreover, the insights gained towards the extent of attenuation of diffusivity show that noble-gas concentrations can be "stored" and "conserved" for a long period of time in the sediments. Hence noble gases have the potential to become a valuable tool to reconstruct past climate change and to study fluid transport through the uppermost part of the continental crust.

Zusammenfassung

Diese Arbeit beschreibt die Anwendung von Edelgasen als Indikator für den Transport gelöster Stoffe und Fluide in lockeren See- und Ozeansedimenten. Atmosphärische Edelgase werden durch Gasaustausch an der Grenzfläche Luft/Wasser abhängig von den lokalen Druck- und Temperaturbedingungen und der Salinität in die Wasserkörper von Seen und Ozeanen eingebracht. Während der Sedimentation am Grund wird ein Teil des sich dort befindenden Wassers (und damit die im Wasser gelösten Edelgase) im Porenraum der wachsenden Sedimentsäule "eingefangen". Generell werden Edelgaskonzentrationen nicht durch biogeochemische Prozesse beeinflusst. Daher können Abweichungen von den erwarteten atmosphärischen Gleichgewichtskonzentrationen verwendet werden, um relevante physikalische Transportprozesse zu identifizieren, welche die Verteilung von gelösten Stoffen in der Sedimentsäule beeinflussen. Die Charakterisierung des Stofftransportes in der Sedimentsäule ist nötig, um die zeitliche Entwicklung von Konzentrationssignalen zu verstehen, die z.B. durch klimatische Veränderungen oder durch den Eintrag von Fluiden aus tieferen geochemischen Reservoirs verursacht werden.

Aktuelle analytische Fortschritte erlaubten zum ersten Mal die Messung von Edelgaskonzentrationen und Isotopenverhältnissen in Seesedimenten auf eine robuste und zuverlässige Art und Weise. Diese Standardmethode wurde in der grössten bekannten Edelgasstudie in den lockeren Sedimenten des *Vansees* angewendet, um die räumliche Verteilung der Freisetzung von He aus der festen Erde zu untersuchen. Die Resultate zeigen, dass die Intensität der Emanation von He räumlich höchst hetereogen ist, das He im Vansee jedoch aus einer einzelnen geochemischen Quelle stammt. Die Isotopensignatur dieser Quelle deutet auf eine Mischung von He aus einer abgereicherten Mantelquelle und aus radiogenem in der Sedimentsäule produzierten He hin. Weiter zeigt die Untersuchung, dass die effektive Diffusivität von He im Porenraum des Sediments viermal kleiner als die molekulare Diffusion von He im Wasser ist. Darüber hinaus ist der ermittelte maximale He-Fluss im Sediment des Vansees ist fünfmal kleiner als der kontinentale He-Fluss, der durch globale He-Budget Studien geschätzt wurde.

Eine noch stärkere Hemmung der diffusiven Transportprozesse wurde in einem Sedimentkern vom *Stockholm-Archipel* beobachtet, wo eine laterale Rutschung vor ungefähr 100 Jahren eine grosse Menge atmosphärischer Gase in die Sedimentsäule einschloss. Das Modellieren des Gasüberschusses zeigt, dass die effektive Diffusivität im Porenraum mindestens drei Grössenordnungen kleiner als die Diffusion im freien Wasser sein muss, um die starke Konzentrationszunahme der atmosphärischen Edelgase zu erklären, die in ungefähr 40 cm Sedimenttiefe (d.h. am oberen Rand der Sedimentrutschung) beobachtet wurde.

Die zwei Fallstudien vom Vansee und vom Stockholm-Archipel zeigen, dass die effektive Diffusion in Sedimenten offenbar durch die Geometrie des Porenraumes begrenzt wird und, unter besonderen Bedingungen, diffusive Prozesse sogar in untiefen Bereichen der

Sedimentsäule praktisch vernachlässigbar werden können.

Obgleich die Qualität der Resultate von Vansee und Stockholm-Archipel der erwarteten experimentellen Präzision entspricht, muss die Standardmethode zur Bestimmung von Edelgaskonzentrationen in Seesedimenten von Experten durchgeführt werden, um erfolgreich angewendet werden zu können. So kann z.B. die Sedimenttextur die Extraktion der Edelgase quantitativ relevant beeinflussen. Ausserdem kann das Heizen der Sedimentproben während der Extraktionsphase eine unkontrollierte Freisetzung von radiogenem He aus den Sedimentkörnern fördern, wodurch die Schlussresultate beeinflusst werden können. Angesichts dieser experimentellen Herausforderungen wurde ein neues analytisches Konzept im Rahmen dieser These entwickelt. Die neue Methode basiert auf der Trennung der Porenwasser- und der Sedimentmatrixphasen durch Zentrifugierung der originalen Sedimentproben. Durch die Zentrifugation wird das Porenwasser vom Rest der Probe getrennt und als eine normale, "reine" Wasserprobe analysiert. Verglichen mit der bisherigen Standardmethode ist die neue Zentrifugierungmethode viel einfacher durchzuführen und daher weniger Benutzer-empfindlich. Sie liefert zudem eine konstant hohe Extraktionseffizienz und fördert nicht die Freigabe von He aus den Sedimentmineralien.

Die neu entwickelte experimentelle Methode wurde weiter angepasst, um Edelgaskonzentrationen von küstennahen Ozeansedimenten aus *Neuseeland* zu bestimmen mit dem Ziel, den Ursprung einer kalten Methanemission durch die isotopische Zusammensetzung von He zu identifizieren. Aus den gesammelten Daten wurde geschlossen, dass ^{3}He-angereicherte, also dem Mantel zuzuordnende Fluide vorzugsweise in der Nähe der Pazifisch-Australischen Subduktionszone freigesetzt werden. Da jedoch der Ursprunug des grössten Teils des terrigenen He als krustal identifiziert wird, scheint das Methan im oberen Teil der Sedimentsäule überwiegend biologisch produziert zu werden. Das Vorkommen von ^{3}He aus dem Erdmantel weist allerdings darauf hin, dass Spuren von thermogenen/abiogenen Methan vorhanden sind. Diese zusätzliche Information kann einer "konventionellen" Analyse der Kohlenstoffisotope des gelösten CH_4 in der Wassersäule nicht entnommen werden.

Zusammenfassend kann gesagt werden, dass Edelgase in lockeren Sedimenten von Seen (und Ozeanen) ideale Indikatoren sind, um den lokale Stofftransport innerhalb des Porenwasserraumes der Sedimentsäule zu charakterisieren. Ausserdem zeigen die Erkenntnisse über das z.T. hohe Mass der Hemmung der Diffisivität, dass Edelgaskonzentrationen "gespeichert" und während einer langen Zeitspanne in den Sedimenten "erhalten" werden können. Folglich haben Edelgase aus Sedimenten das Potenzial ein wertvolles Instrument zu werden, um vergangene Klimaänderungen zu rekonstruieren und um den Transport von Fluiden durch den obersten Teil der kontinentalen Kruste zu studieren.

Chapter 1

Introduction

1.1 Noble gases in the pore water of unconsolidated sediments

In recent years the analysis of noble gases in meteoric waters became a powerful geochemical tool to analyze the dynamics in lakes, oceans, and groundwaters and to reconstruct past climate conditions (for reviews see Kipfer et al., 2002; Schlosser and Winckler, 2002). As noble gases are (geo)chemically inert, no biogeochemical process can alter the atmospheric noble-gas concentrations that are preset in the water body during the last gas exchange with the atmosphere. The few physical processes that do fractionate noble gases in waters are radioactive production (i.e. $^3H \rightarrow {}^3He$, U/Th $\rightarrow {}^4He$), accumulation of terrigenic fluids (from crust and mantle) and secondary, non-atmospheric gas exchange.

As Henry's Law reasonably describes the equilibrium partitioning of noble gases between atmospheric air and water, and as the gas-specific Henry coefficients are mainly affected by the temperature and salinity of the exchanging water mass, the solubility equilibrium concentrations of noble gases directly reflect the physical conditions that prevailed during the air/water partitioning when the water was last in contact with the atmosphere (e.g. Aeschbach-Hertig et al., 1999b; Kipfer et al., 2002, for a review).

This straightforward physical concept builds the basic foundation to use dissolved noble-gas concentrations to analyze and to determine mixing and deep water exchange in lakes and oceans (e.g. Hohmann et al., 1998; Igarashi et al., 1992; Peeters et al., 2000; Sano and Wakita, 1987; Torgersen et al., 1977; Weiss et al., 1991), to reconstruct past climate conditions from (ground) water (e.g. Aeschbach-Hertig et al., 1999b, 2000; Ballentine and Hall, 1999; Beyerle et al., 1998, 2003; Marty et al., 2003; Stute et al., 1992, 1995; Weyhenmeyer et al., 2000), and to analyze past hydraulic conditions (e.g. Stute and Talma, 1998; Ingram et al., 2007; Klump et al., 2007, 2008b; Zhu and Kipfer, 2010).

First experimental techniques for the sampling and the analysis of dissolved noble gases in the pore water of lake sediments were developed by Brennwald et al. (2003). This experimental progress allowed for the first time the well-developed noble-gas systematics of meteoric waters to be applied to the pore water of unconsolidated sediments of lakes in a routine manner. The work revived the old idea to use dissolved noble gases in sediments to reconstruct (palaeo) environmental conditions in lakes and oceans and to analyze the transport of solutes and fluids in the sediment column by noble gases (see Ozima and Podosek, 1983; Brennwald et al., 2004, 2005; Strassmann et al., 2005).

In open waters, i.e. water masses with a free interface to the atmosphere, advection and turbulent mixing affect the (vertical) transport of energy/heat (e.g. temperature) and matter (e.g. salinity, dissolved noble gases) in the same manner (e.g. Schwarzenbach et al., 2003) as exchange is controlled by a corresponding water movement. Hence, in lakes and oceans, dissolved noble-gas concentrations were found to be closely concordant with the expected atmospheric equilibrium concentrations determined by the ambient atmospheric pressure and the local temperature and salinity of the surrounding water mass (e.g. Aeschbach-Hertig et al., 1999b; Craig and Weiss, 1971; Peeters et al., 1997, 2000). Large water bodies sometimes show a small, but characteristic excess of (light) noble gases which is attributed to the dissolution of small air bubbles due to breaking waves at the air/water interface (Craig and Weiss, 1971; Thorpe, 1984; Kipfer et al., 2002).

During sedimentation, water from the water/sediment interface is incorporated into the growing sediment column. Atmospheric noble-gas concentrations in the pore water of sediments are, therefore, expected to agree with the noble-gas concentrations of the overlaying water mass at the time when the sediment was deposited. Brennwald et al. (2003) convincingly affirmed the correspondence of the dissolved noble-gas concentrations in the open water and the pore water experimentally. As lakes - especially closed water bodies (i.e., with no outlet) - are very susceptible to environmental and climate change (e.g. Fritz, 1996; Brennwald et al., 2004) noble-gas concentrations in unconsolidated sediments were considered as archives for reconstruction of past climate conditions as early as 1979 (Barnes, 1979).

Besides environmental reconstruction through atmospheric noble gases, the transient behavior due to the time dependent accumulation/production of terrigenic ^{4}He, tritiogenic and terrigenic ^{3}He and tritium (^{3}H) allows, in principle, to study the transport of dissolved species in the pore water of sediments and to analyze the transport mechanisms of terrestrial fluids through the upper crust (Ballentine et al., 2001; Brennwald, 2004; Stephenson et al., 1994; Strassmann et al., 2005).

Despite the obvious potential, the application of terrestrial noble-gas geochemistry in (unconsolidated) sediments was, until recently, severely limited by a lack of an experimental method to determine noble-gas concentrations in pore waters with the necessary overall precision of 1–2%. This situation changed in 2003 when the first robust experimental method was developed and successfully applied, allowing dissolved noble gases in pore water to be analyzed in a reproducible and routine manner (Brennwald et al., 2003).

However, noble gases and ^{3}H in sediment pore waters are still not widely used in environmental/geochemical research on aquatic systems. The aim of this thesis is to overcome this initial idleness and to spread the geochemical use of noble gases in unconsolidated sediments:

- by applying the recently developed extraction procedure (Brennwald et al., 2003) to more "extensive" and "complex" case studies;
- by simplifying and improving the analytical method so that it can be used in laboratories, where up to now only the analysis of bulk water samples is possible, e.g. to develop a method where only water, but not sediment needs to be extracted.

Noble-gas data from pore waters published in previous works are limited to one or two sediment cores for each studied site and the analyzed sediment cores have a relatively coarse vertical resolution (~ 10 cm, see Barnes and Bieri, 1976; Stephenson et al.,

1994; Brennwald et al., 2003, 2004, 2005; Strassmann et al., 2005; Holzner et al., 2008). Therefore, up to now noble gases in sediments were not applied to study the interactions between the water body, the sediment column and the underlying geochemical reservoirs on the spatial scale of a single lake basin. For instance, the observed heterogeneity of the helium release from solid earth and the attenuation of diffusive transport processes in the sediments are only partly understood. Both topics are still the subject of ongoing scientific speculation due to the lack of high-quality experimental data, characterized by low-resolution profiles and uneven spatial distribution.

The current standard method to determine noble-gas abundances in unconsolidated sediments (Brennwald et al., 2003) requires, mainly during the extraction phase, well-trained personnel to perform the analysis. This method is much more time-consuming than the measurement of noble gases in water or gas samples (the major analytical challenges are listed in the outline of Chapter 5 in the next section). Therefore, a simpler and more reliable concept to degas the pore water is utterly needed in order to widely apply the concepts of noble-gas geochemistry in lacustrine and ocean sediments.

1.2 Outline

This thesis presents the results of three noble-gas studies in unconsolidated sediments from Scandinavia (Stockholm Archipelago), from eastern Anatolia (Lake Van) and from the South Pacific Ocean (off shore from New Zealand). The noble-gas concentration profiles within the sediment column were interpreted in terms of diffusive transport, and the origin of terrigenic fluids was identified. Simple diffusion models were applied to define the relevant parameters that govern the noble-gas exchange/transport in the pore space of sediments.

To achieve the formulated main goals, the work of this thesis is ordered in seven chapters. Chapters 1, 2 and 7 provide an introduction and a final outlook on the application of noble gases in lake and ocean sediments. Chapter 3 describes the recently achieved experimental advancements to determine noble-gas abundances in pore waters of unconsolidated sediments. Chapters 4, 5 and 6 apply the developed methods to the three different case studies with different research focuses.

Chapter 2: Conceptual aspects This short chapter summarizes the main processes determining the fate of noble gases in aquatic systems, such as lakes and oceans, and their sediments. The influence of temperature and salinity on the expected equilibrium concentrations is discussed, with consideration of the local environmental conditions of the case studies presented in the following chapters. The specific isotope composition of helium is discussed in the context of different geochemical compartments/reservoirs from which it emanates.

Chapter 3: An improved method for the analysis of noble gases in the pore water of unconsolidated sediments The standard procedure developed by Brennwald et al. (2003) in order to determine noble-gas abundances in the pore water of lacustrine sediments is based on the heating of the closed sediment samples and a subsequent sediment "blow-out" under ultra high vacuum conditions into a connected extraction vessel.

This procedure may foster the release of radiogenic ^{4}He from the sediment grains in an uncontrollable manner due to the applied heating step. Such local He from the matrix severely hampers the analysis of terrestrial He emission. In addition, this method sometimes yields a partial (and therefore unsuccessful) extrusion of the bulk sediment into the extraction vessel; this implies low extraction efficiency, non-quantitative noble-gas extraction and elemental fractionation. The direct consequence of such an incomplete extraction can be an inability to convert the determined noble-gas concentrations into noble-gas temperatures in a statistically robust manner, i.e. the estimated temperature from the concentration of one single noble gas species significantly deviates from the temperature estimated for the other noble gases, which as a result hampers past climate reconstruction. Moreover, the extraction procedure is experimentally demanding and can only be applied by experienced specialists. In this chapter a new extraction method which involves the centrifugation of the bulk sediment samples will be discussed. It is shown how the experimental problems of the former method can be bypassed and how the determination of the noble-gas content in pore waters can be easily performed by noble-gas laboratories, where up to now only the analysis of bulk water samples is possible. The performance of the new method was tested on sediment samples from Lake Van (Turkey) and was further applied to ocean sediments (see Chapter 6).

Chapter 4: Attenuation of noble-gas transport in laminated sediments of the Stockholm Archipelago The very basic questions, whether and to which extent noble-gas signals are conserved in the sediment column over time, are still unanswered. In particular, it is yet to be defined under which sedimentological conditions noble gases as solutes are not subject to advective and diffusive transport/exchange as well as the resulting concentration "amplitude" damping. In a sediment core from the Stockholm Archipelago (Sweden) sampled at a high resolution in intervals of about 2 cm, the determined noble-gas profiles show that a past mass movement deposited and incorporated strong atmospheric and terrigenic noble-gas excesses. The atmospheric gas surpluses are clearly detectable even after a period of about one century. Such atmospheric noble-gas remains can only be reasonably explained, if the effective diffusion coefficients in the sediment are two to three orders of magnitude lower than those in free water. Otherwise the signals would have been smoothed over the given time and spatial scales.

Chapter 5: Spatial distribution of helium in the sediments of Lake Van Sediments act as a diffusive barrier for the fluids released from solid earth and therefore allow - in principle - to map the terrigenic He emanation at the local scale (e.g. a scale smaller than the lake basin) and to determine the respective terrestrial He flux. In this chapter the He liberation in Lake Van, located in a tectonically active region in eastern Anatolia (Turkey), was successfully studied and the flux of terrigenic He emission was for the first time ever experimentally determined. The results show that the He release occurs very unevenly in the spatial domain and seems to be bound to the steep collapsed structure of an ancient caldera that forms the deep basin of Lake Van. The new results indicate, in contrast to former studies, that the emanating He is not of pure depleted-mantle origin, but rather represents a mixture of mantle and radiogenic He. The lower ^{3}He/^{4}He ratio determined for terrigenic He accumulating in Lake Van gives insights into the terrestrial He release and leads to a new interpretation of the mixing conditions of Lake Van during

1989/90, a low water level period.

Chapter 6: Noble-gas analysis in ocean sediments to characterize active CH_4 seepage off shore from New Zealand Until now the measurement of noble gases in the pore water of ocean sediments was not possible because the fine texture of the sediment matrix hampered the required "blow-out" of the former extraction procedure (Brennwald et al., 2003). The combination of the new extraction method discussed in Chapter 3 with a more powerful centrifuge and ultrasonic disaggregation of the bulk sediment, allows, for the first time, noble gases to be extracted from ocean sediments in a routine manner. The application of this slightly modified extraction method was carried out on ocean sediments collected in the South Pacific, off shore from New Zealand, where a cold CH_4 seepage occurs along an active subduction zone. The goal of this work is to identify the geochemical reservoir related to the cold seepage system by its He isotope signature. The data show that CH_4 emanating at the active subduction zone is labeled by mantle He, whereas fluids in the forearc region are mainly of crustal sedimentological origin.

Chapter 2

Conceptual aspects

Noble gases are ideal tracers for studying physical processes in lakes (Torgersen et al., 1977; Kipfer et al., 1994; Hohmann et al., 1998; Peeters et al., 1997, 2000; Aeschbach-Hertig et al., 2002), oceans (Schlosser et al., 1991) and aquifers (Ingram et al., 2007; Klump et al., 2007, 2008b) because they are not affected by biogeochemical transformations and therefore are in the strictest sense only subject to physical exchange and production processes. Only recently, however, the development of analytical tools to sample and measure noble-gases in the pore water of lacustrine sediments (Brennwald et al., 2003) allowed the concepts of noble-gas geochemistry to be applied to unconsolidated sediments in a routine manner. In Lake Issyk-Kul (Kyrgyzstan) a noble gas anomaly detected in the sediment column was interpreted in terms of lake level changes and effective noble-gas diffusivities were roughly estimated to be smaller than the molecular diffusivities in water by at least two orders of magnitude (Brennwald et al., 2004). From the depletion pattern of dissolved noble gases in the sediments of Lake Soppen (Switzerland) generated by methane ebullition, Brennwald et al. (2005) concluded that diffusive processes in the sediment column must be nearly insignificant in order to preserve the observed depletion of dissolved noble-gas species which were not found to be significantly fractionated by potential kinetic effects related to the formation of methane bubbles. Furthermore, the combination of noble-gas concentration profiles and tritium (^{3}H) measurements in the sediment column of Lake Zug (Switzerland) has been shown to be a robust and straightforward approach to identify the relevant parameters controlling the transport of solutes and fluids in the pore space (Brennwald, 2004; Strassmann et al., 2005).

The present chapter gives a short conceptual overview of the relevant processes and sources affecting the abundance of noble gases in the sediment column of lakes and oceans (Sec. 2.1, see Fig. 2.1). Sediments act as an advective/diffusive barrier (Berner, 1975; Imboden, 1975; Boudreau, 1986; Strassmann et al., 2005) between the overlying water body (i.e. by constraining the solute exchange at the sediment/water interface) and the underlying geological setup (e.g. bedrock, faults, aquifers). The upper boundary conditions for the noble-gas transport in unconsolidated sediments is set by the abundance of noble gases in the water body at the sediment/water interface which in surface water bodies, such as lakes and oceans, generally agrees with the expected atmospheric equilibrium concentrations (Sec. 2.2). In addition to the atmospheric component, helium (He) is often enriched by terrigenic and radiogenic He (with characteristical isotope signatures) emanating from solid earth (Sec. 2.3), and tritiogenic ^{3}He produced by the radioactive decay of ^{3}H present

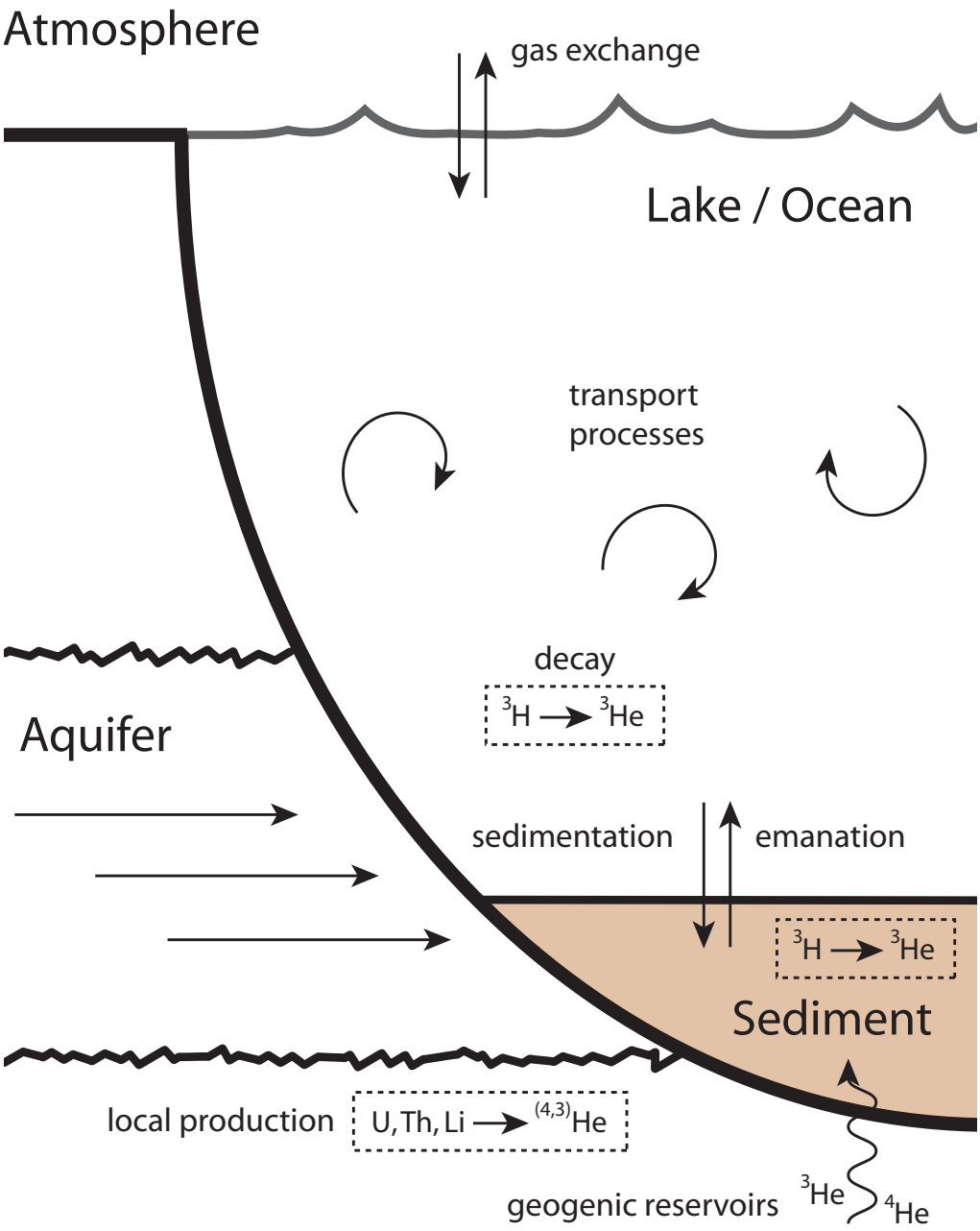

Figure 2.1: Schematic of the different processes affecting the noble-gas concentrations in unconsolidated sediment of lakes and oceans discussed in this thesis.

in surface waters (Sec. 2.4). The tritium concentrations measured in the sediment column can be used to determine the effective diffusivity of noble gases in the pore space with a simple diffusion model, which is described, along with its fundamental assumptions, at the end of this chapter (Sec. 2.5).

2.1 Origin of noble gases in unconsolidated sediments

Atmospheric noble gases - as all other air-borne gas species - generally enter the water phase by gas exchange at the water surface. In lakes and oceans the amount of transferred gases by gas exchange at the air/water interface is only constrained by the partial pressure of each gas at a given altitude and by the temperature and the salinity of the exchanging water mass (Aeschbach-Hertig et al., 1999b). Therefore, the atmospheric noble-gas component is characterized by the presence of all noble gases residing in the atmosphere, i.e. helium, neon (Ne), argon (Ar), krypton (Kr), xenon (Xe) and radon (Rn). As in this thesis only stable noble-gas isotopes are considered, Rn as radioactive species will be excluded from further discussions.

After entering the water phase the dissolved noble gases are distributed by advective and diffusive processes into the water body, depending on its mixing dynamics (Fig. 2.1). During the deposition of allogenic and autogenic sediment particles at the bottom of the water body (i.e. the sedimentation process), small amounts of the water overlying the sediment/water boundary together with all dissolved species, including dissolved (atmospheric) noble gases, become part of the growing sediment column. By further deposition of new sediment particles the pore water is progressively decoupled from the fast water exchange and mixing dynamics of the water body; in particular transport processes by advection and turbulent diffusion are completely attenuated in the pore water of the sediment. The "efficiency" of this decoupling mechanism can however differ by orders of magnitude depending on the sedimentation regime of the studied water body. In the Stockholm Archipelago (Chapter 4) sedimentation rates of about 2 cm/year have been observed (Meili et al., 2000; Persson and Jonsson, 2000), in Lake Van (Chapter 5) the yearly deposition is about 0.5–0.8 mm/year (Lemcke, 1996; Landmann et al., 1996) and in oceans (Chapter 6) sedimentation is in general less than 1 mm/year (except in the vicinity of estuaries, where large amounts of suspended particles are transported by rivers). Sedimentation becomes an important parameter for the modeling of solute transport in the pore space. The gravitational force of particles settling at the bottom of lakes/oceans fosters the compaction of lower sediment layers. The gradual reduction of the pore space due to compaction generates an advective pore water flux towards the water/sediment boundary. This advective flux can be more or less relevant compared to the diffusive processes affecting the concentrations of dissolved species in the pore space (Berner, 1975; Imboden, 1975; Strassmann et al., 2005) depending on the relevant time and spatial scales, as will be discussed in Sec. 2.5.

Non-atmospheric noble gases originate mainly from solid earth and/or are produced by nuclear reactions. Therefore they often enter "from" the bottom of (or are produced in) the sediment column. Hence non-atmospheric noble gases can in some cases set a lower boundary condition (i.e. the liberation of fluids from deeper strata of the planet) and/or a local production term affecting the solute transport in the sediment (Sec. 2.5). However, the sources of non-atmospheric noble gases cannot be so easily defined a priori as in

the case of atmospheric gas equilibration of surface waters since the geological structures which foster/hamper the release/production of geogenic fluids below the sediments differ greatly in the spatial domain and are in general unknown.

The two stable He isotopes, i.e. ^{3}He and ^{4}He, are commonly analyzed to study the emanation of fluids from different strata of the Earth (e.g. crust and mantle) as different geochemical reservoirs are determined by a typical ^{3}He/^{4}He ratio which in turn is a "defining" feature of the concerning reservoir (see Sec. 2.3). He in deep circulating fluids is commonly a mixture of variable shares of primordial ^{3}He released from the Earth's mantle and ^{4}He (and ^{3}He) locally produced in rocks/minerals and sediments. Most of terrigenic He is of radiogenic origin, as the result of the decay of U, Th (and K) and the induced secondary nuclear reactions (Morrison and Pine, 1955; Mamyrin and Tolstikhin, 1984). The non-atmospheric (non-tritiogenic) He components are often referred to as being of *terrigenic* origin. Note that beside He (and Rn, mainly produced by the uranium-radium decay chain) other noble gases are not affected by a significant terrigenic component in surface waters and therefore their concentrations and isotope ratios in unconsolidated sediments are expected to reflect the atmospheric equilibrium values (Brennwald et al., 2003). The terrigenic He release from lacustrine sediments of Lake Van will be discussed in Chapter 5.

In addition, young meteoric waters near the Earth's surface often contain *tritiogenic* ^{3}He which is produced by the decay of ^{3}H. ^{3}H is commonly of "atmospheric origin", as it is either constantly produced by spallation or introduced by atmospheric nuclear bomb tests (see Kipfer et al., 2002, for a review). The produced ^{3}H is rapidly oxidized in the atmosphere to tritiated water (^{3}H^{1}HO), and enters as such into the meteoric water cycle. In lakes and oceans, and depending on the mixing conditions of the concerning water body, when ^{3}H decays to ^{3}He, tritiogenic ^{3}He accumulates in the water column and allows the water renewal rates to be determined (Stute and Schlosser, 2000; Kipfer et al., 2002). Also, in sediments ^{3}H which enters the pore space can lead to tritiogenic ^{3}He accumulation. The coupling of advective/diffusive transport models and radioactive decay of tritium in the sediment column can be used to characterize the relevant parameters which govern the transport of noble gases (and other solutes) in the pore space (see Sec. 2.5).

2.2 Atmospheric equilibrium concentrations in water

The amount of atmospheric noble gases transferred from the atmosphere into water bodies is described reasonably by *Henry's Law*. This law states that an equilibrium exists between the (noble-gas) concentrations in the atmosphere (partial pressure) and the water:

$$p_i = H_i(T, S) \cdot C_i^* \tag{2.1}$$

where p_i is the partial pressure of the noble gas $i = \mathrm{He, Ne, Ar, Kr, Xe}$, H_i is the Henry coefficient (which depends on the water temperature T and the salinity S, see Table 2.1) and C_i^* is the equilibrium concentration in the water phase.

Under common environmental conditions (e.g. T from 0°C to 30°C and S from 0 g/kg to 35 g/kg) the saturation concentrations for all noble gases tend, as is common for weakly soluble gas species, to decrease with increasing temperature and/or salinity (see Fig. 2.2). In this work the noble-gas equilibrium concentrations are calculated using the

Table 2.1: Henry coefficients $H_i(T, S)$ for different water temperatures T and $S = 0‰$ in [bar/(cm^3_{STP}/g)]. STP means Standard Temperature (0℃) and Pressure (1 atm). Heavy noble gases tend to be more "hydrophile" and therefore they are less prone to degas.

T	0℃	5℃	10℃	15℃	20℃
			H_i $[\frac{\text{bar}}{\text{cm}^3_{\text{STP}}/\text{g}}]$		
He	108.3	111.5	114.3	116.6	118.6
Ne	81.89	86.76	91.31	95.55	99.52
Ar	19.01	21.71	24.51	27.39	30.34
Kr	9.306	10.93	12.69	14.58	16.58
Xe	4.580	5.576	6.690	7.920	9.263

parametrizations of Weiss (1971b) for He and Ne, Weiss (1971a) for Ar, Weiss and Kyser (1978) for Kr, and Clever (1979) for Xe (as recommended by Kipfer et al., 2002). The noble-gas concentrations are given as cm^3STP/g which denotes the volume of gas in cm^3 at Standard Temperature (0℃) and Pressure (1 atm) conditions (STP) dissolved per gram (pure) water.

The differences in the solubility behavior between light (He and Ne) and heavy (Ar, Kr, and Xe) noble gases set the physical basis for the use of noble gases to reconstruct past environmental conditions. As atmospheric equilibrium sets the natural boundary of the occurrence of atmospheric noble gases in water, any deviance against the equilibrium concentrations has either to be interpreted in terms of changing environmental conditions (changes in T and/or S) or as an indication of secondary gas/water partitioning as it will be illustrated for the Stockholm Archipelago (Chapter 4), Lake Van (Chapters 3 and 5) and the South Pacific Ocean (Chapter 6). The temperature and salinity dependence of the atmospheric equilibrium concentrations was successfully applied to determine the past continental climate evolution using groundwater (for a review see Kipfer et al., 2002), and to analyze water level fluctuations in lakes (Brennwald et al., 2004). Significant atmospheric noble-gas depletions were observed in the water column of e.g. the Black Sea (Holzner et al., 2008), as well as in organic-rich sediments of lakes which are known to produce methane (Brennwald et al., 2005). In both cases the observed depletion pattern, where the less soluble gas species He and Ne were affected differently than more soluble species Ar, Kr and Xe, allowed the noble-gas fractionation to be interpreted in terms of a secondary gas exchange between gas hydrates (or a free gas phase) and an air saturated water mass. This allowed, for example, the CH_4 emission from mud volcanoes in the Black Sea to be conceptually understood and to be quantified (Schubert et al., 2006; Holzner et al., 2008) and the CH_4 ebullition from lake sediments to be determined (Brennwald et al., 2005). In conclusion, the application of noble gases as palaeoenvironmental proxies is based on the straightforward coupling of simple and robust physico-chemical concepts which mechanistically explain the noble-gas abundance in the water phase.

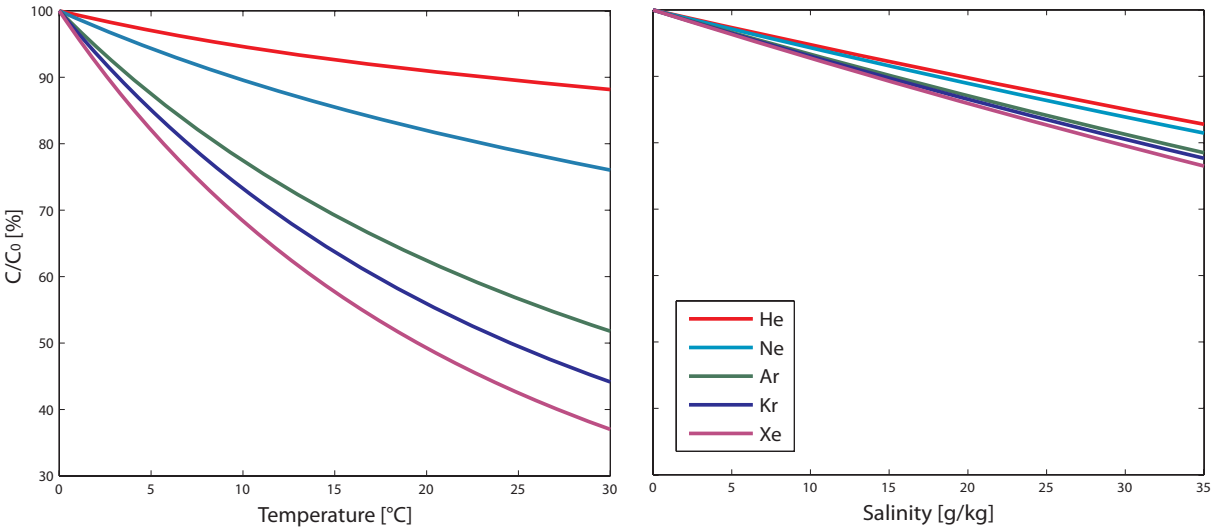

Figure 2.2: Temperature and salinity effect on solubility of noble gases. C/C_0 is the percentage of saturation relative to the initial concentration for 0°C temperature, rsp. 0 g/kg salinity. In general, the light noble gases are less affected by changes in temperature or salinity. Given their low mineralization, changes in salinity have a smaller effect on solubilities in fresh waters. However, in the case of saline lakes (e.g. Lake Van presented in Chapter 5, $S \approx 23$ g/kg) or oceans (e.g. the South Pacific in Chapter 6, $S \approx 35$ g/kg) the influence of salinity becomes important (see Brennwald et al., 2004).

2.3 Helium and He isotopes

Terrestrial He emanates from solid earth in a highly variable manner (Oxburgh et al., 1986). Not only the intensities of the He release, but also its isotope composition depend largely on the geological setup of the studied areas (for a review see Ballentine and Burnard, 2002).

He in the (depleted) mantle has a typical $^3He/^4He$ isotope ratio of $\sim 10^{-5}$ which is the result of the mixing of remains of primordial $^{(3)}$He and $^{(4,3)}$He being produced by nuclear reactions (radiogenic He). The He of the Earth's crust has a lower isotope signature of $^3He/^4He \sim 10^{-8}$, which reflects the higher He production in crustal rocks/minerals that are enriched in incompatible elements U, Th and Li, which control the production of ^{4}He (U, Th) and ^{3}He (Li, for details see e.g. Morrison and Pine, 1955; Mamyrin and Tolstikhin, 1984). The atmosphere is characterized by a constant He isotope ratio of $1.384 \cdot 10^{-6}$ (Clarke et al., 1976), which is the result of a steady state between the liberation of terrigenic He from the mantle and the crust and the He loss into interplanetary space (O'Nions and Oxburgh, 1983). The typical isotope ratios for these different reservoirs of the Earth are summarized in Table 2.2.

The clear separation between the isotope ratios of these three geochemical compartments/reservoirs allows for straightforward determination of the origin of He and therefore of "all other" fluids migrating through the uppermost layers of solid earth such as lake/ocean sediments (see in particular Chapters 5 and 6).

Table 2.2: Typical $^3He/^4He$ ratios for different geochemical reservoirs on Earth.

Reservoir	$^3He/^4He$
Crust	10^{-8}–10^{-7}
Atmosphere	$1.384 \cdot 10^{-6}$
Mantle	10^{-6}–10^{-5}

2.4 Tritium and tritiogenic ^3He

Tritium (^3H) occurs naturally in the atmosphere where it is mainly produced in nuclear reactions induced by cosmic radiation on nitrogen and oxygen nuclei (Craig and Lal, 1961). In addition, in the 1960's, nuclear bomb tests increased the terrestrial tritium budget by orders of magnitude (with a distinct maximum in 1963, see Weiss et al., 1979; IAEA/WMO, 2006).

Tritium enters the hydrologic cycle in the form of tritiated water ("HTO"). ^3H has a half-life $\tau_{1/2}$ of 4500 ± 8 days (Lucas and Unterweger, 2000) and decays to tritiogenic ^3He ($^3He_{tri}$). The ^3H abundance is often expressed in tritium units (TU), i.e. as a normalized $^3H/^1H$ ratio:

$$1\text{TU} = \frac{1 \cdot {}^3\text{H atom}}{10^{18} \cdot \text{H atoms}}$$

From the ^3H and $^3He_{tri}$ concentrations it is possible to assess the time, t, since an isolated water parcel was in contact with the atmosphere (Tolstikhin and Kamenskiy, 1969; Torgersen et al., 1977, 1979). The following equations describe the time-dependent concentrations of both species in an isolated water mass:

$$^3\text{H}(t) = {}^3\text{H}_0 \cdot e^{-\lambda t} \tag{2.2}$$

$$^3\text{He}_{\text{tri}}(t) = {}^3\text{H}_0 \cdot (1 - e^{-\lambda t}) \tag{2.3}$$

where $^3H_0$ is the initial ^3H concentration in the water, and $\lambda = \ln 2/\tau_{1/2}$ denotes the decay constant. These two coupled equations set the physical basis to determine water residence times and the typical renewal rates in lakes/oceans and groundwaters. While $^3H_0$ is usually unknown, it can be calculated as the sum of $^3H(t)$ and $^3He_{tri}(t)$. If both $^3H(t)$ and $^3He_{tri}(t)$ are known, equations 2.2 and 2.3 can be solved for t which is the so called "$^3H/^3He$ water age".

$$t = \frac{1}{\lambda} \ln \left(1 + \frac{{}^3\text{He}_{\text{tri}}(t)}{{}^3\text{H}(t)} \right) \tag{2.4}$$

Despite the successful application of this dating method in aquifers and lakes (Stute and Schlosser, 2000; Kipfer et al., 2002), where water exchange is mainly given by advection, in systems where diffusive exchange or mixing controls the concentration of ^3H and dissolved gas concentrations, the difference in the diffusion coefficients for tritiated water and helium in bulk water may decouple the two concentration signals (Jenkins, 1998; Aeschbach-Hertig, 1994). This is the case for lacustrine sediments, where diffusive processes are mainly responsible for the transport of solutes in the pore space (e.g. Imboden,

1975; Strassmann et al., 2005). In this case the classical concept of "water age" is not permissible. However, the concentration profiles of ^{3}H and ^{3}He still convey information about the water exchange and the involved exchange rates if the transient behavior of the tracers is analyzed by an advective/diffusive transport model (e.g. Strassmann et al., 2005). This is shown in the following section.

2.5 Determination of solute transport in the pore space

The information gained from tritium profiles in the sediment column can be very useful to quantify the effective diffusivity of solutes in the sediments (e.g. Strassmann et al., 2005). By introducing the decay of tritium in the equation for solute transport within the connected pore space the effective diffusivity of the solutes (e.g. ^{3}H) in the sediment column can be determined.

Solute transport in sediments can be described as a combination of advective and diffusive fluxes (Berner, 1975; Imboden, 1975; Strassmann et al., 2005):

$$\phi \frac{\partial c}{\partial t} = \frac{\partial}{\partial z}\left(\phi D_{\text{eff}} \frac{\partial c}{\partial z}\right) - U\phi \frac{\partial c}{\partial z} + \phi r \tag{2.5}$$

where ϕ is the sediment porosity, c the concentration of the dissolved species, t time, z the sediment depth, D_{eff} the effective diffusion coefficient, U the velocity at which pore water moves relative to the sediment surface, and r a source/production term. The effective diffusivity, D_{eff}, is defined in this work as follows:

$$D_{\text{eff}} = \frac{\phi}{a} D_{\text{mol}} \tag{2.6}$$

where a [-] is an attenuation factor, accounting for the effects of "tortuosity" in the sediment column, which may significantly reduce the effective diffusivity in pore waters compared to the molecular diffusivity of dissolved species in bulk water, D_{mol}. With the assumption of no advection ($U = 0$) and no production ($r = 0$) equation 2.5 can be simplified to:

$$\phi \frac{\partial c}{\partial t} = \frac{\partial}{\partial z}\left(\frac{\phi^2}{a} D_{\text{mol}} \frac{\partial c}{\partial z}\right) \tag{2.7}$$

Advective fluxes can be reasonably neglected if the solute transport is dominated by diffusion and hence the respective Peclet number, $Pe = UL/D_{\text{NG}}$ (Schwarzenbach et al., 2003, where $D_{\text{NG}} > 10^{-2}\,\text{m}^2/\text{year}$ are the molecular diffusivities of dissolved noble gases in water) is small (i.e. $Pe < 1$). All presented case studies in this thesis fall in this "diffusive regime", i.e. $UL \ll D_{\text{NG}}$ is valid. In the respective chapters the relevance of effective diffusivity D_{eff} with respect to the transport regime will be discussed. Furthermore, assuming that porosity is constant in time and space, equation 2.7 can be reduced and simplified to a form similar to Fick's second law:

$$\frac{\partial c}{\partial t} = \frac{\phi}{a} D_{\text{mol}} \frac{\partial^2 c}{\partial z^2} \tag{2.8}$$

Equation 2.8 describes the transport of solutes in the pore space that is sometimes strongly attenuated, as will be shown using noble gases as tracers in the case studies of the Stockholm Archipelago (Chapter 4) and Lake Van (Chapter 5). Adapting this simplified transport equation for solutes in the sediment column for the particular case of tritium (i.e. tritiated water) gives:

$$\frac{\partial C_{^3\mathrm{H}}}{\partial t} = \frac{\phi}{a} D_{\mathrm{HTO}} \frac{\partial^2 C_{^3\mathrm{H}}}{\partial z^2} - \lambda C_{^3\mathrm{H}} \tag{2.9}$$

where $C_{^3\mathrm{H}}$ is the tritium concentration, D_{HTO} the diffusion of tritiated water in free bulk water, λ is the decay rate for ^{3}H and ϕ and a determine the attenuation of diffusion as described in equations 2.5 and 2.6. As ϕ is a given parameter, the effective diffusivity in equation 2.6 can be estimated by fitting the results of the diffusive modeling to the measured tritium concentration data in the sediments just by adapting the value of a. The details concerning the application of tritium to determine the effective diffusivities of solutes in the pore space will be further discussed in Chapter 5.

Chapter 3

An improved method for the analysis of dissolved noble gases in the pore water of unconsolidated sediments

Abstract: We developed a new and improved method for the extraction of dissolved noble gases from the pore water of unconsolidated lacustrine sediments. Our previous extraction method is based on thermal dispersion of the bulk sediment under vacuum conditions to degas the pore water. This approach was shown to be prone to numerous experimental difficulties (e.g., the release of He from sediment grains, and incomplete extrusion from the copper tube used as a sample container), which are overcome by our new method. The new method relies on separation of the pore water from the bulk sediment by centrifugation. This allows simpler, faster and more reliable analyses. As only bulk pore water is used for analysis, the new method can easily be adopted by other noble-gas laboratories. Also, the new method can be used to determine the abundance of other dissolved gases such CH_4, N_2 or CO_2.

3.1 Introduction

In recent years the analysis of noble gases in meteoric waters has become a powerful tool for studying mixing dynamics in lakes, oceans, and groundwaters, and for reconstructing past climate conditions (Kipfer et al., 2002; Schlosser and Winckler, 2002). Noble-gas concentrations in sediment pore water have been shown to reflect past noble-gas concentrations in the overlying water body (Brennwald et al., 2003, 2004), and can provide information on transport and gas-exchange processes within the sediment (Brennwald et al., 2005; Strassmann et al., 2005; Holzner et al., 2008).

Until now, the method developed by Brennwald et al. (2003) was the only method available for the quantitative analysis of the concentrations of noble gases dissolved in

Acknowledgments: We highly appreciate the support of Aysegül Feray Meydan, Dr. Mustafa Karabiyikoğlu and Prof. Dr. Sefer Örçen and the staff of the Yüzüncü Yıl University in Van (Turkey) during fieldwork on Lake Van during the past few years. We thank Urs Menet and Heinrich Baur at ETH Zurich for their technical support in the lab. We also thank Dr. D. M. Livingstone (Eawag) for his helpful comments and editing assistance. This work was funded by the Swiss Science Foundation (SNF 200020-109465).

the pore water of lacustrine sediments. This method was successfully used to study the noble-gas abundance in the sediments in various lakes (Brennwald et al., 2003, 2004, 2005; Strassmann et al., 2005), and in the Black Sea (Holzner et al., 2008). Gas extraction is achieved by connecting the bulk sediment sample container to an evacuated extraction vessel. The sample container is then rapidly heated to 150°C, which results in a pressure increase in the sample container. The bulk sediment is then extruded explosively into the extraction vessel ("blow-out"), and the sediment grains are dispersed over the interior surface of the extraction vessel. The pore water is liberated from the sediment matrix and is degassed in the extraction vessel. Chaduteau et al. (2007) recently proposed an extraction method based on flushing the sediment samples with degassed water. However this method was only applied to determine the concentrations of He isotopes, requires a dedicated extraction apparatus, and is time-consuming.

Although the analytical protocol of Brennwald et al. (2003) allows noble-gas concentrations to be determined reliably, it also has several shortcomings. Heating the sediment may cause the gas sample to be contaminated with radiogenic ^{4}He released from the sediment grains, and may also induce chemical reactions that produce large amounts of gases such as CH_4 that interfere with the analysis of noble gases in the pore water sample (see Brennwald et al., 2003). Furthermore, in the specific case of Lake Van (Turkey), quantitative extraction of some sediment samples could not be achieved because part of the bulk sediment remained in the sample container after blow-out, and quantitative degassing of the pore water in this sediment is therefore not possible. In addition, it emerged that the blow-out step needs to be performed by experienced specialists to minimize the number of incompletely degassed sediment samples. The experimental difficulties encountered with the Lake Van sediments are probably the result of the very fine texture of the laminated sediments of this lake.

To overcome the shortcomings of the blow-out method, we developed a new and improved method to extract the noble gases dissolved in sediment pore water. With this new method, a fraction of the pore water is first separated from the sediment matrix by centrifugation. This water sample is then analyzed according to the standard protocol for the analysis of noble gases in water samples (Beyerle et al., 2000). In comparison to our previous method, the new gas extraction method is less experimentally challenging, reduces work load with the noble-gas extraction line, and results in a substantial improvement in reliability. Further advantages of the new method are that it can be directly applied in the quantitative analysis of other dissolved gases in the pore water (e.g. CH_4, N_2 and CO_2), and that it can easily be adopted by any laboratory equipped to conduct gas analyses in common water samples from open water bodies and groundwaters.

3.2 Materials and Procedures

3.2.1 Concept overview

Bulk sediment samples are transferred into sample containers (copper tubes) in the field immediately after sediment coring by squeezing the sediment core with two pistons inserted into both ends of the plastic core liner. The copper tubes, which are attached to the side of the core liner by Swagelok fittings at the chosen sampling depths, are filled with bulk sediment and closed off airtight using two special metal clamps to avoid the

contamination and degassing problems that might result if the sediment were to come in contact with air. For further details on sampling refer to Brennwald et al. (2003).

In the laboratory, the separation of the pore water from the sediment matrix within the still closed sampling containers is achieved by centrifugation. The original sample is split into two aliquots. After centrifugation one aliquot is opened to determine the position of the sediment/water interface. The second aliquot is split at the position of the sediment/water interface with a third clamp. Thereafter, the pore water and the compressed sediment phase are completely separated from each other. The pure pore water phase of the second aliquot is analyzed as a normal water sample following well-accepted protocols for the analysis of noble gases in water samples (Beyerle et al., 2000).

Here we describe and discuss only our new and improved method of extracting the dissolved gases from the sediment pore water.

3.2.2 Centrifugation

To separate the pore water from the bulk sediment, the copper tube containing the bulk sediment sample is split into two aliquots of the same length (~ 20 cm each, Fig. 3.1A). Both aliquots are centrifuged at 2300 rpm, resulting in the release of 1–3 g of pore water from the sediment matrix (Fig. 3.1B). To avoid deformation of the copper tubes during centrifugation, they are held in place by a polypropylene support. The maximum length of copper tube that fits our currently used centrifuge (Heraeus UJ3S) is ~ 20 cm. Of this, 3 cm must remain empty, as this is needed for later connection to the vacuum extraction system. The sediment-filled copper tube between the two sealing clamps of each aliquot has a length of ~ 11 cm.

3.2.3 Separation of pore water and sediment phases

The position of the sediment/water interface depends on the type of sediment (e.g., grain size, porosity) and therefore needs to be determined for each sample or each sediment core individually. To this end, the copper tube containing one sample aliquot is cut open at the end containing the released pore water. The tube is then cut successively shorter in a stepwise manner to determine the position of the sediment/water interface (Fig. 3.1C). The tube holding the other sample aliquot is then pinched off close to the expected sediment/water interface (Fig. 3.1D), but shifted about 5-10 mm toward the water phase to avoid the inclusion of residual sediment grains in the water sample.

3.2.4 Noble-gas analysis

Noble gases dissolved in the pore water separated from the sediment matrix are then extracted and analyzed following our standard protocol for noble-gas analysis in water samples (Beyerle et al., 2000). The only exception to this standard protocol is made necessary by the fact that the connection part of the copper tube (see Fig. 3.1) is too short to be joined to the UHV extraction line using the standard cutting-edge mechanism (Beyerle et al., 2000; Brennwald et al., 2003). We therefore use a rubber O-ring connector to establish a gas-tight connection between the copper tube and the extraction line.

In order to determine the water mass of the sample, the part of the copper tube that contained the analyzed pore water is vacuum dried. The water mass is then given by the

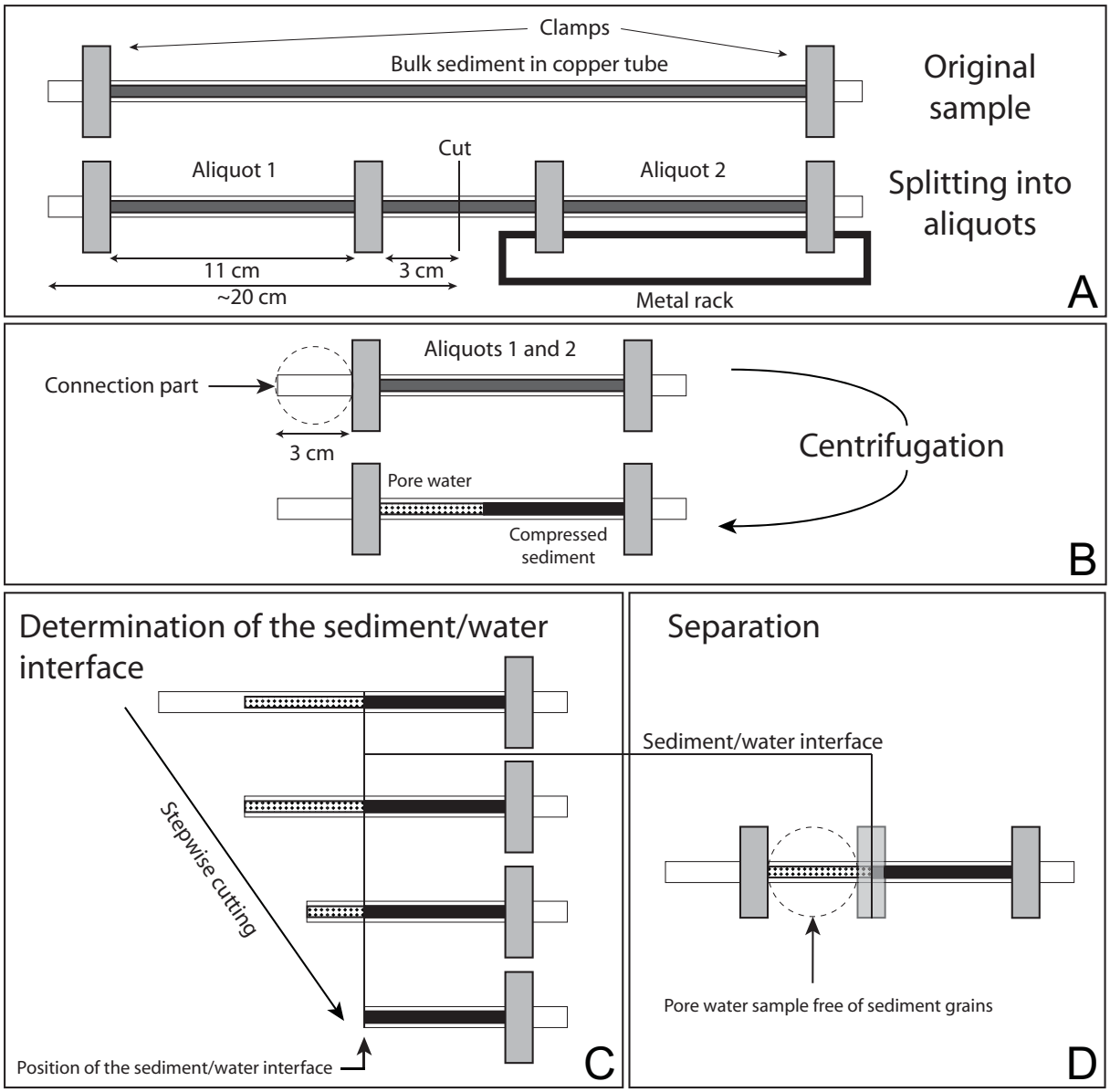

Figure 3.1: Preparation of sediment samples for centrifugation. (A) A copper tube containing a bulk sediment sample is split into two aliquots of the same length with the help of a tailor-made metal rack, leaving a length of about 3 cm on at least one side of each aliquot that is later used to connect the sample to the extraction line. (B) The two aliquots are centrifugated in order to separate a pure pore-water phase from the sediment phase. (C) One aliquot is used to determine the position of the sediment/water interface. (D) The other aliquot is pinched off at the sediment/water interface, yielding a pore-water sample free of sediment grains.

difference of the mass of the tube plus sample before analysis and that of the dry tube after analysis.

3.3 Assessment

We assessed the performance of our new method to determine noble-gas concentrations from unconsolidated sediments in two stages:

- Overall performance and leak test using standard water samples.
- Comparison of the new centrifugation method with the previously used blow-out method as applied to lacustrine sediments.

3.3.1 Performance and leak test

We evaluated the performance of the centrifugation method using water samples from Lake Lucerne (Switzerland), which are used as an internal laboratory standard for the routine analysis of water samples. The noble-gas concentrations in these water samples are therefore very well known and provide a well-defined reference. We applied our new centrifugation protocol to three of these internal standard water samples. The concentrations and isotope ratios of the noble gases measured in these centrifugated water samples agree with the expected concentrations and isotope ratios within the analytical 1σ error (Fig. 3.2; Table 3.1). The slight He excess relative to the expected equilibrium concentration can be explained either by the accumulation of terrigenic He in the water body or by the presence of excess air related to wave formation at the surface of the lake. The results indicate that the copper tubes and sealing clamps remain airtight during the centrifugation process. Further, centrifugation does not result in a significant elemental or isotopic fractionation of noble gases in the water.

3.3.2 Comparison of new and old methods

A comparison of the overall experimental performance of the new method of determining noble-gas concentrations in unconsolidated sediments with the standard "blow-out" protocol of Brennwald et al. (2003) was carried out on samples from two sediment cores acquired from Lake Van in May 2005 (see Fig. 3.3).

Lake Van is located at 1640 m a.s.l. in a tectonically active zone in eastern Anatolia. The lake is about 450 m deep and accumulates terrigenic helium from a depleted mantle source (Kipfer et al., 1994). The sediments of Lake Van are homogeneous and fine-textured, and the first 10-15 m of the sediment column are annually laminated (Landmann et al., 1996; Wick et al., 2003; Reimer et al., 2008). The porosity in the upper few meters is 60-70%. The sediment samples were taken from the sediment cores using the standard procedure described by Brennwald et al. (2003).

From each core two replicate samples were taken for noble-gas analysis. One replicate was split into two sub-samples which were analyzed using the blow-out method of Brennwald et al. (2003). The other replicate was analyzed using the new centrifugation method.

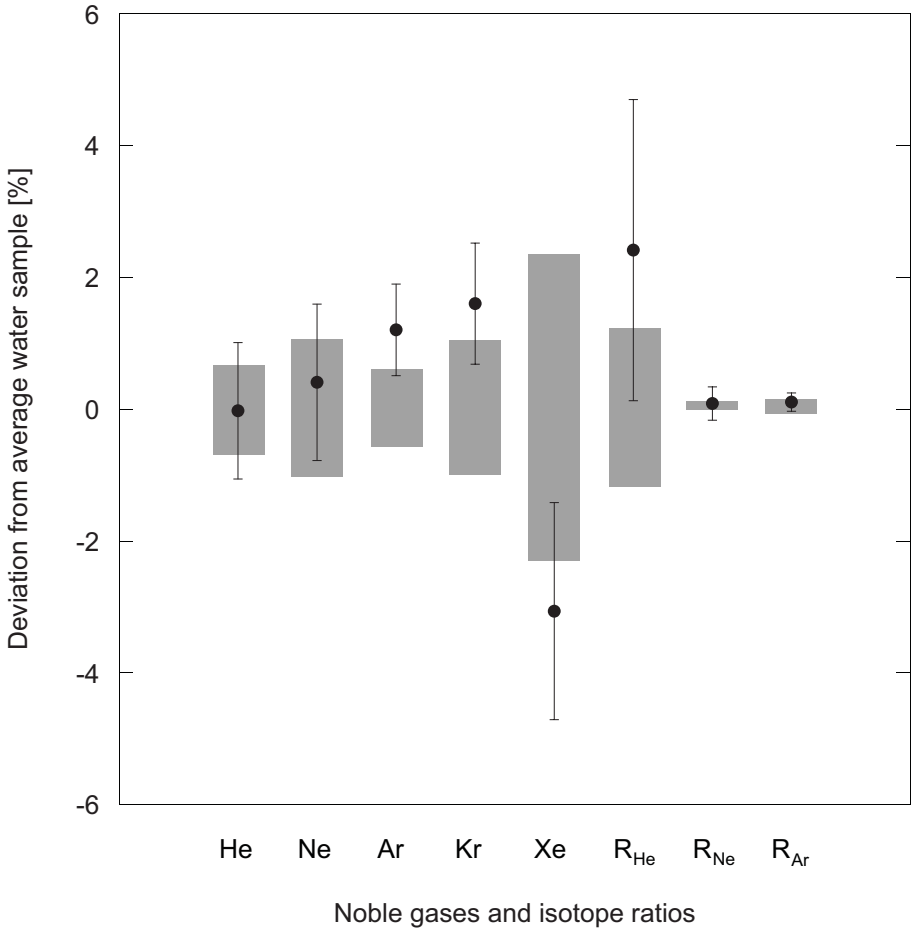

Figure 3.2: Comparison of mean noble-gas concentrations and isotope ratios in three centrifugated standard water samples (black dots) with mean concentrations and isotope ratios in water standards analyzed in the same way as normal (non-centrifugated) water samples (gray shaded areas). R_{He}, R_{Ne}, and R_{Ar} are the isotope ratios $^{3}He/^{4}He$, $^{20}Ne/^{22}Ne$ and $^{36}Ar/^{40}Ar$, respectively. The mean concentrations and isotope ratios of the normal water samples is set to zero on the y-axis, and their standard deviations are given by the gray areas. The data from the centrifugated samples are represented as relative deviations from the corresponding normal water sample data, and the black error bars indicate the standard deviation of the mean. The concentrations and isotope ratios measured in the centrifugated water samples agree with those of the standard samples within the analytical error.

Table 3.1: Noble-gas concentrations and isotope ratios for sediment and water samples from Lake Lucerne and Lake Van. STP = standard temperature (0°C) and pressure (1 atm). Method used (indicated in the sample name): N = bulk water samples measured using the standard protocol for analyzing noble gases in water samples (i.e., non-centrifugated: Beyerle et al., 2000); B1, B2 = sediment samples measured using the blow-out method (Brennwald et al. 2003); C = sediment samples measured using the centrifugation method. *L-Weq*: calculated equilibrium concentrations for Lake Lucerne water samples. *V1-Wm*, *V2-Wm*: measured concentrations for Lake Van water samples.

Sample	z (m)	He (10^{-8} cm$^3_{STP}$/g)	Ne (10^{-7} cm$^3_{STP}$/g)	Ar (10^{-4} cm$^3_{STP}$/g)	Kr (10^{-8} cm$^3_{STP}$/g)	Xe (10^{-8} cm$^3_{STP}$/g)	^{3}He/^{4}He (10^{-6})	^{20}Ne/^{22}Ne	^{40}Ar/^{36}Ar
Lake Lucerne (36.9 m water depth, temperature 3.2°C, salinity $\sim$ 0‰)									
L-Weq		*4.49*	*1.98*	*3.99*	*0.96*	*1.42*	*1.36*	*9.78*	*294.9*
L1-N		4.74	1.95	3.92	0.92	1.42	1.34	9.80	294.5
L2-N		4.96	2.03	4.04	0.95	1.41	1.33	9.79	296.0
L3-N		4.77	1.99	4.03	0.96	1.44	1.33	9.80	294.5
L1-C		4.80	1.98	4.03	0.95	1.36	1.34	9.81	296.2
L2-C		4.80	1.99	4.04	0.96	1.36	1.37	9.76	296.1
L3-C		4.86	2.02	4.07	0.97	1.43	1.38	9.80	293.6
Lake Van V1 (250 m water depth)[a]									
V1-Wm		*4.05*	*1.49*	*3.02*	*7.17*	*1.07*	*2.61*	*9.76*	*295.7*
V1-B1	0.20	4.15	1.39	2.54	0.57	0.85	3.57	9.78	295.8
V1-B2	0.20	4.05	1.38	2.56	0.59	0.90	3.19	9.76	295.4
V1-C	0.20	4.08	1.51	3.09	0.73	1.05	2.77	9.76	297.1
Lake Van V2 (196 m water depth)[b]									
V2-Wm		*3.98*	*1.49*	*3.03*	*7.23*	*1.10*	*2.33*	*9.79*	*294.7*
V2-B1	0.26	4.11	1.40	2.63	0.62	0.97	5.53	9.82	295.7
V2-B2	0.26	4.18	1.46	2.87	0.67	1.08	3.14	9.82	295.4
V2-C	0.26	4.13	1.52	3.09	0.73	1.11	6.36	9.65	296.0
Error B[c] (%)		1.0	1.3	1.1	1.9	2.6	1.0	0.2	0.1
Error C[d] (%)		1.9	1.9	1.9	2.0	2.5	1.7	1.6	0.2

[a]The water sampling station was located in the Ahlat sub-basin about 9 km east of sediment sampling station V1 (Fig. 3.3).
[b]The water sampling station was located in the main basin of Lake Van about 10 km west of sediment sampling station V2 (Fig. 3.3).
[c]Relative standard error for the blow-out extraction method of Brennwald et al. (2003).
[d]Relative standard error for the centrifugation method.

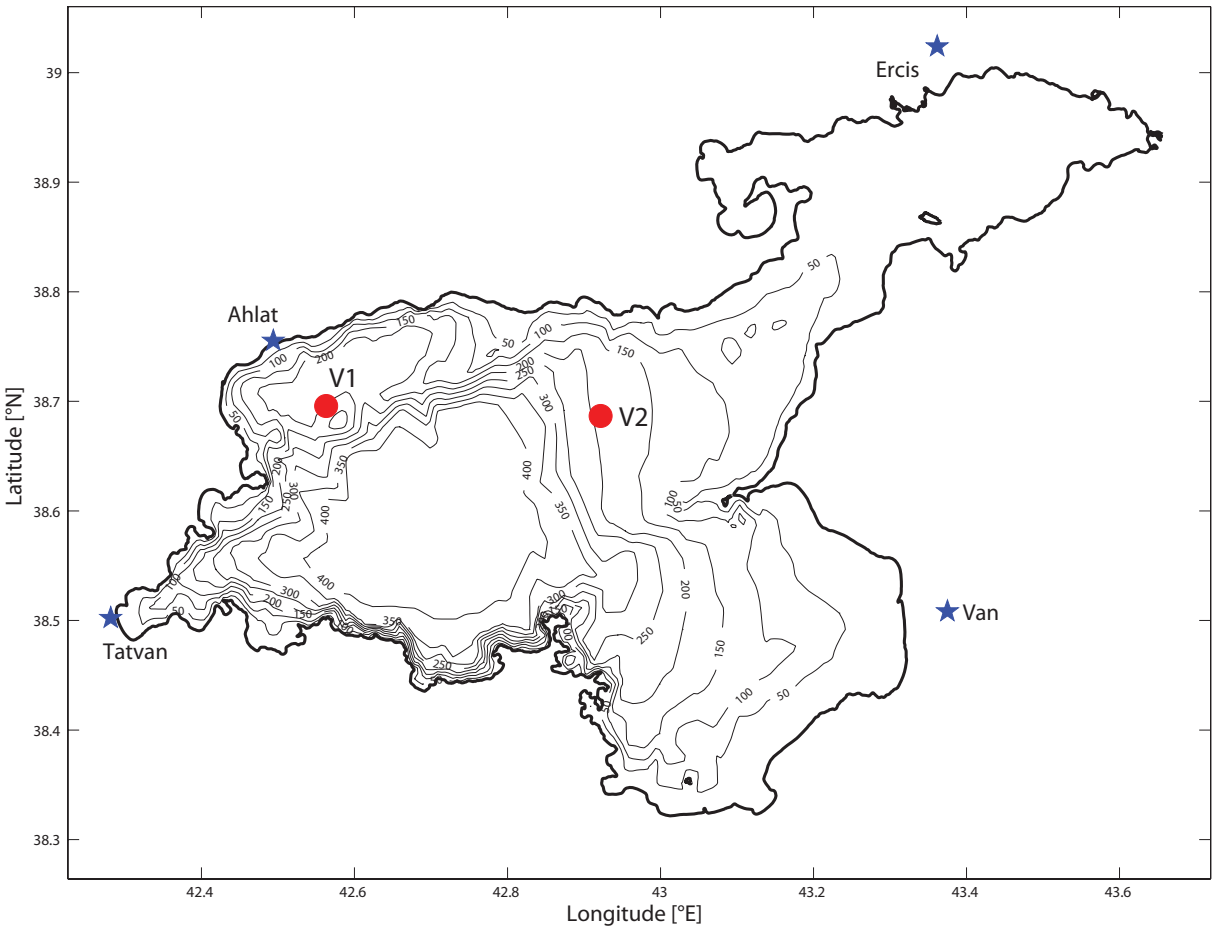

Figure 3.3: Map of Lake Van showing the locations of the sediment sampling stations in 2005 (red dots) and the major cities in the vicinity of the lake (blue stars).

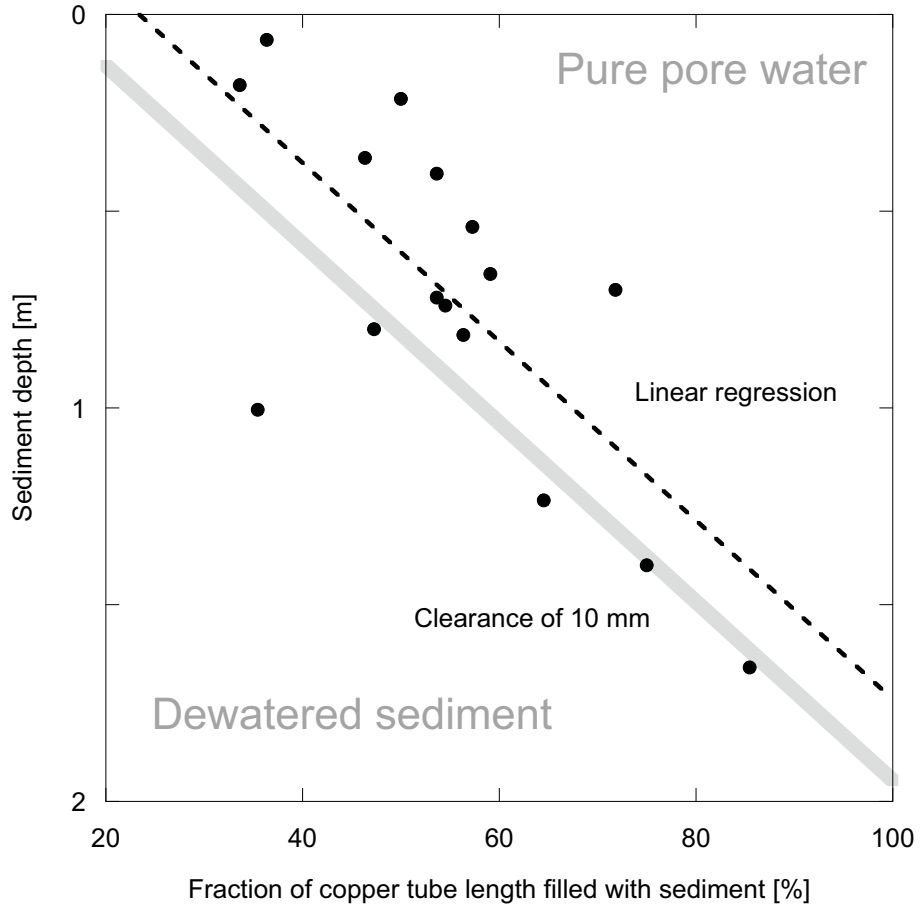

Figure 3.4: Determination of the sediment-water interface for samples from Lake Van (black dots). The dashed line represents a linear regression which allows the geometrical position of the sediment-water interface to be estimated. The gray line represents a clearance of 10 mm.

Various aliquots of samples from other sediment cores from Lake Van were used in centrifugation experiments to assess how well the position of the sediment/water interface could be determined after centrifugation. Inspection of the prepared aliquots showed that the bulk water contained no residual sediment grains. Based on our experience, knowledge of the position of the sediment/water interface in a few centrifugated aliquots is sufficient to define an empirical relationship between the position of the sediment/water interface in the copper tube and the sediment depth (Fig. 3.4). We therefore conclude that in the case of Lake Van the position of the sediment/water interface can be reliably determined from the established empirical relationship. Note, however, that the latter may only apply in the case of homogeneous and fine-textured sediments like those from Lake Van. We therefore suggest that the position of sediment/water interface always be determined experimentally for each individual sample using an aliquot of the same sample.

The linear regression illustrated in Fig. 3.4 suggests that the available water mass becomes very small in samples taken at depths greater than 1.5 m. This poses practical difficulties in setting the third clamp to separate water and sediment (see Fig. 3.1D). Because space within the centrifuge is limited, the maximum sample length (i.e., the

distance between the clamps) is about 11 cm (Fig. 3.1A). This defines the maximum available water mass after centrifugation as ~ 2 g (at least with the copper tubes used in our experiments, which have an inner diameter of ~ 7 mm).

Comparison of the noble-gas concentrations determined by the blow-out extraction method of Brennwald et al. (2003) and our new centrifugation method shows that, in the case of the Lake Van sediment, the former method has a lower extraction efficiency for the heavier noble gases (Table 3.2). This is probably due to incomplete blow-out of the fine-grained sediments of Lake Van.

Table 3.2: Comparison of noble gas concentrations and isotope ratios in the sediments of Lake Van (stations V1 and V2, see Fig. 3.3) as determined by the standard method of Brennwald et al. (2003) (B1 and B2) and by the centrifugation method (C). The data are expressed as the percentage deviation from the measured concentrations and isotope ratios in the overlying water column. ΔV1 and ΔV2 denote the discrepancies between the two extraction methods at each station.

Sample	He (%)	Ne (%)	Ar (%)	Kr (%)	Xe (%)	^{3}He/^{4}He (%)	^{22}Ne/^{20}Ne (%)	^{40}Ar/^{36}Ar (%)
V1-B1	2	-7	-16	-20	-21	37	-0.3	0.1
V1-B2	0	-7	-15	-18	-16	22	0.0	-0.1
V2-B1	3	-6	-13	-15	-12	137	-0.3	0.3
V2-B2	5	-2	-5	-7	-2	34	-0.3	0.2
V1-C	1	1	2	2	-2	6	-0.1	0.5
V2-C	4	2	2	1	1	172	1.5	0.5
ΔV1	-1	8	18	21	17	-23	0.1	0.5
ΔV2	0	7	11	12	8	87	1.8	0.2

With the blow-out method, the discrepancy between the noble-gas concentrations measured in the pore water and in the overlying bulk water increase with increasing atomic mass (Table 3.2). The greatest discrepancy is found in the case of Xe (21%, sample V1-B1). It seems that the blow-out method extracts light noble gases from the sediments of Lake Van more efficiently than heavier ones, whereas the new method does not fractionate noble-gas species (or not appreciably). Brennwald et al. (2003) successfully analyzed sediment samples from two Swiss lakes using the standard blow-out method with a mean extraction efficiency for Xe of $\sim 98\%$ for Lake Lucerne and $\sim 94\%$ for Lake Zug. However, incomplete extrusion of the sediment sample significantly reduces the extraction efficiency of the standard method. A very fine-grained sediment matrix may hamper gas extraction in the blow-out method, as the effective diffusivity is significantly attenuated by an increase in tortuosity that prevents the noble gases from being released from the sediment.

We therefore conclude that the strong depletions of about 10-20% in the concentrations of the heavy noble gases (Ar, Kr, and Xe) measured in the samples extracted using the blow-out method are related to something specific to the matrix of the analyzed sediments that either hindered complete extrusion of the gases from the copper tube, or generated large sediment clumps during the extrusion step. In both cases the sediment structure was apparently able to form a diffusive barrier that hindered complete degassing of the

heavier dissolved noble gases from the sample during the extraction process.

For all noble gases, the samples analyzed using the centrifugation method show concentrations that agree with those in the overlying water to within 4% (Table 3.2), indicating that the textural problem encountered by the blow-out method is completely bypassed by the new extraction procedure. For He, the agreement is slightly less good than for the heavier noble gases, and $^3He/^4He$ ratios in the sediment, especially at sampling station V2, are much higher than in the overlying bulk water (Table 3.2). However, this is to be expected because of the accumulation of mantle He enriched in ^3He at the bottom of Lake Van (Kipfer et al., 1994). He in the sediment column, in contrast to He in the overlying bulk water, cannot be dispersed by strong horizontal turbulent transport.

The measured ^4He concentrations agree with those of the standard method to within 1%; however, the $^3He/^4He$ ratios deviate considerably from those of the standard method. As already pointed out by Brennwald et al. (2003), the standard blow-out method tends to result in an uncontrolled release of He from the sediment matrix in response to the heat applied. A direct comparison of the two methods based on $^3He/^4He$ ratios from the pore water of Lake Van is therefore not feasible.

3.4 Discussion

The results from the centrifugated sediment samples from Lake Van show that centrifugation yields a bulk pore water sample that is free of residual sediment grains. The procedure is experimentally straightforward and results are reproducible. The optical determination of the geometrical position of the sediment/water interface within the centrifugated samples could be achieved in a robust manner. The position of this interface needs to be precisely known in order to obtain the maximum amount of water for the subsequent noble-gas analysis, as the mass of water liberated by centrifugation determines the overall error of the noble-gas determination. Otherwise, if the position is only vaguely defined, the third clamp that separates the sediment from the water has to be set at a safe position near the water end of the sample to keep the water phase clear of sediment. Under such unfavorable conditions our geometrical setting does not always guarantee that the separated water mass is large enough (> 2 g) to allow adequate determination of the noble-gas concentrations.

The centrifugation method described here represents a significant step forward in the analysis of noble gases in the pore water of unconsolidated sediments.

Firstly, the uncontrolled release of He from the sediment grains, which affects the $^3He/^4He$ isotope ratios determined by the blow-out method (Brennwald et al., 2003), is completely avoided by separating the pure pore water from the compressed sediment phase. The pure pore water sample is extracted like a common water sample under normal ambient temperature conditions.

Secondly, the new centrifugation method is more reliable, as it is less operator-sensitive. Also, the formation of gases such as CH_4 as the result of heating that can interfere with the noble-gas measurements is avoided. Moreover, the time needed for gas extraction is considerably shorter, as the extrusion/heating procedure ($\sim$ 30 min) is avoided and drying the sample (which contains only water instead of a water/sediment mixture) after extraction is much faster.

Finally, the new experimental protocol is much easier to handle from both an experimental and a conceptual point of view, making it feasible for other laboratories to apply the method. The centrifugation of the bulk sediment samples intended for noble-gas analysis can be accomplished using commercially available equipment.

3.5 Comments and recommendations

Sample containers The available volume in the cylinders of the centrifuge can severely limit the amount of water that can be separated within the copper tubes during centrifugation, which leads to the occurrence of larger overall errors in the noble-gas analysis because of the limited water mass. The use of larger volumes (by increasing the diameter of the copper tube or the capacity of the centrifuge) would overcome this limitation. This might be of key importance in the case of low-porosity sediments.

Centrifuge By using a centrifuge with a higher angular velocity, it might be possible to separate even samples of low porosity into a water phase and a sediment phase. Large centrifuges rotating at 12,000 rpm are available that produce a force about three times that of the centrifuge used in the present work.

In situ noble-gas analysis in aquifers Our method could also easily be applied to bulk sediments from aquifers to determine $^3H - {}^3He$ water ages and atmospheric noble-gas concentrations with the aim of reconstructing past climate conditions. Because groundwaters are commonly sampled by pumping water from an observation well, the resulting forced water flow may follow preferential pathways from the aquifer to the borehole. Such preferential flow will bias the sampling, since the pumped water may not belong to the local groundwater in which the well is embedded under natural flow conditions. Moreover, it is time-consuming and expensive to sample groundwater from specific depths or aquifers using multi-screen ground-water monitoring wells. The adaptation of the sampling technique of Brennwald et al. (2003) to aquifer materials would allow sediments to be acquired from a drilled core. Our experimental protocols also allow the centrifugation method to be applied to aquifer sediments and hence allow the real noble-gas concentrations present in the aquifer at a precise spatial position to be determined. Such exact spatial information is often ultimately needed to validate state-of-the-art numerical ground-water models.

Analysis of other dissolved gases As the most commonly used techniques for sampling other gases dissolved in sediment pore waters (e.g., CH_4, N_2 or CO_2) are subject to experimental artifacts - e.g., degassing during sampling by syringes or peeper plates - reliable, quantitative determination of the concentrations of these gases still poses an experimental challenge. As the physical properties (solubility, diffusivity, etc.) of most common dissolved gas species lie within the range of those of the noble gases, the centrifugation method is expected to allow the determination of their concentrations also.

Chapter 4

Attenuation of noble-gas transport in laminated sediments of the Stockholm Archipelago

Abstract For the first time a sediment core has been sampled at a vertical resolution of $\sim 2\,\mathrm{cm}$ for noble-gas analysis in the sediment pore water. This high-resolution sampling allowed an excess of atmospheric gases to be identified at a sediment depth of 40 cm. Sedimentological evidence indicates that the observed excess is related to a past mass movement that trapped and conserved the gas surplus for more than a century.

The measured noble-gas concentrations support the hypothesis that, depending on the sediment texture or particular structures in the sediment, effective diffusion of noble gases in the pore space can be strongly attenuated compared to molecular diffusion in bulk water. Moreover, the atmospheric noble-gas abundance in the pore water allows the deposition of sediments originally located near the air/water interface to be clearly identified.

4.1 Introduction

Concentrations of dissolved noble gases in the pore water of unconsolidated sediments were shown to agree with the concentrations of noble gases in the overlying water column (Brennwald et al., 2003). In lakes and oceans, dissolved noble-gas concentrations are in general found in atmospheric equilibrium with respect to the temperature (T) and salinity (S) conditions prevailing during the gas/water partitioning at the water surface (Aeschbach-Hertig et al., 1999b). Therefore atmospheric noble gases in the pore water of sediments have been successfully used to reconstruct past physical and environmental conditions in the deep-water bodies of lakes (Brennwald et al., 2004, 2005), whereby changes

Acknowledgments: We want to thank Prof. Per Jonsson and the staff of the Department of Applied Environmental Science at Stockholm University for their great support during the expedition in the Stockholm Archipelago. Thanks are due to Nora Denecke for the pleasant company and support during the preparation and execution of the field work in Sweden. We are grateful for the improvement of the ^{137}Cs and ^{210}Pb dating provided by Marian Fujak. Further, we thank Ryan North for his helpful comments and editing assistance. This research was possible thanks to funding from the Swiss Science Foundation (SNF 200020-109465).

in noble-gas concentrations were interpreted in terms of changes of physical conditions in the water column in response to climate forcing.

The transport of solutes, e.g. noble gases, in the pore space can be described by advection and diffusion in the bulk sediment (Berner, 1975; Imboden, 1975; Strassmann et al., 2005), where the upper boundary condition for the solute transport in the sediment column is given by the concentrations in the overlying water body. Earlier case studies on lacustrine sediments show that past noble-gas concentrations can be conserved for a long time in the pore space without being subject to significant diffusive exchange (Brennwald et al., 2004, 2005; Strassmann et al., 2005; Pitre and Pinti, 2010). The structure of the sediment or boundaries within the sediment seem to strongly attenuate the diffusive exchange in the pore-water. But the mechanistic understanding of the processes that lead to the observed attenuation still remains vague. Former studies focused on sites with low sedimentation rates (< 0.1 mm/year). Until now the published noble-gas data from unconsolidated sediments have a vertical spatial resolution of ≥ 10 cm, which prevented studying noble-gas concentration changes occurring on time scales of decades. Therefore, the sediment age between the neighboring samples was more than a century.

A higher sampling resolution is utterly needed to interpret the temporal evolution of noble-gas concentration signals in the pore water - in particular to assess if and to which extent the concentration profiles are smoothed by diffusive transport.

In this work, we present noble-gas concentrations and isotope ratios measured in 40 sediment samples taken at 23 different sediment depths separated by vertical intervals of about 2 cm from a sediment core taken in the Stockholm Archipelago. The local high sedimentation rate (see section 4.2) and the high-resolution sampling allowed us to characterize the solute transport on a decadal time scale. Our data add further experimental evidence to the possibility pf strong attenuation of effective noble-gas diffusion in the pore space.

4.2 Study site

The Stockholm Archipelago (Sweden, Baltic Sea) constitutes a geomorphological transition zone between the lake-rich land of Scandinavia and the Baltic Sea. In these semi-enclosed bays, the local conditions favor inflow and retention of settling particles, which leads to very high sedimentation rates of several centimeters/year (Meili et al., 2000). The undisturbed sediment accumulation (especially in the deep regions) allows annual varves to form and to reach thicknesses of up to 5 cm (Meili et al., 2000; Persson and Jonsson, 2000).

At the chosen sampling location of 59°20.99'N / 18°27.94'E (36 m water depth), a maximal varve thickness of about 2 cm was found as determined by optical inspection in the uppermost $\sim$ 12 cm of the sediment column. Within the uppermost $\sim$ 15 cm, the sediment is hardly layered and the water content is high due to incomplete compaction (Fig. 4.1).

The extremely high sedimentation rates easily allowed the annual depositions to be distinguished on a macroscopic level (i.e. using the color of the different layers). Therefore, a sedimentological disturbance, i.e. an abrupt change of the appearance (and texture) of the sediment, was clearly visible at a depth of 40 cm in the core. Compared to the laminated structure of the overlying sediment column, the zone below the disturbance is

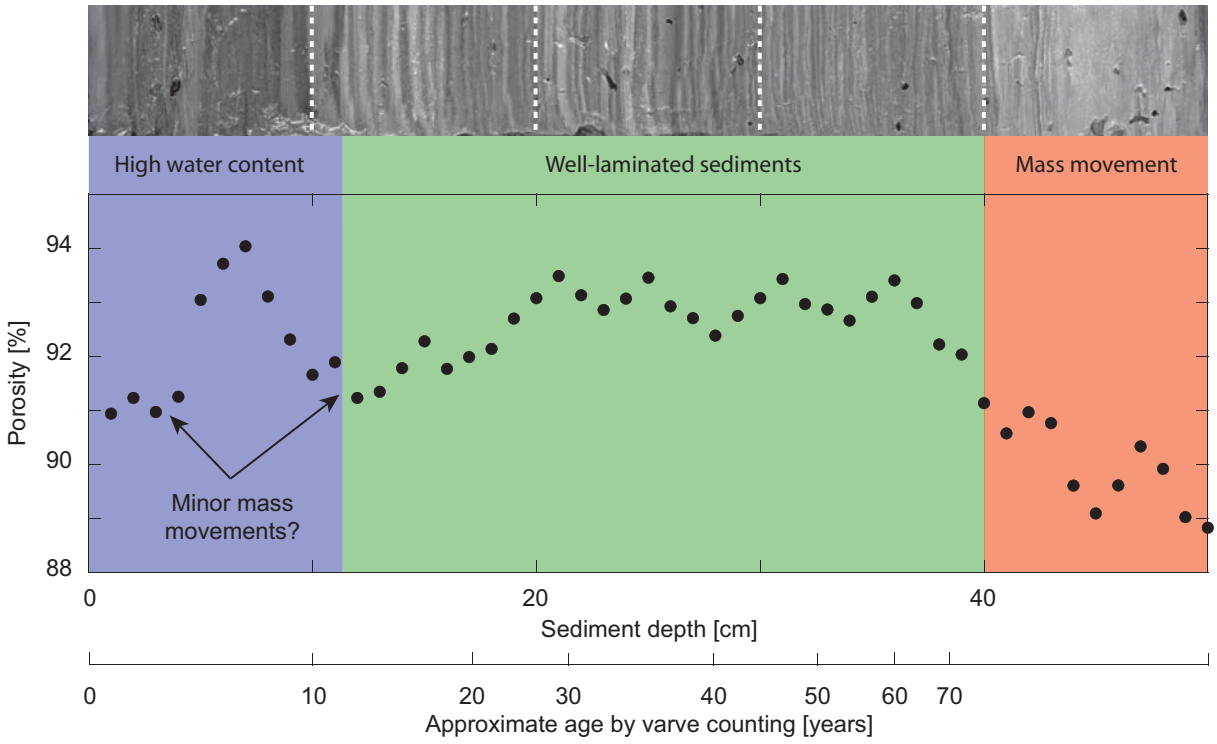

Figure 4.1: Macroscopic structure and porosity profile determined for the sediments at the noble-gas sampling station in the Stockholm Archipelago. In the topmost 12 cm of the sediment (blue shaded area) annual laminations are present, but lamination is not as well defined as in deeper parts of the sediment column. In general, the porosity increases towards the sediment/water interface. Two local porosity minima may indicate minor mass movements. However the porosity in the first 5-6 cm of sediment may be an artifact generated by water loss from the liner during the transport from Sweden to Switzerland. In the middle part of the sediment column (green shaded area) annual laminations can be clearly observed and the porosity is virtually constant. Below 40 cm depth a mass movement is present: the sediment color is lighter, the porosity decreases with depth and no lamination is visible (red shaded area). The age scale is based on optical varve counting which is confirmed by ^{137}Cs and ^{210}Pb dating (see sections 4.3.2 and 4.4.2).

characterized by a lighter color, a more homogeneous texture and lower porosities (see Fig. 4.1). A first estimation of the age of the sediment layers was possible by varve counting (Fig. 4.1), and identified the sedimentological disturbance to be older than 80 years. However, as the laminations in the upper part of the core are not completely undisturbed (e.g. sediment layers without visible lamination), we also used radiometric ^{137}Cs and ^{210}Pb dating to reliably determine the age of deposition of the disturbance (see sections 4.3.2 and 4.4.2).

4.3 Methods

4.3.1 Noble-gas sampling and analysis

A 1.03 m long sediment core taken by a gravity corer was sampled for noble-gas analysis using the method of Brennwald et al. (2003). Bulk sediment was transferred from the plastic liner containing the core into small copper tubes which were air-tight closed with two special metal clamps (Brennwald et al., 2003).

The samples were taken at vertical intervals of about 2 cm. The distance between each sample approaches the geometrical limits of the applied sampling technique (Brennwald et al., 2003). Due to geometrical constraints it is questionable if samples taken in even smaller intervals would belong to the depth where the copper tubes are attached on the liner. In order to fill a larger number of samples/copper tubes, more bulk-sediment volume is required. During the transfer of the sediment into the copper tubes, two pistons, on both sides, push the core material out of the liner. Sediment with higher porosity often flows better out of the core being squeezed. As the uppermost part of the sediment column normally shows a strong porosity gradient (i.e. the porosity decreases with depth), the upper samples tend to be filled with sediment prior to the bottom samples. Therefore, the bottom samples are filled and closed after a certain volume of bulk sediment has already, preferentially, left the plastic liner from the upper part of the sediment core. If this volume exceeds the volume of bulk sediment present between each sampling depth, it is possible that the uncertainty of the effective sampling depth for the bottom samples covers the range of the adjacent samples, i.e. the depth resolution at the lower part of the core is not as adequate as in its upper part. Moreover, as the squeezing procedure can displace the original position of the liner with respect to the frame holding the core with the inserted pistons, a shift in the order of a few millimeters is normal, but can be greater if more sediment volume is needed to flush and fill more samples. Access to the metal clamps ($\sim$ 4 cm width), which need to be tightly closed in order to seal the copper tubes, must also be guaranteed. Removal of the copper tubes from the liner in order to close the clamps is not an option as air contamination of the remaining samples would likely occur.

In total 40 samples from 23 different sampling depths were collected from a single sediment core. During the sampling in the Stockholm Archipelago the observed displacement of the plastic liner with respect to the holding frame during the squeezing procedure was $\sim$ 1 cm. This observation and the calculated amount of sediment volume pushed out of the core to fill the samples yield uncertainties for the acquisition depth of the samples between $\pm$0.5–3.3 cm.

The noble-gas abundances in the pore waters were determined by the extrusion method

of Brennwald et al. (2003) at the Noble Gas Laboratory of the Swiss Federal Institute of Science and Technology (ETH) in Zurich. Technical details about the gas purification line and the mass spectrometric noble-gas determination are described in Beyerle et al. (2000). The applied analytical protocol yields He, Ne, Ar and Kr concentrations with an overall error of 1.2%, and Xe concentrations with a slightly higher error of 1.6% (see Table 4.1).

4.3.2 ^{137}Cs and ^{210}Pb dating and sediment porosity

A second sediment core was recovered at the same location as the core used for noble-gas analysis. This second core was opened and cut vertically into two halves. One half was used to visually inspect the macroscopic structure of the sediment column (e.g. annual lamination and mass movements, see Fig. 4.1). The other half was sampled at vertical intervals of 1 cm for ^{137}Cs and ^{210}Pb dating to determine the age of the sediment (Pennington et al., 1973; Ritchie et al., 1973; Appleby and Oldfield, 1978; Appleby, 2001).

In order to determine the ^{137}Cs and ^{210}Pb activities, the sediment samples were vacuum dried. From the weight difference before and after desiccation, the porosity profile of the sediment column at the sampling site was reconstructed (see Fig. 4.1). We assumed a solid-sediment density of $\sim 2.6\,\mathrm{g/cm^3}$ (quartz) to calculate the porosity. Note that the true porosity may be lower than the calculated values because the sediments at the Stockholm Archipelago are rich in organic matter, which in general shows a lower solid-sediment density. However, this porosity bias does not affect the further interpretation of the porosity profile and the modeling of solute transport.

The porosity is not only a relevant factor which characterizes the transport of dissolved gases in the pore space (see sections 4.3.3 and 4.4.3), but it is also a simple and straightforward parameter to detect structural changes of the sediment matrix. For instance the textural change at 40 cm sediment depth is characterized by a distinct change in porosity and in the water content (see Fig. 4.1).

4.3.3 Diffusion model

A simple diffusion model reflecting the transport equation for nonreactive solutes given in Strassmann et al. (2005) was used to determine the most relevant transport parameters, such as the effective diffusivities, that control the migration of noble gases (and other solutes) in the connected pore space of the sediment column, with the assumption that advective transport generated by sedimentation and compaction is negligible (for more comprehensive modeling see Berner, 1975; Imboden, 1975; Strassmann et al., 2005):

$$\phi \frac{\partial C_i}{\partial t} = \frac{\partial}{\partial z}\left(\phi \cdot D_{\mathrm{eff},i} \frac{\partial C_i}{\partial z}\right) \tag{4.1}$$

$$D_{\mathrm{eff},i} = \frac{\phi}{a} D_{\mathrm{mol},i} \tag{4.2}$$

where C_i is the concentration of the dissolved noble gas i = He, Ne, Ar, Kr, Xe. The effective diffusivity, $D_{\mathrm{eff},i}$, was parametrized by the molecular diffusivity of noble gases in free water, $D_{\mathrm{mol},i}$, and the porosity, ϕ, being scaled by the dimensionless factor a.

Note that in principle the effective diffusivity, $D_{\mathrm{eff},i}$, includes all the possible processes affecting the solute diffusion in the pore space. Therefore, in contrast to many other sediment transport models where parameter a only reflects tortuosity, we use a as a scaling parameter that covers and integrate all processes that may attenuate solute diffusion in the pore water on a macroscopic level. This includes tortuosity, but also solute retention caused by double porous media, sorption or trapping of solutes in dead pores or gas bubbles, or any other unidentified process attenuating (macroscopic) diffusion.

The exclusion of advection from the transport model is reasonable, if the Peclet number $Pe = UL/D_{\mathrm{NG}}$ is small (where U is the sedimentation rate, L is the relevant length scale and D_{NG} is the molecular diffusivity of noble gases, Schwarzenbach et al., 2003). For small Peclet numbers ($Pe < 1$) the overall solute transport is dominated by diffusion. At the sampling site we estimate a sedimentation rate U of 0.5 m/100 years and a relevant length scale L of 0.5 m (see Fig. 4.1) which yields $UL \sim 2.5 \cdot 10^{-3}\,\mathrm{m^2/year}$, which is much smaller than the molecular diffusivity of noble gases ($D_{\mathrm{NG}} > 10^{-2}\,\mathrm{m^2/year}$). Hence setting $Pe < 0.3$ shows that the transport at our site is expected to be mainly of a diffusive nature. A continuous, time-independent function for porosity at different depths was constructed by linear interpolation of the calculated porosity profile (spatial resolution of ~ 1 cm). For sediment depths > 0.5 m a constant porosity of 89% (i.e. the lowest porosity determined in the core) was assumed.

4.4 Results and discussion

4.4.1 Noble-gas profile in the pore water of the sediment column

Table 4.1 lists, for all 40 samples collected in the Stockholm Archipelago, the measured noble-gas concentrations for He, Ne, Ar, Kr and Xe as well as the ^{3}He/^{4}He, ^{20}Ne/^{22}Ne and ^{36}Ar/^{40}Ar ratios and their average experimental errors. The results are plotted in Fig. 4.2 as relative concentrations normalized by the expected concentrations and isotope ratios of air saturated water for local temperature and salinity conditions ($T = 4$°C and $S = 11$ g/kg). Note that the concentration differences in replicate samples taken at the same sediment depth (e.g. at 32, 40, 44, 46 or 48 cm depth) are the result of the strong vertical concentration gradients and the slight vertical offset of the replicates caused by sediment squeezing during sampling.

Upper section of the sediment core Between 0-40 cm depth the concentrations of all atmospheric noble gases (Ne–Xe) approach the expected saturation concentrations and remain more or less constant. The constant noble-gas concentrations being close to the expected equilibrium concentrations indicate undisturbed trapping of water from the sediment/water interface into the sediment pore space (see Brennwald et al., 2003; Strassmann et al., 2005).

The He concentration increases slightly with depth due to accumulation of terrigenic $^{(4)}$He, which is either produced in-situ by radioactive decay of Th and U in the sediment matrix, or is injected from deeper strata (Dyck and Da Silva, 1981; Stephenson et al., 1994; Brennwald, 2004).

Some samples seem to be affected by degassing during sampling. In these samples, the Ne concentrations (see Fig. 4.2, black triangles) are lower ($< 80\%$) than the expected

Table 4.1: Measured concentrations, isotope ratios, concentrations corrected for degassing and average uncertainties for samples from the Stockholm Archipelago. For some samples re-determination of noble gas abundances allowed the exclusion of measurements where air contamination was suspected (these samples are identified by a 5-digit final number). STP = standard temperature (0°C) and pressure (1 atm).

Sample	z (m)	Concentrations (cm^3_{STP}/g)					Isotope ratios			Corrected concentrations (cm^3_{STP}/g)			
		He 10^{-8}	Ne 10^{-7}	Ar 10^{-4}	Kr 10^{-7}	Xe 10^{-8}	$^3He/^4He$ 10^{-6}	$^{20}Ne/^{22}Ne$	$^{36}Ar/^{40}Ar$ 10^{-3}	He 10^{-8}	Ar 10^{-4}	Kr 10^{-7}	Xe 10^{-8}
Saturation concentration		4.49	2.19	4.12	1.00	1.50	(calculated for $T = 4$°C and $S = 11$ g/kg)						
SE,331,2867	0.02	5.81	2.04	4.37	1.06	1.72	1.19	9.76	3.390	6.57	4.55	1.09	1.76
SE,331,2877	0.04	6.54	2.00	4.27	1.04	1.68	1.04	9.79	3.383	7.65	4.50	1.07	1.72
SE,331,28771	0.04	6.51	2.01	4.46	1.10	1.78	1.07	9.78	3.379	7.57	4.69	1.14	1.82
SE,331,28641	0.06	7.24	1.93	4.44	1.09	1.73	1.06	9.79	3.385	8.90	4.77	1.14	1.79
SE,331,2885	0.08	7.15	1.92	4.10	0.98	1.55	0.96	9.82	3.387	8.88	4.42	1.03	1.61
SE,331,28851	0.08	6.98	1.96	4.35	1.07	1.67	1.01	9.76	3.383	8.41	4.64	1.11	1.72
SE,331,2887	0.10	11.6	2.24	4.30	1.01	1.57	0.74	9.79	3.386	11.6	4.30	1.01	1.57
SE,331,28871	0.10	6.63	1.29	3.44	0.91	1.55	0.70	9.78	3.385	11.9	4.33	1.06	1.75
SE,331,28711	0.12	9.10	1.85	4.07	0.98	1.61	0.76	9.77	3.382	11.9	4.47	1.05	1.69
SE,331,2863	0.14	13.0	1.92	4.23	1.04	1.64	0.64	9.79	3.385	16.1	4.56	1.09	1.70
SE,331,28631	0.14	14.8	2.27	4.83	1.18	1.86	0.61	9.81	3.381	14.8	4.83	1.18	1.86
SE,331,2882	0.16	11.1	1.56	3.51	0.90	1.53	0.58	9.76	3.385	17.3	4.15	1.00	1.66
SE,331,28821	0.16	12.7	1.83	4.12	1.02	1.66	0.55	9.80	3.384	16.7	4.54	1.09	1.75
SE,331,2891	0.18	17.5	2.33	4.67	1.11	1.73	0.54	9.83	3.387	17.5	4.67	1.11	1.73
SE,331,28911	0.18	20.3	2.66	5.44	1.30	1.99	0.56	9.80	3.381	20.3	5.44	1.30	1.99
SE,331,2894	0.20	27.4	2.52	5.55	1.37	2.15	0.46	9.83	3.391	27.4	5.55	1.37	2.15
SE,331,2879	0.22	9.33	1.08	2.73	0.74	1.32	0.47	9.81	3.384	18.6	3.61	0.89	1.53
SE,331,28791	0.22	13.3	1.39	3.91	1.07	1.80	0.48	9.81	3.382	22.7	4.81	1.23	2.01
SE,331,2890	0.24	18.2	2.04	4.67	1.20	1.96	0.46	9.81	3.384	20.6	4.87	1.23	2.00
SE,331,28901	0.24	13.7	1.52	3.71	0.98	1.66	0.48	9.82	3.386	21.8	4.42	1.10	1.82
SE,331,2892	0.26	13.6	1.41	3.77	1.03	1.74	0.48	9.85	3.381	23.1	4.62	1.18	1.93
SE,331,28921	0.26	14.7	1.66	3.97	1.05	1.75	0.45	9.80	3.383	21.7	4.58	1.16	1.89
SE,322,2883	0.28	12.8	0.98	2.97	0.87	1.55	0.43	9.83	3.390	26.6	4.01	1.06	1.82
SE,331,28831	0.28	11.4	0.99	2.83	0.80	1.46	0.42	9.81	3.384	23.5	3.81	0.98	1.71
SE,331,28781	0.30	16.0	1.50	3.76	1.00	1.69	0.42	9.78	3.382	25.9	4.52	1.13	1.86
SE,331,2895	0.32	24.5	1.93	4.46	1.19	1.98	0.40	9.81	3.385	30.1	4.79	1.25	2.05
SE,331,28951	0.32	38.9	3.13	6.75	1.72	2.71	0.40	9.82	3.383	38.9	6.75	1.72	2.71
SE,331,2881	0.34	11.1	0.64	2.13	0.66	1.28	0.36	9.86	3.391	26.4	3.08	0.85	1.56
SE,331,28721	0.36	11.6	0.83	2.59	0.77	1.40	0.38	9.85	3.394	25.7	3.60	0.96	1.67
SE,331,2886	0.38	23.8	1.23	3.43	1.01	1.76	0.30	9.86	3.389	44.2	4.38	1.19	2.00
SE,331,2884	0.40	76.0	2.78	7.40	2.11	3.43	0.24	9.84	3.392	76.0	7.40	2.11	3.43
SE,331,28841	0.40	55.5	1.97	5.87	1.72	2.80	0.27	9.85	3.390	66.1	6.24	1.78	2.89
SE,331,2873	0.42	15.7	0.85	2.61	0.78	1.42	0.33	9.88	3.390	34.4	3.62	0.97	1.69
SE,331,28731	0.42	21.2	1.21	3.44	1.01	1.77	0.34	9.85	3.389	39.8	4.41	1.19	2.02
SE,331,2875	0.44	72.5	2.65	7.05	1.95	3.11	0.27	9.86	3.393	72.5	7.05	1.95	3.11
SE,331,28751	0.44	30.6	1.14	3.48	1.05	1.80	0.27	9.87	3.391	59.2	4.54	1.25	2.06
SE,331,2876	0.46	58.7	2.35	5.83	1.62	2.60	0.27	9.85	3.387	58.7	5.83	1.62	2.60
SE,331,28761	0.46	77.6	2.94	7.16	2.00	3.21	0.25	9.88	3.391	77.6	7.16	2.00	3.21
SE,331,2870	0.48	116	4.26	9.08	2.46	3.80	0.27	9.86	3.395	116	9.08	2.46	3.80
SE,331,28701	0.48	186	6.88	14.7	3.93	5.90	0.27	9.87	3.390	186	14.7	3.93	5.90
Average error (%)		1.1	1.2	1.1	1.2	1.6	1.6	0.2	0.1	2.2	1.2	1.2	1.6

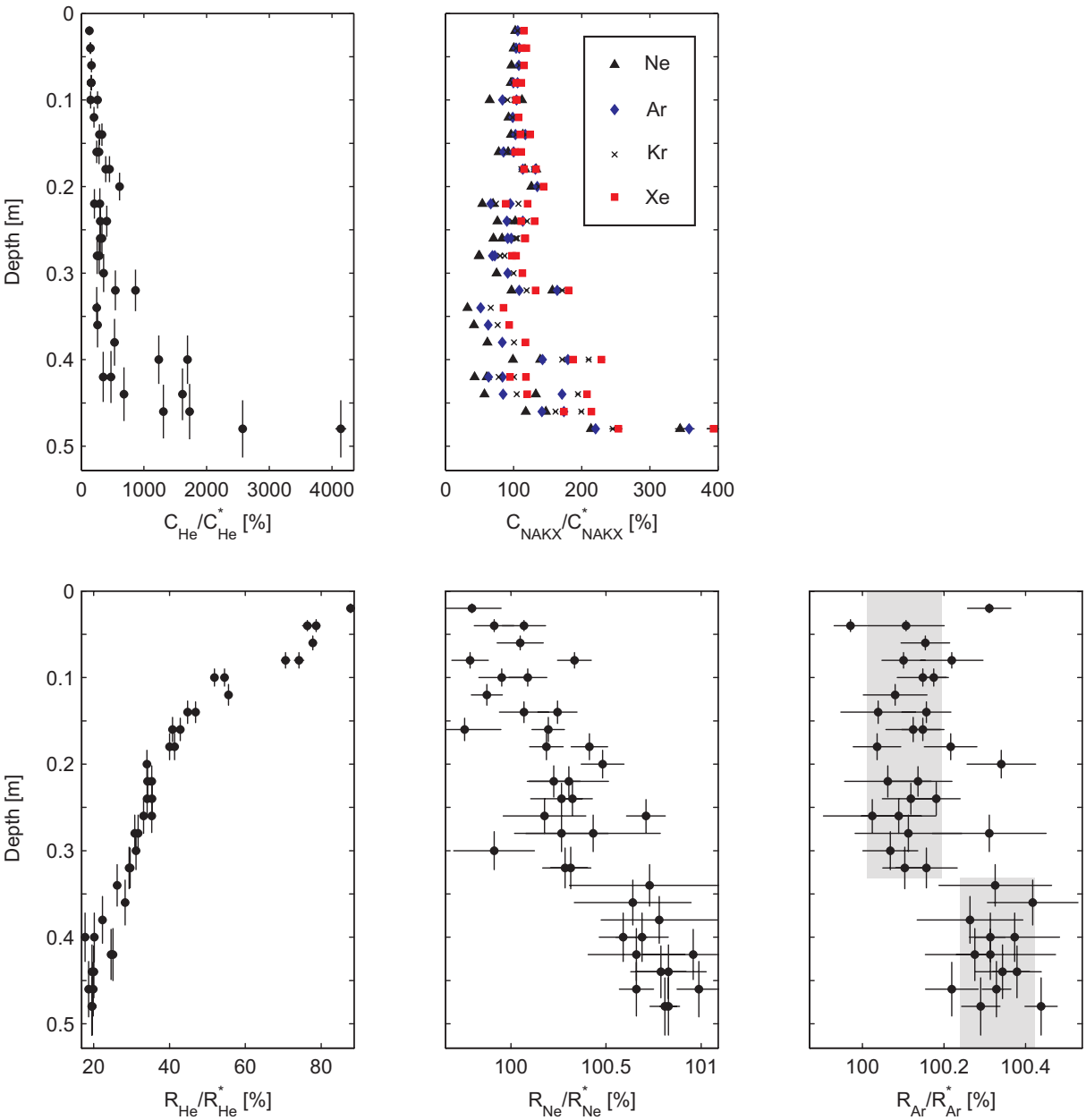

Figure 4.2: Noble-gas concentrations and isotope ratios (^{3}He/^{4}He, ^{20}Ne/^{22}Ne and ^{36}Ar/^{40}Ar) relative to the expected equilibrium values for air saturated water ($T = 4$°C and $S = 11$ g/kg). NAKX = Ne (black triangles), Ar (blue diamonds), Kr (black crosses) and Xe (red squares). Note that the depth uncertainties for the NAKX concentrations are not plotted for clarity, but are the same as for He concentrations. The concentration errors are in general smaller than the plotted symbols (Table 4.1).

saturation concentration. With increasing atomic mass (from Ar to Xe), the deviations of the measured noble-gas concentrations relative to the expected equilibrium concentrations is generally decreasing, as the more soluble gases are less subject to secondary gas exchange (Kipfer et al., 2002; Holzner et al., 2008). This systematic noble-gas depletion pattern is indicative of degassing processes (Brennwald et al., 2003). Again, we note that the samples from the lower part of the sediment core were collected after the ones at the top of the sediment column (see section 4.3.1). Therefore, we assume that the observed degassing occurred during sampling (lasting for more than 30 minutes) due to gas bubbles that formed in the sediment core as a result of the pressure decrease during recovery of the core. However, such degassing processes only lower the measured noble-gas concentrations; from this point of view the concentrations given in Table 4.1 are minimum estimates.

Atmospheric noble-gas excess in the lower part of the sediment core Below 40 cm depth we observed strong concentration fluctuations with large supersaturations of all - atmospheric and non-atmospheric - noble gases. In contrast to the upper part of the sediment column, where the measured concentrations of atmospheric noble gases agree reasonably with the expected equilibrium concentrations, supersaturations of up to 200-400% characterize the sediment in this depth range of the core (see Fig. 4.2). As atmospheric noble gases enter meteoric water only by air/water partitioning, the atmospheric noble-gas surpluses can only be explained by trapping of significant volumes of atmospheric air. In contrast to the supersaturations measured in the pore water by Pitre and Pinti (2010), noble-gas adsorption on sediment particles cannot account for the gas excesses presented in this work.

Firstly, in the case of the noble-gas profile from the Stockholm Archipelago the extent of the observed supersaturations is similar for all atmospheric noble-gas species (i.e. the excess has an atmospheric noble-gas composition). Secondly, as it will be discussed in the next paragraph, Ne and Ar are enriched in light isotopes. Thirdly, the He excesses are one order of magnitude larger than the excesses for Ne, Ar, Kr and Xe. All these facts negate adsorption as the cause of the observed noble-gas surpluses, as adsorption favors in general the enrichment of heavy elements and isotopes (Podosek et al., 1980, 1981; Mamyrin and Tolstikhin, 1984; Ozima and Podosek, 2002).

Due to the presence of atmospheric noble-gas excesses, the textural change at a sediment depth of 40 cm (see Fig. 4.1) is interpreted as the result of a mass movement that originated from near-surface regions (e.g. the shore). The mass movement entrained air that was deposited and trapped in the bulk sediment of the Stockholm Archipelago.

Ne and Ar isotopes The isotope ratio for Ne ($^{20}Ne/^{22}Ne$) and Ar ($^{36}Ar/^{40}Ar$) in the mass movement is higher ($\sim 0.8\%$ and $\sim 0.3\%$, respectively) than in the upper part of the sediment column where the noble-gas concentrations are very similar or agree with the respective atmospheric equilibrium ratios (see Beyerle et al., 2000). The depth at which enrichment of the light ^{20}Ne and ^{36}Ar isotopes occurs (see Fig. 4.2, gray areas), agrees well with the depth of the change in sediment texture (in Fig. 4.1). The slight geometrical offset between the gas anomaly and the textural change may be related to the spatial heterogeneity of the mass movement (i.e. the thickness of the disturbance may be different in space) or to the advective pore-water displacement relative to the sediment matrix due to compaction of the bulk sediment (Imboden, 1975).

Conceptually, the enrichment of the light noble-gas isotopes can be understood as kinetic fractionation during gas/water partitioning which can be described by a Rayleigh process (Holocher et al., 2003; Brennwald et al., 2005; Zhou et al., 2005; Klump et al., 2007, 2008a). At the time of deposition of the mass movement, atmospheric air bubbles were entrained into the moving water/sediment mass. During the descent towards the bottom of the basin, the lighter isotopes fractionated faster into the water phase than the heavier isotopes, because their molecular diffusivity is slightly higher (Rayleigh, 1896).

It appears most reasonable to us that during a turbulent event such as a mass movement, dissolution of entrapped air bubbles is not complete, e.g. some of the air bubbles escape towards the water/air interface. Under such circumstances, a slight light isotope enrichment of the dissolved gas phase can be expected, as the escaping gas bubbles are enriched in heavier isotopes that dissolve at a slower rate during the kinetic gas partitioning process.

He isotopes The He concentrations in the deeper part of the core also significantly exceed the concentrations measured in the upper part of the sediment column close to the sediment/water boundary. In contrast to the other noble gases, which are of purely atmospheric origin, the He excess is one order of magnitude larger.

The ^{3}He/^{4}He isotope ratio in the pore waters is lower than that of air-saturated water (^{3}He/^{4}He $= 1.36 \cdot 10^{-6}$, Weiss, 1970) throughout the entire sediment core, which indicates that isotopically heavy terrigenic He accumulates in the sediment pore water. The isotope ratio of the excess He in the bottom samples (^{3}He/^{4}He $\sim 2.3 \cdot 10^{-7}$) is higher than that determined in the North Sea (^{3}He/^{4}He $\sim 1.45 \cdot 10^{-7}$, Oxburgh et al., 1986). The higher ratios are attributed to the atmospheric He excess originating from the mass movement (^{3}He/^{4}He$_{\mathrm{atm}} > {}^3$He/^{4}He$_{\mathrm{terr}}$). The ^{3}He/^{4}He ratio of terrigenic He can be estimated by subtracting the atmospheric $^{(3,4)}$He excess which can be assumed to be proportional to the Ne excess. Tritiogenic ^{3}He produced by the decay of ^{3}H is negligible, because the concentration of ^{3}He produced by the decay of 5 TU (i.e. the ^{3}H concentration before the nuclear tests in the sixties) is more than one order of magnitude smaller than the measured ^{3}He concentrations. The correction for the atmospheric He excess results in ^{3}He/^{4}He $\sim 1.5 \cdot 10^{-7}$ for the terrigenic He component in the mass movement, which agrees closely with the isotope signature of terrigenic He in the North Sea (Oxburgh et al., 1986).

The presence of large amounts of terrigenic He below 40 cm depth indicates that the sediment overlying the mass movement or the mass movement itself, form a barrier where the effective He diffusivity is considerably lower than in the laminated sediment above. Such "boundary" strongly attenuates the upward migration of solutes emanating from deeper strata and allows terrigenic He to accumulate.

Assuming that the observed Ne degassing is a diffusion-controlled process, the measured He concentrations can be corrected by adding the "degassed" He component, which is proportional to the respective Ne depletion multiplied by a factor $D_{\mathrm{mol,He}}/D_{\mathrm{mol,Ne}}$. The He concentration profile corrected for degassing is shown in Fig. 4.3 and Table 4.1 (where the corrected concentrations for Ar, Kr and Xe are also listed). Compared to the uncorrected data, the corrected He concentration profile is more homogeneous and is less scattered. In particular, the concentrations of samples taken at the same sediment depth tend to be more consistent with each other. Between 0–40 cm depth the corrected He concentration increases linearly with depth ($\partial C_{\mathrm{He}}/\partial z \approx 8.1 \cdot 10^{-9}$ cm^{3}STP/g/cm). From a depth

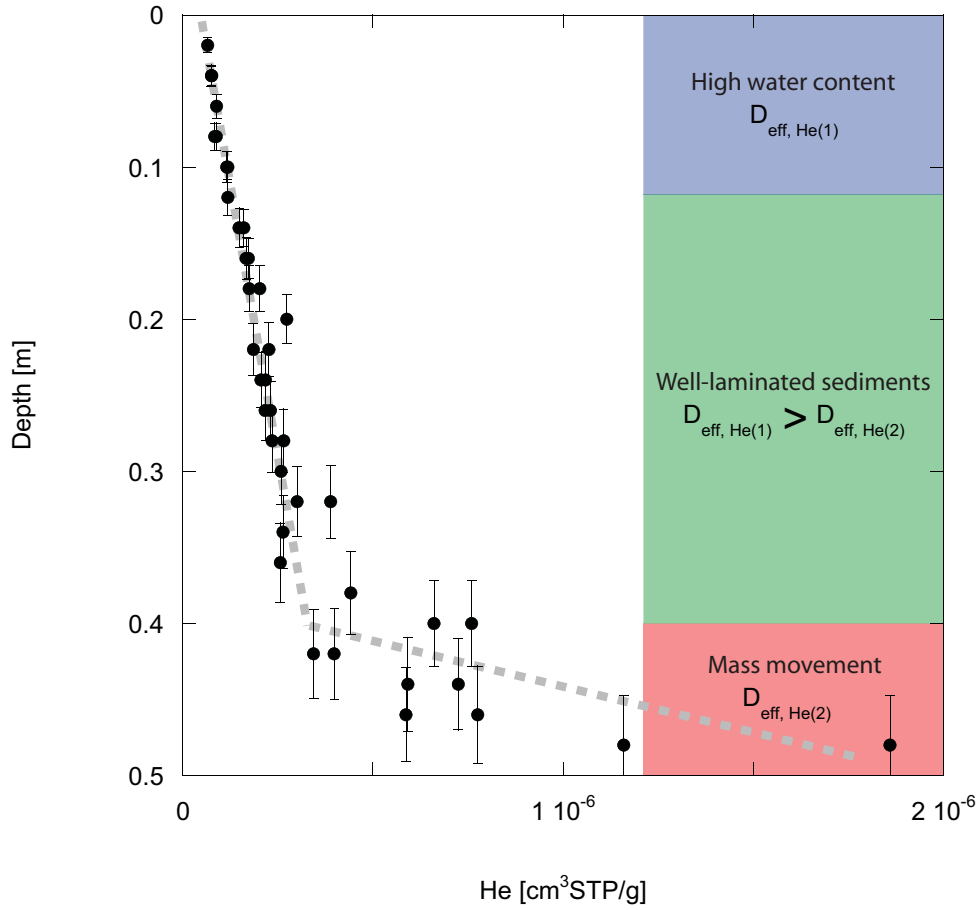

Figure 4.3: He concentration profile corrected for degassing effects. The amount of "degassed" He was calculated from the Ne depletion with respect to the expected atmospheric equilibrium concentration multiplied by a factor $D_{\mathrm{mol,He}}/D_{\mathrm{mol,Ne}}$ (i.e. the degassing process is diffusion-limited). The corrected He profile shows two intervals with different diffusive behavior (i.e. different effective diffusivities, $D_{\mathrm{eff,He(1)}}$ rsp. $D_{\mathrm{eff,He(2)}}$). The colored areas on the right side of the figure correspond to the macroscopic structure and porosity sections of Fig. 4.1.

of 40 cm the He concentration profile is characterized by a much stronger concentration gradient ($\partial C_{\mathrm{He}}/\partial z \approx 95 \cdot 10^{-9}$ cm^{3}STP/g/cm), as already observed in the non-corrected profile. The upward flux of terrigenic He is given by Fick's law ($j_{\mathrm{He}} = -D_{\mathrm{eff,He}} \cdot \partial C_{\mathrm{He}}/\partial z$). Neglecting the in-situ production of terrigenic He by the radioactive decay of U and Th isotopes, the He flux can be considered constant throughout the sediment core. The larger He concentration gradient below 40 cm therefore indicates that the effective He diffusivity is strongly reduced in the mass movement as compared to the sediment above.

4.4.2 Sediment dating and porosity

Dating In order to assess the temporal evolution of dissolved noble gases in the pore water, we dated the sediments using ^{137}Cs and ^{210}Pb. The measured activities for both isotopes and the estimated ages are given in Table 4.2. In the upper part of the core the ^{137}Cs and ^{210}Pb ages tend to agree with each other. In the lower part of the sediment core the ^{210}Pb ages are generally lower than the ^{137}Cs ages - although both ages agree within 25%. The lower ^{210}Pb ages most likely result from uncertainties in the correction of the measured ^{210}Pb activities for the in-situ production of ^{210}Pb in the sediment grains (see Table 4.2).

The two ^{137}Cs activity maxima for 1986 (Tschernobyl) and 1960 (atomic bomb tests) are found within the sampled depth range at 12 cm and 24 cm. The ^{137}Cs activities (Fig. 4.4) are highly compatible with the varve chronology. Therefore we used ^{137}Cs results as a rough estimate for the sedimentation history.

By linearly extrapolating the sediment age-depth relation defined by the ^{137}Cs peaks corresponding to 1986 and 1960, the age of the mass movement is estimated to be older than 80 years (which is in coarse agreement with the ^{210}Pb dating). As compaction is affecting the lower part of the well-laminated section of the sediment (i.e. the sediment age is higher than estimated from the sedimentation rate in the upper part of the core, see Fig. 4.1), we assumed for modeling purposes that the mass movement was deposited $\sim$ 100 years ago (which also agrees reasonably well with the age determined by varve counting, see Fig. 4.1).

Porosity Three different sections can be distinguished in the porosity profile (see Fig. 4.1): a high water-content section at the top of the analyzed sediment column, a constant porosity section related to well-laminated sediments, and a section of decreasing porosity in proximity of the depth range of the mass movement.

The water content in the upper 12 cm (first section, blue) reaches 94%, but the section also contains two local minima at $\sim$ 4 cm and at $\sim$ 12 cm. The first minimum is most probably the result of water loss from the sediment core during transportation from Sweden to Switzerland (confirmed by the presence of water at the bottom of the expedition containers). The second minimum seems to be related to the stepwise change in the measured ^{3}He/^{4}He ratio profile at about the same depth (see Fig. 4.2). The change in the shape of the porosity and ^{3}He/^{4}He profiles over this depth range supports the hypothesis that a slight difference in solute transport properties of the pore space may be present at the interface of the first and the second section.

Table 4.2: Measured ^{137}Cs and ^{210}Pb activities, ^{210}Pb activities corrected for in-situ production ($^{210}Pb_u$) and estimated sediment age. The two ^{137}Cs activity peaks for Tschernobyl (1986) and the nuclear bomb tests in the sixties are indicated by bold fonts.

z (m)	^{137}Cs (Bq/kg)	^{210}Pb (Bq/kg)	$^{210}Pb_u$ (Bq/kg)	^{137}Cs age (a)	^{210}Pb age (a)
0.01	429±48	276±34	223±24	1	2
0.02	520±60	309±50	267±36	3	3
0.03	568±69	287±70	240±50	4	5
0.04	607±70	222±47	194±33	6	6
0.06	645±78	278±76	221±55	10	9
0.07	596±69	280±55	246±39	11	11
0.08	678±77	222±44	177±31	13	13
0.09	596±69	280±55	246±39	15	14
0.10	806±92	210±49	157±35	17	16
0.11	906±103	212±50	156±35	18	17
0.12	731±84	158±40	111±29	**19**	19
0.13	887±100	183±38	142±27	21	20
0.14	524±60	152±38	111±27	23	22
0.15	180±23	148±42	112±30	26	23
0.16	123±16	156±41	112±29	28	25
0.17	117±15	200±39	149±28	30	27
0.18	103±14	179±43	135±31	32	28
0.19	74±10	165±33	126±24	34	30
0.20	77±16	203±65	160±47	36	31
0.21	70±8	151±25		39	33
0.22	62±18	152±85	122±62	41	34
0.23	77±14	153±56	115±41	43	36
0.24	102±21	137±63	122±46	**45**	38
0.25	69±24			47	39
0.26	52±7	161±44	115±32	49	41
0.28	25±11	120±103	85±74	54	44
0.29	21±5	139±38	91±27	56	45
0.32		182±62	134±45	62	50
0.33		136±56	58±40	65	52
0.34		160±47	98±34	67	53
0.36		120±56	61±41	71	56
0.40		178±53	94±38	80	63
0.42		93±52	9±37	84	66
0.44		103±46		88	69
0.46		124±51	38±37	93	72
0.48		120±41	30±30	97	75
0.50		125±48	59±35	101	78

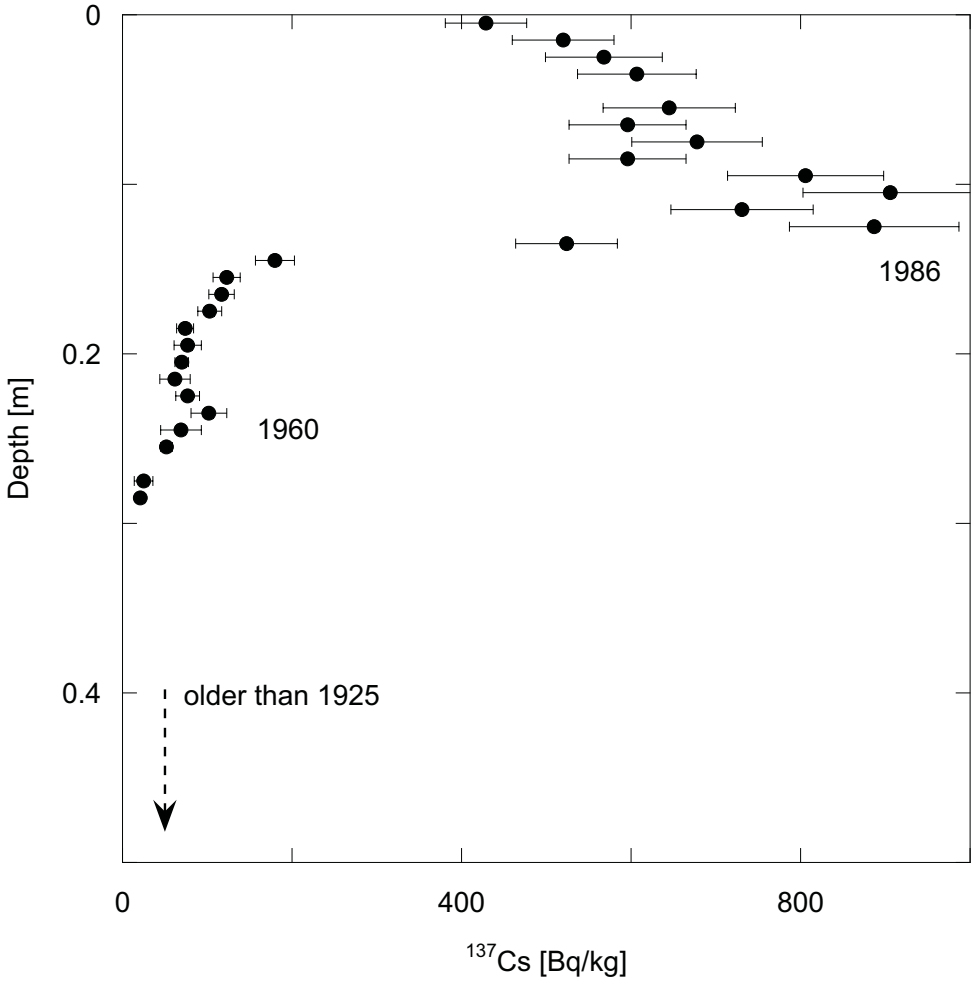

Figure 4.4: ^{137}Cs activity measurements from a second core taken at the same position as the one for noble-gas analysis. ^{137}Cs activity peaks for Tschernobyl (1986) and the nuclear tests in the sixties are well identified at depths of 12 cm and 24 cm, respectively.

4.4.3 Modeling of the noble-gas concentrations in the sediment column

In order to assess the solute transport within the sediment column by physical/numerical modeling, in the uppermost 40 cm of the sediment column the initial noble-gas concentration profile was set to atmospheric equilibrium with respect to the local temperature and salinity conditions ($T = 4$℃, $S = 11\,\mathrm{g/kg}$). Below 40 cm depth the atmospheric noble-gas concentrations in the mass movement were set to 300% of the expected saturation concentrations (see Fig. 4.5, gray dotted line), which approximately corresponds to the average concentration measured in the two deepest samples.

At the upper boundary, located at the water/sediment interface, atmospheric equilibrium concentrations were held constant for the entire simulation. At the lower boundary, immediately below the sedimentological intrusion, a constant concentration of 300% of the saturation was set.

As shown before, the solute transport for the given conditions is mainly driven by diffusion, whereas any advective component can be neglected.

The relevant time span for the simulation of the diffusive transport of solutes in the pore space was approximated from the ^{137}Cs dating and set to 100 years, which roughly corresponds to the estimated age of the mass movement.

In order to fit the model parameter for diffusivity attenuation a to the measured concentration data, a standard least squares method was chosen. As discussed above, Xe is less affected by degassing than the other lighter noble gases (see Fig. 4.2) and the measured concentrations in the upper part of the core agree with the expected equilibrium concentrations. Therefore we chose Xe as the target of our modeling exercise. In Fig. 4.5 the measured and the corrected Xe concentrations are compared. In general the measured Xe concentration profile hardly deviates from the one corrected for degassing. The use of corrected concentrations therefore cannot significantly improve the fit of a. Hence, we decided to use the Xe measurements without any correction for degassing as a reference concentration profile for the least squares fitting process to determine the effective diffusivity.

The modeling results show that the measured supersaturations just above and below the upper boundary of the mass movement in a depth range of $\sim 35 - 45$ cm can only be reasonably reproduced within the respective depth interval if the effective diffusivity is strongly attenuated (see Fig. 4.5). The attenuation parameter a in equation 4.2 needs be set to a value of ~ 1000 (Fig. 4.5, red line) to adequately maintain the sharp concentration increase at a depth of 40 cm, with a depth interval of about 15 cm (40–25 cm depth) for the simulated time period of 100 years. Such attenuation of the effective diffusivity indicates that noble gases from the mass movement only moved a few centimeters over 100 years within the pore space. Although caution needs to be exercised in drawing final conclusions, we reason, both from the experimental data and the modeling exercise, that the effective diffusivity, $D_{\mathrm{eff},i}$, near the mass movement is about three orders of magnitude smaller than the diffusivity of Xe in bulk water ($D_{\mathrm{mol,Xe}} \sim 7.8 \cdot 10^{-10}\,\mathrm{m^2/s}$).

A simpler approach to estimate the effective diffusivity can also be done by dimensional scaling using the relation $L = \sqrt{2 D_{\mathrm{eff}} t}$ with a characteristical diffusion path $L = 0.15\,\mathrm{m}$ (see Fig. 4.5) and a typical time span of $t = 100$ years. This rough approximation leads to $D_{\mathrm{eff}} = 3.6 \cdot 10^{-12}\,\mathrm{m^2/s}$, which is also about three orders of magnitude smaller than

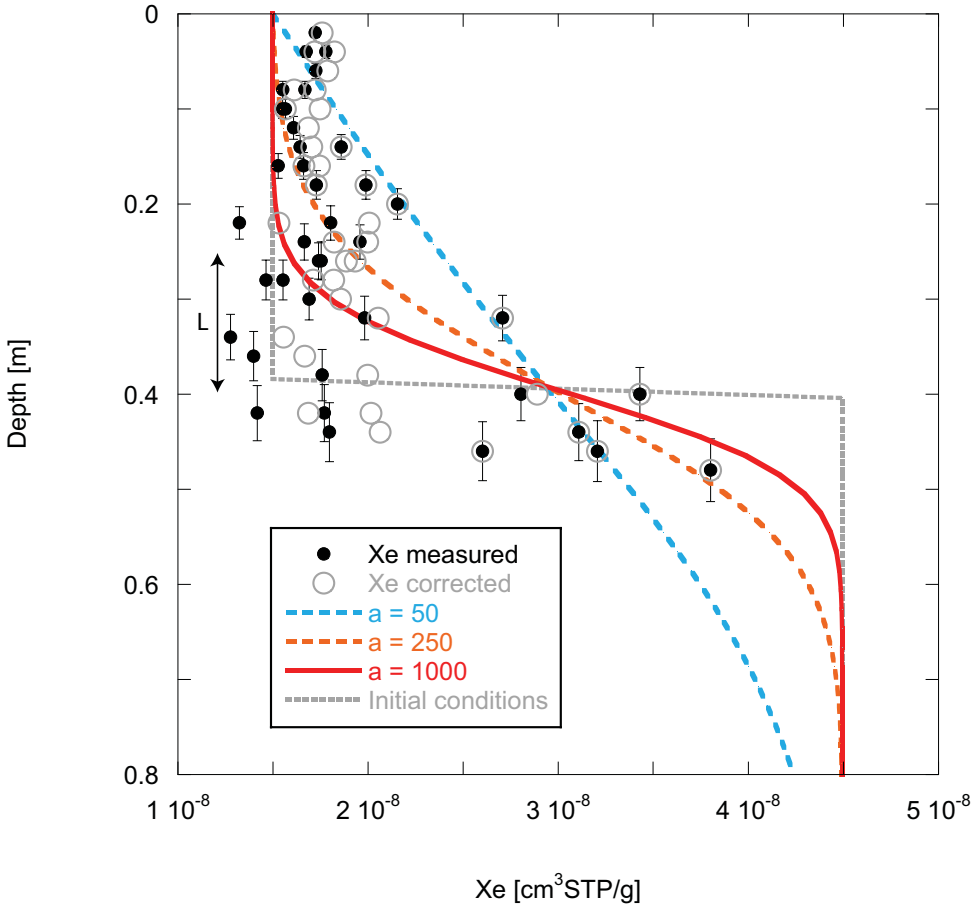

Figure 4.5: Results for the diffusion model applied on an initial steplike Xe concentration profile (300% saturation below 40 cm depth). The simulation time span (t) was set to 100 years and different values for a (the parameter for attenuation of diffusion, see equation 4.2) were used. The results of the numerical simulation were also compared with an estimate of the effective diffusivity, D_{eff}, from the relation $L = \sqrt{2D_{\text{eff}}t}$ with $L = 0.15$ m. Modeling the degassing-corrected concentrations of He and Ne would result in an even stronger diffusive transport suppression (not shown). The Xe concentrations corrected for possible degassing effects are shown as gray circles. As Xe is a large gas species, it is rather soluble. Therefore the differences between the corrected and the uncorrected Xe concentrations are small and do not significantly influence our modeling exercise and the respective results.

molecular diffusivity of Xe in bulk water (i.e. $D_{\text{eff}} \sim 4.6 \cdot 10^{-3} \times D_{\text{mol,Xe}}$).

Consequently, our finding shows that the sediment structure, e.g. the observed mass movement, may significantly attenuate the effective diffusive exchange of solutes in the pore space of unconsolidated sediments even if the sediments have relatively high porosities (see also Brennwald et al., 2004; Strassmann et al., 2005; Pitre and Pinti, 2010). Our results provide evidence that such horizontal barriers are effective in suppressing apparently diffusive transport which may even become virtually negligible, and might limit the solute exchange within the pore space over centuries, or even longer time scales.

The numerical modeling, the dimensional scaling, and the He emanation all agree that the effective diffusivity in the pore space is strongly attenuated in the mass movement.

Such low-diffusive behavior lets us speculate that a "closed" (or "separated") pore space has to be present in the sediment column where virtually no macroscopic diffusion (or any gas exchange) alters the stored concentration signals over time. The observed lower porosity near the mass movement ($\sim 5\%$ lower compared to the overlying sediment column, Fig. 4.1) seems to be indicative of a sediment-controlled diffusion barrier. From this point of view, the role of porosity as a mechanistic control of the effective diffusivity may be largely underestimated in our simple diffusion model, where the scaling of the effective diffusivity is mainly done by the trimming of the attenuation factor a. For future modeling it may be of interest to express the attenuation of diffusivity, paying more attention to changes in the sediment texture.

However, it does not seem physically realistic to justify the observed attenuation of effective diffusivity only by considering diffusion in the pore water phase of the sediments, as our study implies an attenuation of the effective diffusivity 1000 times larger than the attenuation of diffusion by "tortuosity effects" presented by other surveys (see e.g. Boudreau, 1986; Maerki et al., 2004). To conceptually explain the observed strong attenuation of the solute transport into the sediment pore space we offer the following hypothesis which takes in account all observational (noble-gas) evidence, i.e. a mass movement from the air/water interface which embedded significant amounts of air (bubbles). The presence of gas bubbles trapped in the sediment body of the Stockholm Archipelago might explain the strong attenuation of effective diffusivity. Such a gas phase would limit the transport of noble gases in the pore space by constraining the effective noble-gas exchange to the gas exchange through the molecular boundary between non-mobile gas bubbles and stagnant pore water. However, this poses the question whether gas bubbles are expected to exist within the sediment matrix. The observed Xe supersaturation of 200% ($3 \cdot 10^{-8}\,\text{cm}^3\text{STP/g}$) translates to the incorporation of $0.34\,\text{cm}^3\text{STP/g}$ of unfractionated air per gram of water. Due to the hydrostatic load of the water column, the total pressure at the water/sediment interface at 36 m is 4.6 times higher than the atmospheric pressure at the water surface ($\sim 1\,\text{atm}$). The in-situ gas volume in the sediment per unit mass of pore water is therefore about $7.3 \cdot 10^{-2}\,\text{cm}^3\text{/g}$. To dissolve this amount of air ($N_2 \sim 0.27\,\text{cm}^3\text{STP/g}$) completely, a pressure of about 13 atm is needed which exceeds the total pressure at the sampling site by more than a factor of 2.5. In conclusion, the buried air in the mass movement does not dissolve completely but also remains in the form of gas bubbles that are trapped within the sediment matrix.

The presence of gas bubbles in the sediment implies the trapping of noble gases in these bubbles. Because the noble gases are poorly soluble, only a very small fraction of the noble gases will be dissolved in the pore water, where the solute diffusion occurs. The much

larger noble-gas fraction trapped in the stationary gas bubbles would not be available for diffusion in the pore space on a macroscopic level. The presence of gas bubbles in the sediment is therefore consistent with the very strong attenuation of effective noble-gas diffusivity in the sediment. However, the nature of the processes that keep air bubbles trapped in the sediment remains unknown. The same mechanism might also be involved in the strong noble-gas diffusion attenuation observed in other sediments (e.g. Brennwald et al., 2004, 2005; Pitre and Pinti, 2010).

As the Peclet number, Pe, calculated using the effective diffusivity determined for the sediments of the Stockholm Archipelago, is three orders of magnitude larger than the one resulting using molecular diffusivities in bulk water. Due to the massive attenuation of diffusive transport, advection (i.e. sediment burial and pore-water displacement due to sediment compaction) is the dominant transport mechanism affecting the observed noble-gas profiles.

4.5 Conclusions

Our results demonstrate that dissolved noble-gas supersaturations generated by a single mass movement in the past can be stored as a "steplike" concentration feature for more than 100 years within the pore waters of the sediment column. The mass movement or the gas bubbles induced by the mass movement in the sediments seem to restrict the diffusive transport in the pore space to a few centimeters over a century and, hence, reduce the effective diffusivities by at least three orders of magnitude compared to diffusivity in bulk water. Such suppression of diffusion lets us also speculate that a part of the dissolved gases is trapped in "closed" pores or separate structures that are not connected with the open pore space and therefore are not part of the diffusive-transport domain of the pore water where solutes can be diffusively exchanged.

The observed degassing phenomenon precludes further in-depth investigations of the origins of the measured excesses and the mechanisms responsible for the observed isotopic fractionation, which leads to the distinct enrichment of light Ne and Ar isotopes near the mass movement below $\sim$ 40 cm depth. However, the observed enrichment of light gas isotopes indicates that some kind of kinetic process has to control the gas dissolution in response to the formation of the mass movement.

The observed degassing during sampling can only be overcome by much faster sampling techniques which are currently not available. An adaptation of the standard sampling technique by Brennwald et al. (2003) is needed in order to shorten the time necessary for high-resolution sampling in organic-rich sediments with high porosities.

Our results add further evidence to the observation that certain types of sediment can conserve noble-gas concentrations for a very long time, as the diffusive exchange is massively attenuated (Brennwald et al., 2004; Strassmann et al., 2005). This therefore illustrates the usefulness of sediments as noble-gas archives for reconstruction of palaeoenvironmental conditions using similar approaches as with dissolved noble-gas concentrations in groundwaters.

Even if the details of the mechanisms resulting in the unexpectedly strong attenuation of effective noble-gas diffusion in the pore space could not be resolved in this study, our results suggest that the attenuation of effective diffusivity is related to the textural and formational properties of the sediment. The structural differences between the varved

sediments and the mass-flow deposit are directly related to concentrations and the isotopic signature of the dissolved noble gases in the pore water. The strong attenuation of effective diffusivity seems not to result from the tortuosity of the sediment matrix alone, because the extent of the compaction and cementation of the sediment resulting in a tortuosity corresponding to the observed value of the diffusion scaling factor, $a \sim 10^3$, would be expected to require considerably more time (several millennia) than the age of the sediment studied here (a few decades). Therefore, an as-yet unidentified process seems to be responsible for the unexpectedly strong diffusion attenuation. While the trapping of noble gases in stationary gas bubbles is conceptually consistent with our data, further work aimed at the microscopic processes is required to fully elucidate the mechanisms resulting in the strong attenuation of effective noble-gas diffusivity in the pore space on a macroscopic level as it has been done successfully in groudwater to understand the formation of excess air in porous media (Holocher et al., 2003; Klump et al., 2007, 2008a).

Last but not least, the observed noble-gas excess allows the origin of the harboring sediment mass to be identified near the air/water interface as the noble-gas surplus has to stem from the atmosphere. Hence, atmospheric noble gases have the potential to identify mass movements being released from shallow water depths.

Chapter 5

Spatial distribution of helium in the sediments of Lake Van (Turkey)

Abstract In this study, the largest ever carried out to measure noble gases in the pore water of unconsolidated sediments in lakes, the emission of He from the sediments of Lake Van was successfully mapped on the local scale. The main input of He to the water body occurs at the borders of a deep basin submerged in the lake, which is probably the remains of a collapsed caldera. The $^3He/^4He$ ratio identifies the He injected into Lake Van as a mixture of He released from a depleted mantle source and radiogenic He most probably produced in the sediment column ($^3He/^4He \sim 2.2 \cdot 10^{-6}$). Two distinct isotopic compositions can be distinguished in the He emitted into the lake, one of which characterizes the shallow water and the other the deep water. However, both of these are related to the same source of terrigenic He. These new findings provide direct experimental evidence that the release of He from the solid earth is highly spatially heterogeneous on local and regional scales. Moreover, the signature of the He that emanates into the water column of Lake Van is strongly affected by the mixing conditions prevailing in the overlying water body. This fact misled previous studies to interpret the terrigenic He in Lake Van as being only of depleted mantle origin ($^3He/^4He \sim 10^{-5}$).

5.1 Introduction

5.1.1 Global He emission

Geochemical quantification of the release of helium from the solid earth is based mainly on the radiogenic heat budget of the planet, which is governed predominantly by the radioactive decay of ^{40}K to ^{40}Ar, and of ^{232}Th, ^{235}U, and ^{238}U to ^4He. Three distinct $^3He/^4He$ isotope ratios for primordial He from meteorites ($\sim 10^{-4}$), atmospheric He ($1.4 \cdot 10^{-6}$)

Acknowledgments: We thank Aysegül Feray Meydan, Ismet Meydan, Münip Kanan, Mete Orhan, Mehmet Sahin, Dr. Mustafa Karabiyikoğlu, Prof. Dr. Sefer Örçen and the staff of Yüzüncü Yıl University in Van for their invaluable support during the Lake Van expeditions over the last few years. Thanks are also due to Frank Peeters, Heike Kaden and Andrea Huber of the University of Konstanz, and to Mike Sturm, Thomas Kulbe, Flavio Anselmetti and Mona Stockhecke of the Sedimentology Group at Eawag for their pleasant company during the field work on Lake Van. Further, we thank Ryan North and David M. Livingstone for their helpful comments and editing assistance. This work was funded by the Swiss Science Foundation (SNF 200020-109465).

and radiogenic He (with ^{3}He from an α-induced nuclear reaction involving ^{6}Li leading to $^3\mathrm{He}/^4\mathrm{He} \sim 10^{-8}$: see Morrison and Pine, 1955; Mamyrin and Tolstikhin, 1984) are considered to model He emission on a global scale (O'Nions and Oxburgh, 1983). The atmospheric He composition is interpreted as the result of the steady state between production and emission from the solid earth, and loss from the atmosphere to interplanetary space. The $^3\mathrm{He}/^4\mathrm{He}$ ratio (and the He abundance) in the atmosphere therefore sets an upper boundary when quantifying the He fluxes both from the oceans and from the continents.

5.1.2 Experimental quantification of the He fluxes

The flux of He from the upper mantle into the oceans ($3 \cdot 10^9\,\mathrm{atoms} \cdot \mathrm{m}^{-2}\mathrm{s}^{-1}$) was estimated by Craig et al. (1975) from ^{3}He surpluses (with respect to the expected atmospheric equilibrium concentrations) determined on the East Pacific Rise. However, until now only very few direct measurements have been available to assess He release from the continents, which in theory are responsible for most of the terrestrial He release (Mamyrin and Tolstikhin, 1984; Ballentine et al., 2002).

Various studies during the past few decades have tried to quantify continental He emission based on noble-gas and He concentrations i) in ground waters (Andrews et al., 1985; Torgersen and Clarke, 1985; Martel et al., 1989; Stute et al., 1992; Marty et al., 1993; Pinti and Marty, 1995; Tolstikhin et al., 1996; Pinti et al., 1997; Castro et al., 1998a,b); ii) in crater lakes (Sano et al., 1990; Collier et al., 1991; Igarashi et al., 1992; Kipfer et al., 1994; Aeschbach-Hertig et al., 1996b, 1999a, 2002) and other lakes (Aeschbach-Hertig et al., 1996a; Hohmann et al., 1998; Peeters et al., 2000; Kipfer et al., 2002); and iii) in gas wells (Sano et al., 1986). A major constraint in calculating the He fluxes is given by the average renewal rates of lake bottom water and groundwater, and by the residence time of gas in gas wells. These turn out to be notoriously difficult to determine. Moreover, the often-found spatial and temporal heterogeneity in the He emission severely limits its determination. As a result, data-based studies that directly determine He emission on a local scale still remain scarce.

Although the earth's global He budget is understood conceptually, a mechanistic understanding of local-scale continental He emission is still lacking. Various observations suggest that He emission is focused on particular geological structures within the crust, and is related to tectonic activity in extension zones, fault zones, calderas, and volcanoes (Mamyrin and Tolstikhin, 1984; Oxburgh et al., 1986; Oxburgh and O'Nions, 1987; Ballentine and Burnard, 2002). These observations form the basis of the common assumption that the release of He from the continents into the atmosphere is highly variable in space and time (on long time-scales). However, the fast mixing processes that occur both in air and in water commonly prevent the atmosphere and hydrosphere from recording and tracking the specific points of terrestrial He release. Up until now, therefore, there has been hardly any direct evidence that would allow determination of the spatial variability of He emission on regional and local scales (i.e., a few kilometers or less).

5.1.3 Using lacustrine sediments to assess He release

Lacustrine sediments represent an ideal geochemical environment for assessing local He emission, thus, in principle, allowing fluid transport in the uppermost part of the continental crust to be studied. The transport of He within the sediment column can be described by advection and molecular diffusion, where He migrates through the connected pore water space of the sediment (Berner, 1975; Imboden, 1975; Strassmann et al., 2005). As a porous medium, lacustrine sediments suppress the strong horizontal (and vertical) transport (e.g., turbulent diffusion) which dominates in the overlying bulk water (Lerman et al., 1995; Schwarzenbach et al., 2003). In contrast to the bulk water, lacustrine sediments are therefore in principle able to record and store the spatial signals of the local He emission. From this conceptual point of view, lake sediments are very suitable for analyzing the variability of the He flux on spatial scales smaller than the diameter of the lake being studied.

In this work we present ^{3}He, ^{4}He, ^{20}Ne and ^{3}H concentration data measured in the pore water of the sediments of Lake Van (Turkey) between 2004 and 2007.

Lake Van represents an ideal study site to observe and characterize the terrestrial He flux from the earths crust and mantle. The release of He into the lake seems to be under the control of certain geological and tectonic features, such as fault lines and volcanic activity (Degens et al., 1984; Şaroğlu et al., 1992). The lake is known to accumulate terrigenic He from a depleted mantle source (Kipfer et al., 1994; Kaden et al., 2005, 2006, 2010).

In order to study the He release and to quantify the terrestrial He emission, we determined the solute transport in the sediments (e.g., the effective diffusivity in the pore space) by analyzing the vertical distribution of ^{3}H in the sediment column (see Strassmann et al., 2005). Based on the vertical concentration gradients of He within the sediment column and the calculated effective diffusivity, local He fluxes were estimated at the geographical positions of the cores within the lake basin.

This data set allows, for the first time ever, the heterogeneity of He release to be assessed on a spatial scale that is characteristic of the basin and morphology of the lake being investigated (for the bathymetry of Lake Van see: Seyir Hidrografi ve Oşinografi Dairesi, 1990). The He data from Lake Van yield insights into the transport of crustal and mantle-derived fluids in a region that is continental, but seismically and volcanically active.

5.2 Methods

5.2.1 Study site - Lake Van

Lake Van, the largest soda lake on earth, is located in a tectonically active region of eastern Anatolia (Turkey) at ~ 1650 m a.s.l. (Fig. 5.1). The lake has a maximum depth of 457 m, a surface area of $\sim 3600\,\mathrm{km}^2$, and a total water volume of $\sim 606\,\mathrm{km}^3$. Lake Van (Van Gölü in Turkish, Behra Wanê in Kurdish or Vana litč in Armenian) is the third largest terminal lake on earth, which, in combination with the volcanic environment, explains its high salinity (22 g/kg) and exceptionally high pH (~ 10) (Kempe et al., 1991; Kipfer et al., 1994).

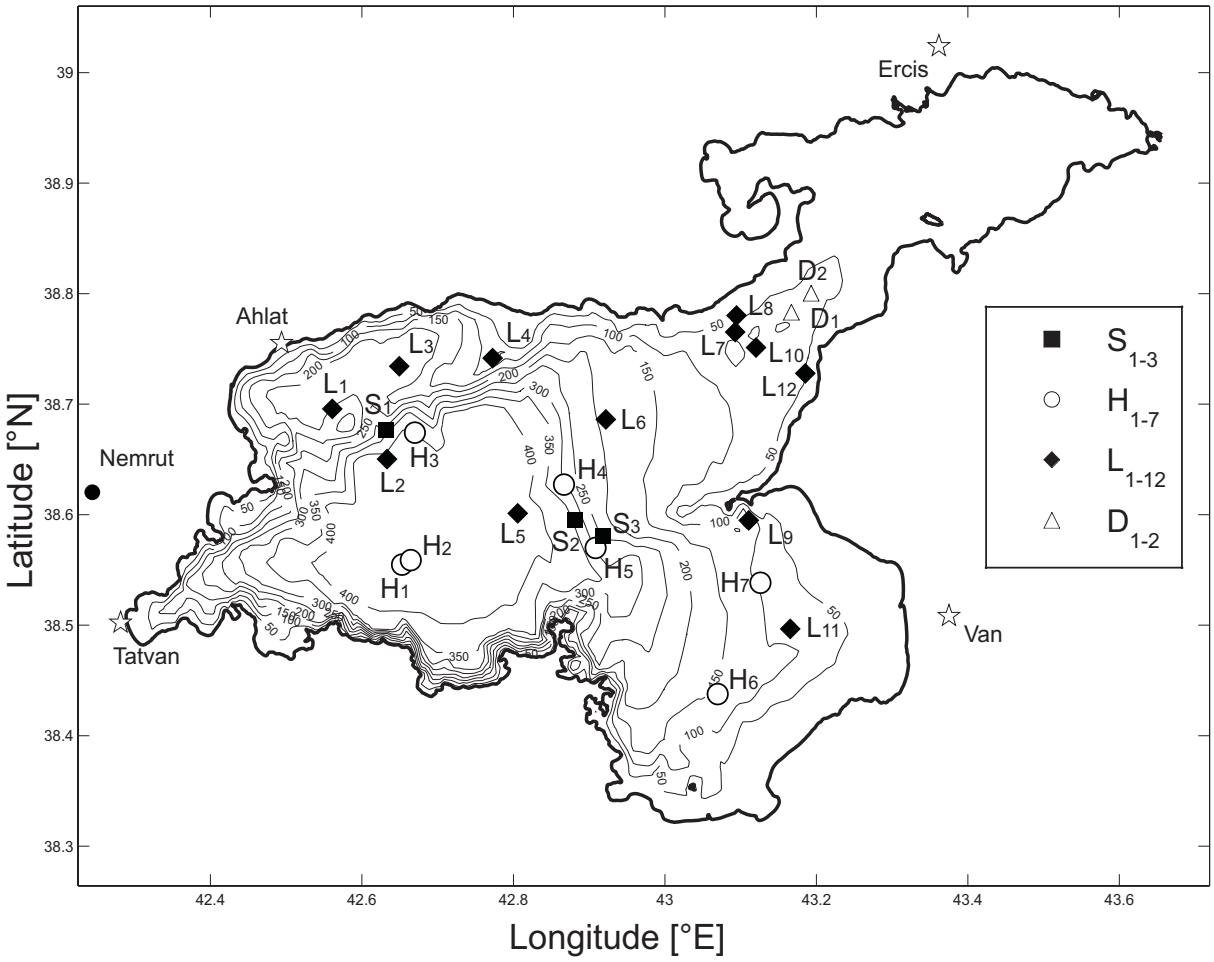

Figure 5.1: Bathymetry of Lake Van (Seyir Hidrografi ve Oşinografi Dairesi, 1990) and the location of the sampling stations. "Low-gradient" (L-cores), solid diamonds; "high-gradient" (H-cores), empty circles; "hot-spots" (S-cores), solid squares. The major cities of Van, Tatvan, Ahlat and Erciş are shown as stars and the Nemrut crater lake as a solid dot.

The sediments of Lake Van are annually laminated (Lemcke, 1996; Landmann et al., 1996) and have porosities of between 60% and 90% in the uppermost few meters. The uppermost 2 m are characterized by dark-brownish varved clays. Because of its very well preserved varves, Lake Van is of prime importance for paleoenvironmental research in eastern Anatolia (Lemcke, 1996; Landmann et al., 1996; Wick et al., 2003; Litt et al., 2009). The lake reacts very sensitively to changes in climate: changes in the precipitation regime, for instance, induce strong lake-level fluctuations (Kadıoğlu et al., 1997; Kılınçaslan, 2000; Kaden et al., 2005, 2006, 2010). The finely varved sediments therefore have the potential to store information related to past environmental conditions prevailing in the surrounding region over several 100 ka (Litt et al., 2009). Moreover, Lake Van and its catchment are located at an important cultural crossroads that has been influenced by more than 3000 years of human cultural evolution (Previté-Orton, 1971; Lang, 1980; Salvini, 1995; Chahin, 2001; Salvini, 2005). The sediments of the lake may therefore hold the key that would allow the rise of mankind in this "cradle of civilization" to be studied (Wick et al., 2003; Litt et al., 2009)

Until now, sedimentological surveys in Lake Van were limited to the uppermost 10 m of the sediment column (Reimer et al., 2008; Litt et al., 2009). An International Continental Scientific Drilling Program (ICDP) project in Lake Van beginning in 2010 aims to recover cores longer than 300 m that will cover up to 500,000 years of sedimentological records (http://van.icdp-online.org). A seismological ICDP pre-site survey (Demirel-Schlueter et al., 2005; Litt et al., 2009) has identified the possible existence of geological structures, such as fault zones, in the sediments. Such structures are a key target of our study, as they might separate the basin of Lake Van into different zones of He emission, possibly marking spots or lines of enhanced He and fluid emission.

5.2.2 Experimental methods

The sampling and noble-gas analysis methods employed are described in detail by Brennwald et al. (2003). The cores were taken with an Uwitec (http://www.uwitec.at) gravity corer. After recovery on board, each core was squeezed and the bulk sediment was transferred into small copper tubes. Each tube was sealed air-tight on both ends with two special clamps to avoid air contamination in the sample.

Noble-gas concentration and isotopic analyses were carried out in the Noble Gas Laboratory at the Swiss Federal Institute of Science and Technology in Zurich. Following the experimental standard protocol for noble-gas extraction from lacustrine sediments (Brennwald et al., 2003), the samples were heated up to 150 °C and forcibly extruded into an extraction vessel under ultra high vacuum (UHV) conditions. The released gases were transfered by water vapor extraction in a UHV purification line. After purification, the noble-gas concentrations and the isotope ratios were determined in two static mass spectrometers, according to well-established experimental protocols commonly used to determine noble-gas abundances in water samples (Beyerle et al., 2000).

Tritium concentrations were determined using the ^{3}He ingrowth method (Torgersen et al., 1977; Bayer et al., 1989; Roether, 1989; Beyerle et al., 1999, 2000). To separate the pore water necessary for ^{3}H determination from the sediment matrix, three sediment cores taken in 2005 were split into sections approximately 10–15 cm long. The content of these sections was transferred to the plastic cylinders of a table centrifuge and centrifugated at

$\sim$ 4000 rpm for 60-90 minutes. The sediment-free water was then transferred into standard copper tubes used for water sampling (Beyerle et al., 2000). The water in the copper tubes was degassed as in "common" water samples in order to remove all atmospheric gases (Beyerle et al., 2000; Strassmann et al., 2005). The degassed pore-water samples ($\sim$20–40 g water) were stored in the copper tubes for about six months to allow ^{3}He to accumulate from the decay of ^{3}H. Note that previous experiments (Stiller et al., 1975; Strassmann et al., 2005) showed that the ^{3}H/^{1}H ratio, and therefore the ^{3}H activity, is not affected by centrifugation. The tritiogenic ^{3}He produced was determined according to the analytical protocol of Beyerle et al. (2000), using a high-sensitivity compressor source designed to measure ultra-low ^{3}He concentrations (Baur, 1999).

5.3 Results and discussion

5.3.1 He concentration profiles

The dissolved He concentrations determined in the pore-water phase of all cores are plotted in Fig. 5.2. From the 140 collected samples, six were affected by major experimental problems (air contamination or partial extrusion of the sample during gas extraction). The data related to these samples are not reported.

Eight samples from two cores taken in the Erciş basin (cores D_1 and D_2) appear to be strongly degassed, as the concentrations of all atmospheric noble gases from Ne to Xe are strongly depleted with respect to their expected atmospheric equilibrium concentrations. The depleted noble-gas pattern is in line with the observation that cores from the Erciş basin produced large amounts of gas (most probably CH_4) during sampling (large gas bubbles were visible in the cores).

For all the other 126 samples the average concentration of atmospheric Ne agreed within $\sim$ 3% with the expected equilibrium concentration, and therefore their corresponding He concentrations were judged to be unaffected by degassing.

The He concentration profiles can be grouped into three different classes, characterized by distinct and different depth-dependent increases in the He concentration within the pore water of the sediment column (Fig. 5.2). When discussing He emission and ^{3}H concentrations as a means of characterizing the solute transport in the connected pore-water space, we will refer to the three classes as "low gradient" (cores $L_1 - L_{12}$), "high-gradient" (cores $H_1 - H_7$) and "hot-spot" (cores $S_1 - S_3$).

In the "low-gradient" cores the He concentration increases only slightly with sediment depth. The "high-gradient" cores show a distinctly more pronounced vertical gradient, with the concentration increasing by about 50% over a depth of $\sim$ 1 m. Compared to the first two types, He emission at the "hot-spot" sites seems to be much greater, as the profiles show a very large vertical gradients. The measured He concentrations reach supersaturations of about 300% (about 10^{-7} cm^{3}STP/g or greater) within the length of a core (< 1.5 m).

5.3.2 He isotope ratios and the correction for tritiogenic ^{3}He

The measured ^{3}He/^{4}He ratios shown in Fig. 5.3 are significantly larger than the atmospheric equilibrium ^{3}He/^{4}He ratio of $1.36 \cdot 10^{-6}$ (Weiss, 1970). Besides terrigenic ^{3}He, a

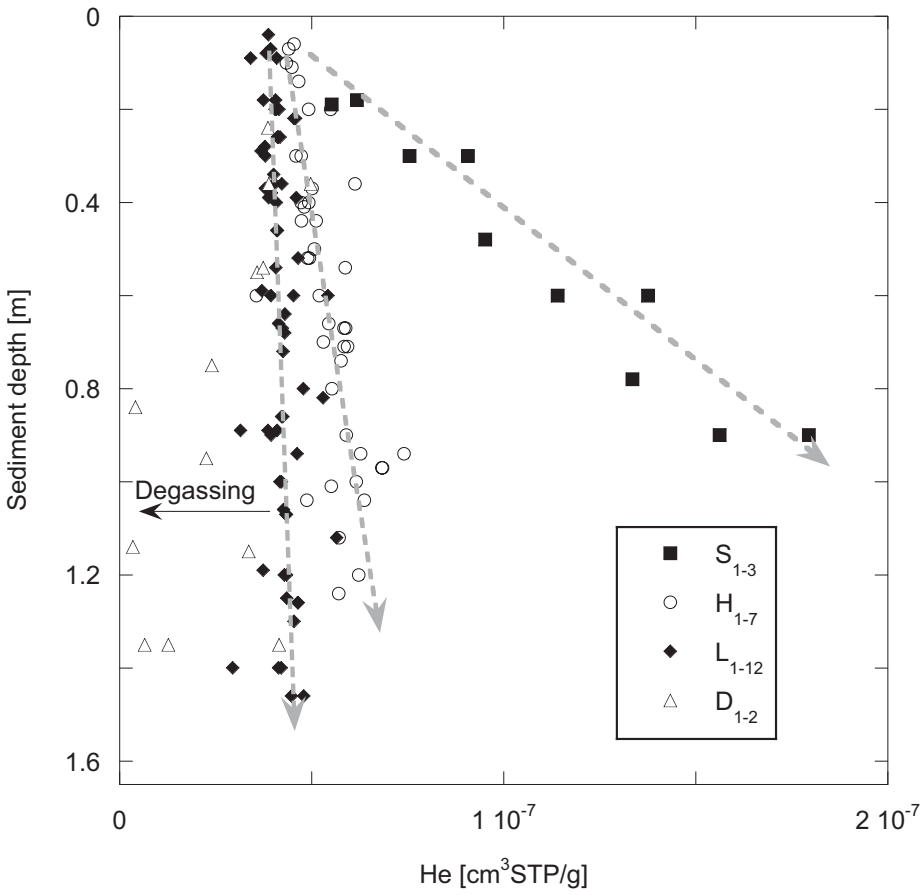

Figure 5.2: Helium concentration profiles in different sediment cores: "low-gradient" cores (L_{1-12}), "high-gradient" cores (H_{1-7}), "hot-spot" cores (S_{1-3}) and cores affected by degassing (D_{1-2}). The location of each core is given in Figure 5.1. The "hot-spot" cores show He supersaturations of up to 300%.

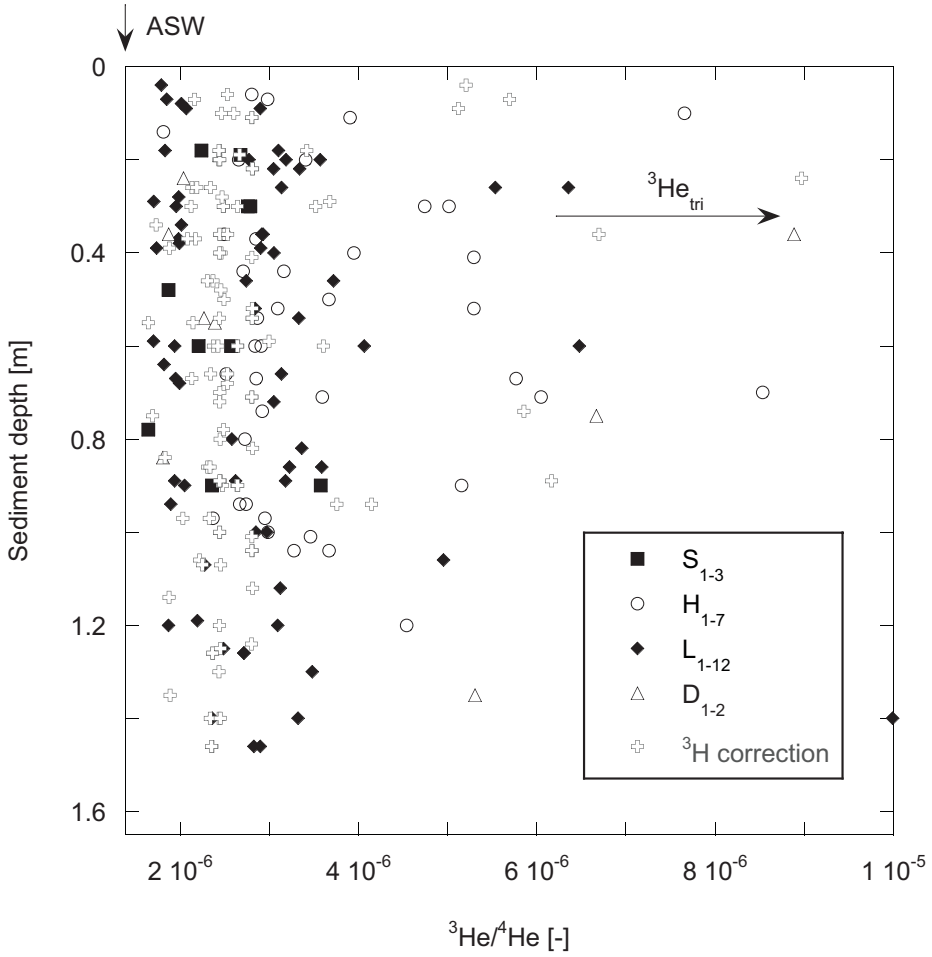

Figure 5.3: Helium isotope ratio profiles for the sampled sediment cores. ASW indicates the $^3He/^4He$ ratio of air-saturated water. The scattering can be mainly attributed to tritium decay, which can be corrected by subtracting the tritiogenic ^3He component using the tritium concentrations measured by Kipfer et al. (1994) (the corrected values for all measured samples are shown as gray crosses).

tritiogenic ^3He component may be present in the topmost part of the sediment column.

The tritium profiles acquired by Kipfer et al. (1994) in the open water column of Lake Van provide an estimate of the amount of tritiogenic ^3He being produced at the water depth of each site where a sediment core was taken. Kipfer et al. (1994) concluded that prior to 1990, deep-water renewal occurred every 1–2 years, and tritiogenic ^3He accumulation in the open water body (and therefore also in the sediments) was therefore found to be negligible. However, starting in the early 1990s deep-water renewal ceased in response to a rise in water level. This rise resulted from enhanced freshwater input to the uppermost part of the water column (Kaden et al., 2005, 2006, 2010), which led to a strong vertical density gradient and to the stabilization of the water column. As a result, vertical transport within the water column was strongly suppressed. Subsequently, tritiogenic ^3He started to accumulate in the deep water of Lake Van as the dissolved gas species were disconnected from the gas exchange occurring at the air/water interface,

thus preventing them from escaping from the water body. Kaden et al. (2005, 2006, 2010) show that the ^{3}H concentrations measured in the water column of Lake Van in 2005/2006 (~ 8 TU) were the result of ^{3}H decay since 1990 (~ 20 TU) and do not reflect any relevant vertical mixing which would have significantly affected ^{3}H evolution in the lake during the previous 15 years. Under the assumption that the deep water of Lake Van was stagnant between 1990 and 2005/2006, the ^{3}H concentrations measured in the lake in 1990 (Kipfer et al., 1994) and 2005/2006 (Kaden et al., 2005, 2006, 2010) allow the accumulation of tritiogenic ^{3}He at the sediment/water interface to be reconstructed.

We used a polynomial function to fit the measured ^{3}H concentrations in order to obtain a continuous ^{3}H concentration as a function of water depth for 1990 and 2005/2006. For each sediment station depth, we then calculated the relative amount of ^{3}He produced by ^{3}H decay from 1990 to 2006. The correction for tritiogenic ^{3}He is based on the assumption that the tritiogenic ^{3}He concentration in the sediments corresponds to the tritiogenic ^{3}He produced in the water at the same depth. The ^{3}He/^{4}He isotope ratio data, corrected for the tritiogenic ^{3}He produced locally in the sediment, are shown in Fig. 5.3 (gray crosses). The corrected ^{3}He/^{4}He ratios converge to the same range as the uncorrected data of ~ 2–$2.5 \cdot 10^{-6}$ at a sediment depth of 1.5 m. The almost constant ^{3}He/^{4}He ratio profiles corrected for tritiogenic ^{3}He suggest that He originates from the same terrigenic source.

However, as the tritiogenic ^{3}He component is not very well constrained for each station, we use the uncorrected ^{3}He concentrations and uncorrected ^{3}He/^{4}He isotope ratios in the further discussion in order to avoid artifacts being introduced by a somewhat "loose" ^{3}H correction.

Besides the uppermost samples in the cores being affected by ^{3}H, some samples show ^{3}He/^{4}He ratios which appear to be too low (i.e. ratios below the range of $2 - 2.5 \cdot 10^{-6}$ which characterizes most of the samples). This is most probably due to the uncontrolled release of ^{4}He from the sediment matrix due to excessive heating of the samples during noble-gas extraction (Brennwald et al., 2003).

5.3.3 Tritium modeling and effective diffusivity

As the tritium input into the deep water of Lake Van is known (Kipfer et al., 1994; Kaden et al., 2006, 2010), the temporal evolution of ^{3}H at the sediment/water interface can be used to characterize the transport of solutes in the pore water of the sediment column, as ^{3}H is trapped in the pore water and further transported in the pore space by advective and diffusive exchange (e.g., Berner, 1975; Imboden, 1975; Strassmann et al., 2005). Sediments are known to limit solute transport in the pore water (e.g., Strassmann et al., 2005). The sediment pore water can therefore often be reasonably described as a purely diffusive domain.

The mean sedimentation rate in Lake Van is 0.5–0.8 mm/year (Landmann et al., 1996; Lemcke, 1996). Hence, the annual advective displacement due to sedimentation is about 30–70 times smaller than the characteristic annual distance Δz for diffusive transport calculated from the relation $\Delta z \sim \sqrt{2 D_{\mathrm{mol}} t}$ (where D_{mol} is the molecular diffusion rate in water) for tritiated water and He. Furthermore, Landmann et al. (1996) show that the first few meters of the sediment column in Lake Van are quite homogeneous with respect to water content, and that the sediment is hardly affected by further compaction over a time-scale of less than 10 ka BP. According to Landmann et al. (1996), this time-scale

corresponds to a sediment depth of about 5 m, which is much greater than the length of our cores (< 2 m). We therefore assumed that advective pore-water fluxes due to sediment burial and compaction of the bulk sediment (Berner, 1975; Imboden, 1975; Strassmann et al., 2005) are negligible and that the solute transport is mainly of diffusive nature.

The effective diffusivity D_{eff} (see equation 5.3 below) can be estimated by modeling the measured tritium profile in the sediments (Fig. 5.4). A simple diffusion model for tritiated water (HTO) similar to that employed by others (Berner, 1975; Imboden, 1975; Strassmann et al., 2005), but neglecting advective processes and assuming constant porosity, was applied to quantify the tritium transport, as follows:

$$\frac{\partial C_{^3\text{H}}}{\partial t} = \frac{\phi}{a} D_{\text{HTO}} \frac{\partial^2 C_{^3\text{H}}}{\partial z^2} - \lambda C_{^3\text{H}} \tag{5.1}$$

where $C_{^3\text{H}}$ [TU] is the tritium concentration in tritium units, D_{HTO} [m^2s^{-1}] is the self-diffusion coefficient of tritiated water (Mills, 1973), ϕ [-] is the sediment porosity, a [-] is a scaling factor for the attenuation of diffusivity, λ [s^{-1}] is the decay rate of tritium (Unterweger et al., 1980), z [m] is the depth in the sediment, and t [s] is time.

The porosity was calculated from the water loss as determined from the weight of the empty sampling containers and the weight of the desiccated samples after extraction. From the porosities determined for individual samples we reconstructed a mean porosity profile (with sediment depth) by assuming that the vertical porosity profile is the same throughout the entire lake. However, according to our determination, based on 22 samples from seven cores taken at different positions in Lake Van, the porosity varies hardly at all over the depth range investigated. For modeling purposes we therefore assumed a constant porosity, $\phi = 0.63$, for all cores, which corresponds to the mean of the measured porosities (see Fig. 5.5).

The temporal evolution of ^{3}H in the open deep water of Lake Van was used as a boundary condition for the model. Further, we assumed that ^{3}H enters the sediment column only by diffusion. We modeled the diffusive transport of ^{3}H in the sediment for a time span of 15 years (i.e., until 2005, the year of acquisition of the cores intended for ^{3}H analysis). As an initial condition, the tritium concentration in the sediment column was set to zero. The upper time-dependent boundary was set to $C_{^3\text{H}}(z = 0, t) = C_{^3\text{H},0} \cdot e^{-\lambda \cdot t}$, where $C_{^3\text{H},0} = 20.1$ TU is the average tritium concentration in the water body determined in 1989-1990 (Kipfer et al., 1994) and $\lambda = 1.78 \cdot 10^{-9}\,\text{s}^{-1}$ is the decay rate for ^{3}H (Unterweger et al., 1980). The assumption of 20.1 TU at the sediment/water interface in 1989/1990 is reasonable, as Kaden et al. (2010) demonstrated that the values of ~ 8 TU in Lake Van measured in 2005/2006 can be directly explained by the decay of ^{3}H starting from an activity of ~ 20 TU in the stagnant water column.

Fig. 5.4 shows the modeled depth profiles for ^{3}H in the pore waters of the sediment column for the year 2005 and for different values of the diffusivity attenuation parameter a. Least-square fitting yielded a best estimate for a of ~ 2.67; thus $\phi/a = 0.24$, implying that diffusive transport occurs about four times more slowly in the pore water of Lake Van than in the bulk water.

The estimate of a obtained from the ^{3}H modeling allows the effective diffusivity D_{eff} for He (see section 5.3.4, equation 5.3) to be scaled. Hence, D_{eff} is also about four times smaller than the diffusivity D_{mol} of He in bulk water. Note, however, that the absence of tritium in the sediment column, which was assumed as an initial condition for the

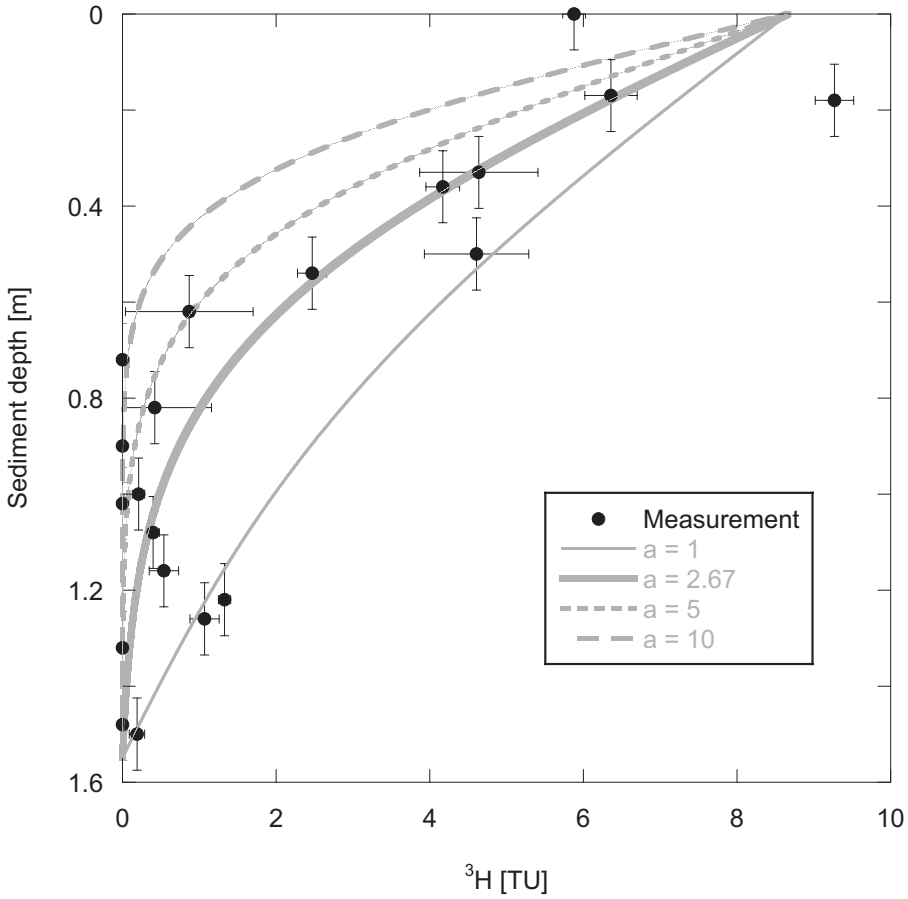

Figure 5.4: Measured tritium profile (black dots) and simulations for $a = 1$ (thin line), $a = 2.67$ (thick line), $a = 5$ (fine dashed line), and $a = 10$ (coarse dashed line) in tritium units (TU). The initial concentration at the water/sediment interface is set to 20.1 TU in 1990 (Kipfer et al., 1994). The curves represent the tritium concentration profiles after a period of 15 years, affected by diffusive transport and radioactive decay. The time span is chosen to fit, at the end of the simulation, the acquisition period of the cores intended for tritium analysis in 2005.

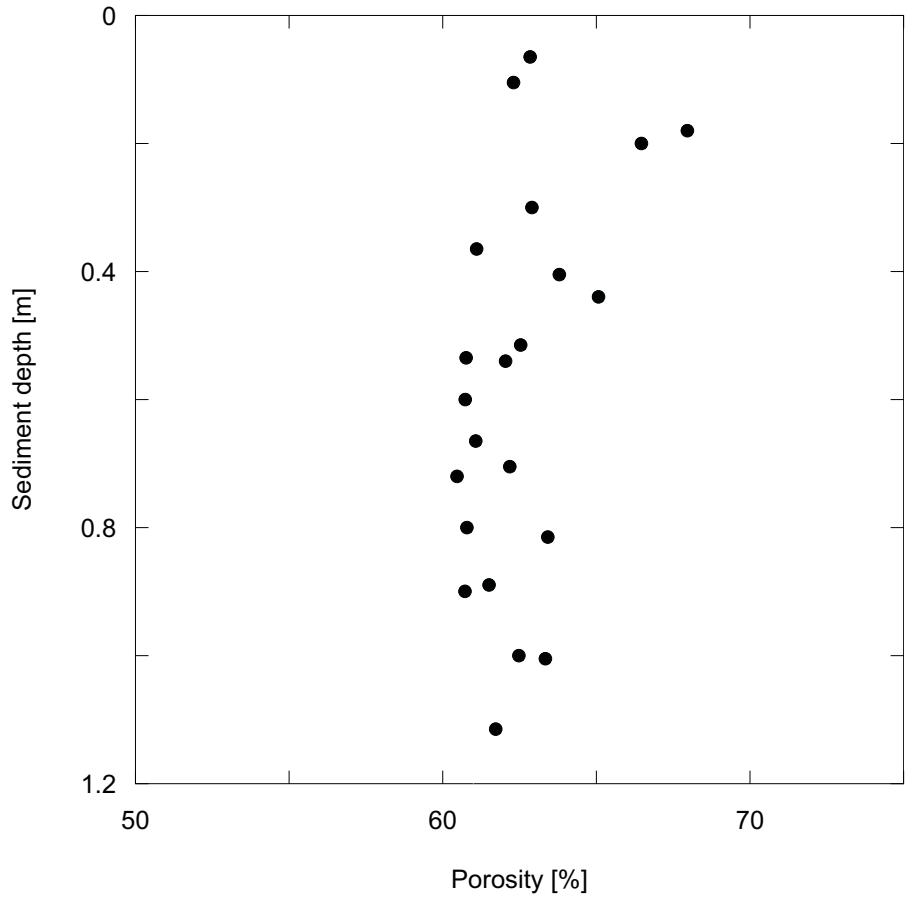

Figure 5.5: Porosity profile determined from the weight of the empty sampling containers and the weight of the desiccated samples after noble-gas extraction.

Table 5.1: Fit parameters for linear regression $C(z) = C_0 + \frac{\Delta C}{\Delta z} \cdot z$ of He concentration data for different cores from the same class, where C_0 is the concentration at the sediment/water interface, $\frac{\Delta C}{\Delta z}$ is the vertical concentration gradient, and z is the depth within the sediment column. The He concentrations at $z = 0$ agree well with the average of the measured water samples of $(3.9 \pm 0.6) \cdot 10^{-8}$ cm^{3}STP/g.

Release type	C_0 [10^{-8}cm^{3}STP/g]	$\frac{\Delta C}{\Delta z}$ [10^{-8}cm^{3}STP/g/m]	Flux J [10^8atoms/m^2/s]
Low-gradient (L)	4.0	0.28	1
High-gradient (H)	4.4	1.6	5
Hot-spot (S)	3.5	14	50

modeling, implies that the resulting effective diffusivity is a "maximum" value. In fact, it is likely that tritium produced during the nuclear bomb tests in the mid-1960s entered the sediments before 1989/1990. The very low ^{3}H concentrations measured below ~ 0.8 m (nearly ^{3}H-free water) may therefore indicate an even stronger attenuation of diffusivity.

5.3.4 Estimation of the He fluxes

In order to determine the terrigenic He emission, the measured He concentrations need to be converted into fluxes. The He flux in the sediments can be calculated from the He concentrations using Fick's law and the determined effective diffusivity D_{eff}, because both the linear increase in the measured concentrations and the nearly constant isotope ratio indicate that the diffusive He transport operates at steady state.

$$J = -D_{\text{eff}} \frac{\partial C}{\partial z} \tag{5.2}$$

$$D_{\text{eff}} = \frac{\phi}{a} D_{\text{mol}} \tag{5.3}$$

where J [atoms $\cdot$ m^{-2}s^{-1}] is the flux, $\frac{\partial C}{\partial z}$ [atoms $\cdot$ m^{-4}] is the vertical concentration gradient, D_{mol} [m^{2}s^{-1}] is the diffusion coefficient for He in bulk water (Jähne et al., 1987), and ϕ and a are as defined in equation 5.1.

The parameters of the linear fit characterizing the He concentration profiles are given in Table 5.1. The fitted concentrations at the surface ($z = 0$) are slightly different for each "release class" ($< 1 \cdot 10^{-8}$ cm^{3}STP/g), which does not affect the flux estimation.

Equation 5.2 and the best estimate of a (~ 2.67) allow the measured concentration profiles to be converted into local He fluxes for each core location. Again - as in the case of concentration - three types of He emission can be distinguished which are characterized by different terrestrial He fluxes: "low-gradient" $J_L = 1 \cdot 10^8$ atoms $\cdot$ m^{-2}s^{-1}, "high-gradient" $J_H = 5 \cdot 10^8$ atoms $\cdot$ m^{-2}s^{-1} and "hot-spot" $J_S = 50 \cdot 10^8$ atoms $\cdot$ m^{-2}s^{-1}.

Notably, even J_S is about five times smaller than the average continental He flux of $2.8 \cdot 10^{10}$ atoms $\cdot$ m^{-2}s^{-1} calculated by O'Nions and Oxburgh (1983), and about one order of magnitude smaller than the He flux of $2 - 3 \cdot 10^{11}$ atoms $\cdot$ m^{-2}s^{-1} estimated

for Lake Van by limnological means (Kipfer et al., 1994). The two estimates originate from either general geochemical arguments (O'Nions and Oxburgh, 1983) or from physical determination of the mixing conditions in water bodies (Kipfer et al., 1994). Hence, these flux estimates were determined over much larger spatial scales (100–1000 km) than those of our determination, which is strictly local in nature. Compared to former "regional-global" studies, our work is constrained to considerably smaller spatial scales, which allows identification of the actual transport processes that allow He to emanate. Such local studies complement the "regional-global" estimates, whose large scales only allow the driving transport process to be identified on a conceptual level. As already pointed out, the He flux in the sediments of Lake Van is mainly diffusive. The attenuation of diffusion that controls the local He emission in Lake Van may explain why the local flux estimates are much smaller than those focusing on "regional-global" scales. Such large-scale "budget" approaches integrate not only over diffusive transport processes, but over all potentially relevant transport processes, regardless of whether they have been observed or not.

5.3.5 Spatial distribution of He emission

According to our data, He emission within the basin of Lake Van is spatially very heterogeneously distributed, even within distances of only a few kilometers (Fig. 5.1). Stations with "low-gradients" and "high-gradients" are found in close proximity to "hot-spot" stations (< 5 km). However, cores of the same "type" have very similar fluxes independent of their individual location, and therefore seem to be indicative of particular tectonic or geological settings. These geological regions can be mapped within Lake Van using the flux estimates.

The largest He fluxes are observed at the margins of the deep, main basin near Tatvan (Fig. 5.1, solid squares), which is separated by very steep basin slopes from the lateral shallow subbasins of Erciş, Ahlat and Van (see the bathymetry of Seyir Hidrografi ve Oşinografi Dairesi, 1990). The location of the "hot-spot" cores (Fig. 5.1, solid squares) corresponds to the morphology of the deep basin of Lake Van.

This circular basin structure may originate from a collapsed volcanic caldera (Litt et al., 2009). Our results on the He flux lend support to this hypothesis, as the fault structures that facilitated the collapse of the caldera would act today as pathways which would foster and stimulate the emission of He (and most probably other fluids), leading to the enhanced He fluxes at the "hot-spot" cores. The absence of such pathways of preferential He emission at "low-gradient" and "high-gradient" sites might explain why the fluxes there are much smaller. A seismic survey within the framework of the ICDP project "PaleoVan" showed that the Tatvan basin is bounded by faults which suggest ongoing subsidence of the basin (Demirel-Schlueter et al., 2005; Litt et al., 2009). Such subsidence processes are likely to generate further pathways of preferential fluid escape just at the edges of the basin in zones where the largest He fluxes were determined. Seismic lines across the steep border of the main basin indicate the presence of structures in the sediment column that may facilitate the release of geogenic fluids. In particular, seismic data from the upper part of the steep slopes of the Tatvan basin (at the position of sediment core S_3) reveal vertical disruptions that cut through the well-laminated sediment layers and along which the accumulation of a gas or liquid phase cannot be excluded (e.g.,

Litt et al., 2009). In conclusion, the seismic data agree with the analysis of the He fluxes. Both lines of evidence may indicate that the collapse of a large caldera generated structures which now operate as pathways of preferential fluid migration.

The spatial distribution of the cores with "low" and "high" fluxes (J_L and J_H) shows a distinct north-south gradient. Interestingly, cores taken near the northern part of Lake Van, close to the active volcanoes Nemrut and Süphan, show lower He fluxes ("low-gradient" cores L_1-L_4, L_6-L_8, L_{10}-L_{12}) than cores taken in the southern part of Lake Van, in the vicinity of the intrusive and metamorphic rocks of the Bitlis massif ("high-gradient" cores H_1, H_2, H_4-H_7). In conclusion the "low-gradient" and "high-gradient" cores tend to follow the north-south zonation of the geological provinces of Lake Van: the volcanic rocks of Nemrut and Süphan in the north and the crystalline rocks of the Bitlis massive in the south. Higher He fluxes are observed in the southern region of the lake near the Bitlis massif and its crustal rocks (opposite the fault region which characterizes the north: Şaroğlu et al., 1992). This might explain why the He in the sediments of Lake Van consists of a mixture of mantle and crustal components (see below) rather than being purely of mantle origin, as observed in water samples from the Nemrut volcano (Aeschbach-Hertig et al., 1991; Kipfer et al., 1994).

Surprisingly, most active faults (Şaroğlu et al., 1992) are located north of Lake Van and do not seem to provide preferential pathways which could foster the release of terrestrial fluids and He. Hence, the spatial distribution of "low" and "high" He fluxes seems to be controlled by the occurrence of geological units and associated rocks, and not solely by tectonic structures.

5.3.6 Characterization of the source of He

The nearly constant isotopic signature of terrigenic He in the sediment thoughout the lake suggests that only one type of terrigenic He is injected into the lake. The observed $^3He/^4He$ ratio indicates that the injected He is a mixture of two components: isotopically light He from a depleted mantle source, similar to the one observed in Lake Nemrut (Kipfer et al., 1994), and isotopically heavy He, most probably radiogenic He produced in sediments or crustal rocks.

The identification of the source of terrigenic He is illustrated in Fig. 5.6. The concentrations of excess ^{3}He, excess ^{4}He and ^{20}Ne are shown. We define "excess He" as the surplus concentration of the He isotopes with respect to those in air-saturated water (ASW) as calculated from the the temperature and salinity of the water:

$$^iHe_{EX} = {}^iHe_m - {}^iHe_{ASW} \tag{5.4}$$

where $i = 3, 4$ and the subscripts "m" and "ASW" indicate the measured and air-saturated water concentrations, respectively (Weiss, 1971a,b; Weiss and Kyser, 1978; Clever, 1979; Kipfer et al., 2002).

Extrapolation of the He isotope signature to a terrigenic gas composition void of any atmospheric air ($^{20}Ne = 0$) yields the $^3He/^4He$ ratio of the terrigenic He component released into Lake Van. The two areas delimited by gray dashed lines in Fig. 5.6 represent the trends identified for the sediment samples from the different sites in Lake Van; the area with the larger gradient $\frac{\Delta(^3He_{EX}/^4He_{EX})}{\Delta(^{20}Ne/^4He_{EX})}$ corresponds to samples from deep-water sediment cores ($z > 200\,m$), whereas the area with the smaller gradient corresponds to samples from

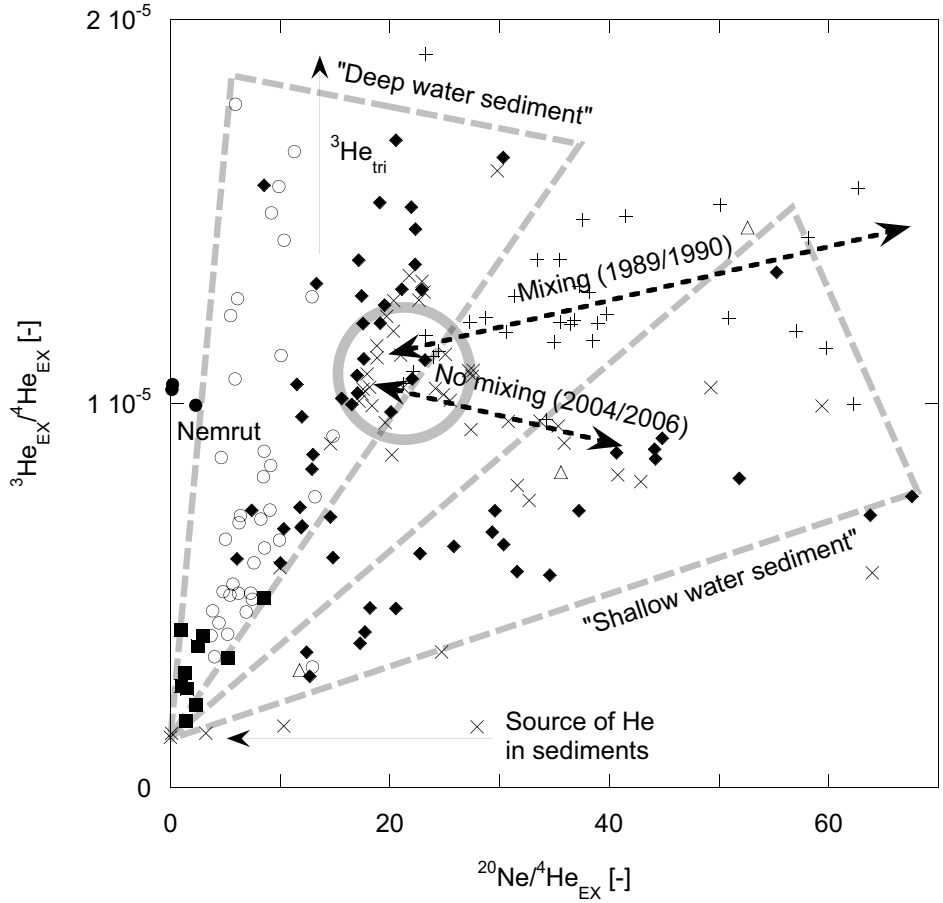

Figure 5.6: Relationship between $^3\mathrm{He}_{\mathrm{EX}}/^4\mathrm{He}_{\mathrm{EX}}$ and $^{20}\mathrm{Ne}/^4\mathrm{He}_{\mathrm{EX}}$ isotope ratios of sediment and water samples. Upright and diagonal crosses indicate water samples taken in 1989/1990 and 2005/2006, respectively. The general trends for water samples taken in a mixing (1989/1990) and a stagnant (2005/2006) water body are plotted as dashed black lines. The remaining symbols have the same meaning as in Figures 5.2 and 5.3. $^i\mathrm{He}_{\mathrm{EX}}$ with $i = 3, 4$ is the excess component of the He isotopes with respect to the expected equilibrium concentrations calculated from the in situ temperature and salinity. The intersection of the sediment trends towards air-free (i.e. ^{20}Ne-free) composition yields the $^3\mathrm{He}/^4\mathrm{He}$ ratio of the terrigenic He source. The resulting ratio of $2.2 \cdot 10^{-6}$ identifies the emitted He to be a mixture of a radiogenic He component (most probably generated by nuclear reactions within the sediment column, $^3\mathrm{He}/^4\mathrm{He} \sim 10^{-8}$) and an He component from a depleted mantle source, as observed in the nearby crater lake, Lake Nemrut (solid dots, see also Kipfer et al., 1994).

shallow-water cores. Both the shallow-water and deep-water sediment clusters of noble-gas abundances tend towards the same terrigenic He component. Both trends define the $^3He/^4He$ ratio of the ^{20}Ne-void terrigenic He component to be $\sim 2.2 \cdot 10^{-6}$.

5.3.7 He accumulation and mixing dynamics in Lake Van

Our He measurements in the sediment pore water allow the previous interpretation of the He dynamics in the open water column of Lake Van to be modified and extended. Kipfer et al. (1994) interpreted the non-atmospheric ^3He abundance in Lake Van to be the result of a minor tritiogenic ^3He component due to the decay of ^3H in the water column and a major component of He from a depleted mantle source (MORB-type) being injected into Lake Van. The presence of He from a depleted mantle source has been clearly demonstrated for Lake Nemrut, the nearby volcanic crater lake. According to Kipfer et al. (1994), the He abundance in Lake Van during the late 1980s could be explained by rapid deep-water renewal, because otherwise the accumulation of tritiogenic ^3He would have resulted in much higher $^3He/^4He$ ratios that were not observed at that time in the water column.

The data of Kipfer et al. (1994) are plotted in Fig. 5.6 and are compared with recent noble-gas measurements from water samples collected between 2004 and 2006 in Lake Van (see also Kaden et al., 2006, 2010). For comparison, the noble-gas measurements from Lake Nemrut are also plotted, as these data define and identify the injected mantle He (note that these water samples were acquired in 2006, but the data agree well with the results of Kipfer et al., 1994).

The first data set of 1989/1990 was acquired when the water level of Lake Van was low, and complete deep-water renewal was assumed to occur within 1–2 years (Kipfer et al., 1994). After the mid-1990s the lake level started to rise in response to enhanced freshwater input. A strong salinity-driven stabilization of the water column therefore occurred, as a freshwater layer developed in the topmost few meters. The increased density stabilization of the water column can be expected to significantly reduce deep-water exchange, as has been shown for the Caspian Sea (Peeters et al., 2000) and Crater Lake, Oregon (Collier et al., 1991). Recent measurements of transient tracers such as SF_6, CFCs and ^3H in Lake Van (Kaden et al., 2005, 2006, 2010) prove that, at least during the last decade, virtually no deep-water renewal occurred, causing the deep-water body to become stagnant.

A stagnant water column is expected to accumulate non-atmospheric He (Kipfer et al., 2002). Therefore, especially in the bottom water near the sediment/water interface, the He isotope signature would be expected to shift toward the signature of He released from the sediments, as such accumulation occurs more or less continuously over the time-scale given by the renewal rate of the overlying lake water (less than a few decades, see Kipfer et al., 2002).

Measured noble-gas abundances in the waters of Lake Van have indeed changed significantly during the last 15 years. In 1989/1990 Lake Van was characterized by an almost constant $^3He/^4He$ ratio throughout the water column, which was found to be the result of effective deep-water renewal. Fifteen years later, however, the water samples of 2005/2006 appeared to be enriched in ^3He compared to the concentrations of ^4He and ^{20}Ne. Such a relative increase in ^3He is expected if a water body is stagnant and accumulates tritiogenic ^3He (i.e., if there is no significant deep-water renewal), as is the case in Lake Van during

phases of increasing water level, when deep-water renewal ceases (Kaden et al., 2005, 2006, 2010). However, the noble-gas trends - that of 1989/1990 and that of 2005/2006 - intersect each other ($^3He_{EX}/^4He_{EX} \sim 10^{-5}$, $^{20}Ne/^4He_{EX} \sim 20$) just at the noble-gas composition characterizing the pore water of the uppermost part of the sediment column of Lake Van (the area delimited by the gray circle in Fig. 5.6).

The fact that the noble-gas isotope signatures of the bottom-water samples is confined to the region of isotope signatures also found in the sediment samples clearly indicates that the observed injection of terrigenic He into the water column of Lake Van is explained by the presence of He released from the sediments into the open water column. The terrigenic $^3He/^4He$ ratio found in the pore waters further indicates that the He originates from a single source. As the $^3He/^4He$ ratio of the terrigenic He released from the sediments into Lake Van is about four times smaller than the postulated isotope ratio for He from a depleted mantle source (Kipfer et al., 1994), it follows that Kipfer et al. (1994) underestimated the tritiogenic ^3He abundance in the water column of Lake Van in 1989/1990. Such a higher tritiogenic ^3He abundance would correspond to a lower renewal rate than that derived by Kipfer et al. (1994).

Using the $^3He/^4He$ ratio of terrigenic He released from the sediments ($\sim 2.2 \cdot 10^{-6}$), it is possible to recalculate the amount of tritiogenic ^3He present in the water column in 1989/1990 by subtracting both the atmospheric equilibrium component and the terrigenic ^3He component, which is proportional to the ^4He excess. The resulting $^3H/^3He$ water ages (Kipfer et al., 2002) have an average value of ~ 9 years (~ 14 years for the bottom water), which is about four times larger than the 1–2 year water age estimated by Kipfer et al. (1994). This finding is in line with the SF_6, CFC and ^3H dating results of Kaden et al. (2005, 2006, 2010) and supports the idea that the tritiogenic ^3He concentrations in 1989/1990 were underestimated by Kipfer et al. (1994).

5.4 Conclusions and outlook

Our tritium measurements show that the effective diffusivity in the pore space is attenuated compared to the diffusivity in bulk water ($D_{\text{eff}} \approx 0.25 \cdot D_{\text{mol}}$). Such attenuation of the effective diffusivity agrees with the findings of Strassmann et al. (2005), who assumed a fourfold reduction in diffusivity to explain the tritium profile measured in the sediments of Lake Zug (Switzerland). Brennwald et al. (2004) showed that in Lake Issyk-Kul (Kyrgyzstan) the molecular diffusivities for noble gases would have to be at least two orders of magnitude lower than the diffusivities in bulk water in order to explain the measured atmospheric noble gas concentrations, which were interpreted in terms of a low lake level. Brennwald et al. (2005) proposed a very low vertical diffusion in the sediment column of Soppensee (Switzerland) to explain the observed strong depletion of atmospheric noble gases due to CH_4 ebullition, which did not lead to any detectable isotopic fractionation in Ne and Ar. Hence our data, in agreement with our earlier studies (Brennwald et al., 2004, 2005; Strassmann et al., 2005), again imply that the diffusive exchange is significantly attenuated in the pore water of laminated or varved sediments, such as those found in Lake Van.

To our knowledge, our noble-gas measurements in the sediments of Lake Van yield, for the first time ever, direct experimental evidence that the He emission occurs heterogeneously on spatial scales of less than a few kilometers. The observed maximum terrestrial

He flux of $5 \cdot 10^9$ atoms $\cdot$ m^{-2}s^{-1} correlates well with seismic features (e.g., Litt et al., 2009) along which terrigenic fluids may preferentially migrate in the sediments of Lake Van. Even at such "hot-spots", however, the flux is five times lower than the expected continental flux (O'Nions and Oxburgh, 1983). The determined local He fluxes are about one order of magnitude lower than those determined from a physical mixing model of Lake Van (Kipfer et al., 1994), which indicates either i) that our measurements do not cover all types of terrigenic He emission in the lake, with some strong emissions still not identified, or ii) that the vertical mixing rates determined in the early 1990s (Kipfer et al., 1994) were overestimated.

The spatial distribution of the local He fluxes determined from single cores reveals that strong He emission is confined to a circular feature that follows the steep borders of the main basin of Lake Van. This spatial distribution supports the idea that the deep basin of the lake was formed from the collapse of an old volcanic caldera which produced deep conduits that act as pathways for the preferential emission of He (and probably other fluids). Furthermore, the observed strong north-south gradient in the local He flux, with low fluxes in the north and high fluxes in the south, indicates that He emission from the intrusive metamorphic rocks of the Bitlis massif is greater than that from the volcanic rocks of the active Nemrut and Süphan volcanoes.

The He injected into Lake Van is identified as a unique single component that can be understood as a mixture of radiogenic He and He from a depleted mantle source, producing the observed ^{3}He/^{4}He ratio of about $2.2 \cdot 10^{-6}$. Although local He fluxes in individual cores may differ by a factor of 50 (Table 5.1), the injected He originates from the same terrigenic source. The identified terrigenic He is isotopically heavier than assumed in previous work (Kipfer et al., 1994).

Our study is the first to determine the spatial distribution of He emission at scales smaller than the lake basin. However, as only short cores (< 2 m) were analyzed, our results are confined to the uppermost few meters of the sediment column. Insights into large-scale vertical He transport are expected from the long (> 300 m) cores that will be taken during the upcoming ICDP drilling project at Lake Van. New results based on data from these cores are expected to provide insight into the nature of vertical fluid transport (advective and diffusive) and the mixing of different fluid phases to produce the He composition observed in the pore water space of the sediments of Lake Van.

Chapter 6

Noble-gas analysis in ocean sediments to characterize active CH_4 seepage off shore from New Zealand

Abstract Recent development of analytical methods to determine noble-gas abundances in the pore waters of unconsolidated sediments easily allow noble-gas concentrations and isotope ratios to be measured in lakes in a routine manner. We applied these techniques for the first time on ocean sediments from the South Pacific off shore from New Zealand with the aim to characterize the origin of an active cold methane seepage system using the $^3He/^4He$ ratio of the pore waters of the sediment column. The results show that in the vicinity of the Pacific-Australian subduction zone more ^{3}He-rich fluids emanate compared to the forearc stations located near the shore of New Zealand. However, the He isotope signature in the sediment column indicates that only a minor part of He emanating from deeper strata originates from a (depleted) mantle source. Hence, the largest amount of He in the pore water is locally produced by radioactive decay of U and Th in the sediment minerals, also suggesting that the source for the largest fraction of CH_4 is located in a surface-near geochemical reservoir. This finding is in line with a $\delta^{13}C$ study in the water column which concludes that CH_4 is most likely of biological origin and it is formed in the upper meters of the sediment column.

6.1 Introduction

Noble gases are ideal tracers to study the transport of other dissolved species in unconsolidated sediments (Brennwald et al., 2005; Strassmann et al., 2005). In particular, as He emanates from solid earth into the atmosphere, the origin of other solutes emanating from the same geogenic reservoir can be determined in a straightforward manner using the He concentrations and isotope ratios measured in the sediment column.

The development of a method for sampling and determination of noble gases in the pore water by Brennwald et al. (2003) allowed for the first time the measurement noble gases in unconsolidated sediments in lakes in a routine manner. A major experimental problem

Acknowledgments: We want to thank the SONNE cruise crew at IFM-GEOMAR, and in particular Matthias Haeckel, for giving us the possibility to sample and analyze the sediments from the South Pacific. This research was funded by the Swiss Science Foundation (SNF 200020-121853).

encountered by applying the method of Brennwald et al. (2003) to ocean sediments is that the utterly needed complete extrusion of samples having very fine texture and relatively low porosity ($\leq 60\%$) cannot always be achieved, i.e. a part of the bulk sediment remains in the copper tube used as sample container in the form of compact clusters. As the presence of these clusters severely attenuates the degassing process, noble-gas extraction results often to be incomplete.

Our recent work to improve the analytical method to determine noble-gas abundances in the pore water of unconsolidated sediments shows that the known experimental limitations of the method by Brennwald et al. (2003) can be overcome by the complete separation of pore water from the sediment matrix by centrifugation of the *bulk* sediment samples within the ultra high vacuum sealed copper tubes (Tomonaga et al., 2010, submitted). In this study we adapted for the first time the centrifugation method (Tomonaga et al., 2010) to ocean sediments acquired in the vicinity of an active cold methane seepage system off shore from New Zealand (Faure et al., 2006, 2009), in order to determine noble-gas abundances.

In the Black Sea noble gases were found to yield valuable information about the origin of methane being injected into the water column by high-intensity seeps. Noble-gas abundances allowed the functional and tectonic relation of CH_4 emission and mud volcano activity to be studied (Holzner et al., 2008). Therefore, using the same concepts we aim to characterize the geochemical origin of methane at cold seeps off shore from New Zealand - in particular using He isotopes to determine the origin of the ascending fluids.

6.2 Study site

The three sediment cores being sampled for noble-gas analysis were taken in the South-West Pacific, off shore from New Zealand in the vicinity of the Pacific-Australian subduction zone (see Fig. 6.1). The region, stretching along the gas-hydrate-bearing Hikurangi Margin, is known for the emanation of cold fluids, e.g. methane is released from the sediments into the water column (Faure et al., 2006). This cold seepage environment also offers a habitat for particular biological communities (Sommer et al., 2009).

The first core for noble-gas analysis was taken at "Rock Garden" in the immediate vicinity of the subduction zone in about 660 m water depth. As the name of this station implies, the presence of rocks only allows small cores of maximum length of 1 m to be taken. Inspection by a remotely operated vehicle (ROV) at this site showed active macroscopic bubble emission at the sediment/water interface (Naudts et al., 2009). The other two stations, "Reference" and "Bear's Paw", are located at Omakere Ridge closer to the shore of New Zealand at 1180 m and 1100 m depth (for detailed maps of the sites see Linke et al., 2009).

All the sediment samples were taken in March 2007 during the SONNE-Cruise 191 lead by IFM-GEOMAR (cruise information: http://www.ifm-geomar.de).

6.3 Methods

The samples for noble-gas analysis were acquired in the field using our standard sampling technique (see Brennwald et al., 2003). Immediately after core recovery on the ship, the

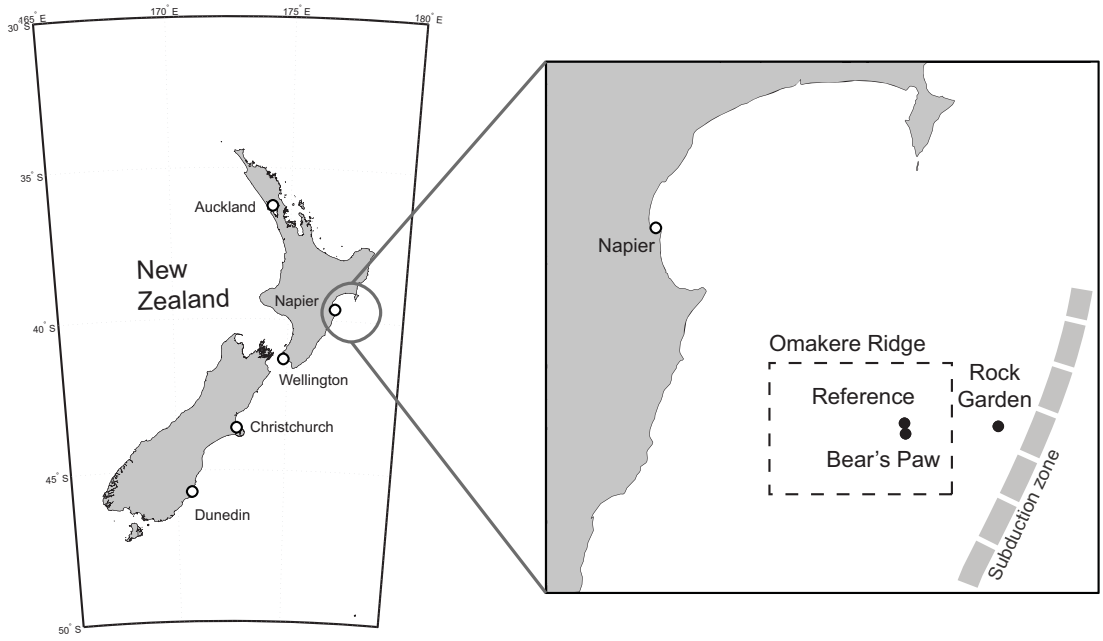

Figure 6.1: Position of the three sampling stations for the sediment cores intended for noble-gas analysis located off shore from New Zealand (solid dots). "Rock Garden" is in the vicinity of the Pacific-Australian subduction zone. The water depth at "Rock Garden" is 660 m, at "Reference" 1180 m and at "Bear's Paw" 1100 m. The position of the major cities is given by empty circles.

bulk sediment was transferred into small copper tubes (inner diameter $\sim$ 6 mm, length $\sim$ 50 cm) by squeezing of the sediment core by moving two pistons along the axis of the plastic liner. The copper tubes being attached to the side of the liner by Swagelok fittings, were filled with sediment and sealed airtight by closing two metal clamps to avoid air contamination and degassing (see Beyerle et al., 2000; Brennwald et al., 2003).

Noble-gas concentrations and isotope ratios were determined by applying our newly developed centrifugation method (Tomonaga et al., 2010). The centrifugation allows separation of the pore water from the sediment matrix within the closed copper tubes. The position of the sediment/water interface after centrifugation is needed in order to set a third clamp to completely separate pore water phase form compressed sediment matrix. After successful separation of the two phases, the pure pore water was analyzed using the well accepted protocols of Beyerle et al. (2000) to determine noble-gas abundances in common water samples. As the amount of sediment samples for noble-gas analysis was very limited (i.e. no replicates available), we chose to roughly approximate the geometrical position of the water/sediment interface using aliquots of samples from the Gulf of Cadiz. These sediments have a similar texture (e.g. grain size and porosity) as the sediments from New Zealand and therefore are expected to react in the same way to the centrifugation process (i.e. the same volume of separated pore water is expected). The sediment/water interface was found to be located below $\sim$ 1.5 cm from the top clamp of all centrifugated aliquots.

Small adaptations of the geometrical arrangement were needed to fit the closed copper tubes into a centrifuge with a fixed angle rotor (Centrikon H-401-B with a A6.9 rotor).

This newly used centrifuge rotates at least three times faster than the centrifuge (Heraeus UJ3S) previously used in the centrifugation experiments by Tomonaga et al. (2010) and hence, the water and sediment matrix phases are significantly better separated by the applied ten times stronger force.

Due to the smaller volume available for each cylinder of the centrifuge rotor the sample length between the two sealing clamps was confined to 9.5 cm. The aluminium fittings necessary to hold and support the sampling containers were designed according to the inner dimensions of the standard centrifugation bottles (made of polypropylene, 500 mL) where they were inserted together with the sample for the centrifugation process. The bottles act as a protection shell for the rotor and allow to simply tare the weight of each sample with water ($\pm$0.01 g) in order to avoid imbalance on the rotor. The total weight of one centrifuge-ready sample (copper tube, clamps, fittings and polypropylene container) is about 1.5 kg. The used rotor can run with a maximum weight of 6 kg at 9000 rpm. In our experiments three samples were simultaneously centrifugated in order to avoid any overloading.

Prior to the high-speed centrifugation step the samples are put in an ultrasonic bath ($\sim$ 30 minutes) in order to loosen the connection between the bulk sediment matrix and the copper tube wall. Then the samples are centrifugated for 2 h at 7000-7500 rpm. Afterwards the centrifugated samples are again placed in an ultrasonic bath. The samples are then centrifugated for a second time using a swing rotor centrifuge (a Heraeus UJ3S, see Tomonaga et al., 2010) for 2-3 h at 2300-2600 rpm. Both steps are needed to orientate the sediment/water interface perpendicular to the axis of the copper tube, as such configuration facilitates the final mounting of the third clamp which separates the "pure" water from the sediment matrix phase.

6.4 Results and discussion

The results are listed in Table 6.1 as raw concentrations of He, Ne, Ar, Kr and Xe and isotope ratios (^{3}He/^{4}He, ^{20}Ne/^{22}Ne and ^{36}Ar/^{40}Ar). In Fig. 6.2 the data are plotted as saturations with respect to the atmospheric equilibrium concentrations expected for "Rock Garden" being calculated for a temperature of 6°C and 35 g/kg salinity.

In general, the applied method to extract noble gases from the pore water of ocean sediments was successful, as the determined concentration profiles for the atmospheric noble gases coincide nearly with the expected atmospheric equilibrium concentrations. The isotope ratios of Ne and Ar agree well with the expected ratios for air saturated water (ASW). Also the ^{3}He/^{4}He ratio close to the sediment/water boundary reasonably agrees with the isotopic composition of ASW. However, the deeper part of the sediment column at all three sites is enriched in He relative to ASW which indicates the presence of terrigenic He.

Some samples in the upper part of the sediment cores were probably not completely extracted, as the measured Ar, Kr and Xe concentrations are smaller than the expected equilibrium concentrations (see Fig. 6.2, samples below 100% air saturation). The inspection of the inner part of the sampling containers after noble-gas extraction and desiccation identified small amounts of sediment remaining in the copper tubes which indicates that the separation of water and sediment was not absolutely complete. As shown for the case of our formerly used "blow out" method, degassing of such sediment chunks is often

Table 6.1: Measured concentrations and isotope ratios for samples taken in the South Pacific Ocean off shore from New Zealand. STP = standard temperature (0°C) and pressure (1 atm). The average errors are higher than the errors given in Brennwald et al. (2003) as the water mass is confined to only ≤ 2 g.

Sampling station	z (m)	He (10^{-8}cm$^3_{\mathrm{STP}}$/g)	Ne (10^{-7}cm$^3_{\mathrm{STP}}$/g)	Ar (10^{-4}cm$^3_{\mathrm{STP}}$/g)	Kr (10^{-7}cm$^3_{\mathrm{STP}}$/g)	Xe (10^{-8}cm$^3_{\mathrm{STP}}$/g)	^{3}He/^{4}He (10^{-6})	^{20}Ne/^{22}Ne	^{36}Ar/^{40}Ar (10^{-3})
"Bear's Paw"	0.01	2.92	1.15	2.98	4.00	1.26	1.51	10.9	3.33
	0.18	25.9	10.3	8.52	8.62	1.76	1.41	9.80	3.38
	0.38	13.3	3.31	4.16	4.89	1.39	1.08	9.76	3.43
	0.58	8.42	1.10	2.26	3.57	1.36	0.71	9.66	3.37
"Reference"	0.85	5.68	1.82	3.56	4.45	1.27	1.22	9.76	3.38
	2.09	4.65	1.18	2.91	4.72	1.26	1.08	9.58	3.41
	3.10	12.3	2.76	3.98	5.30	1.40	0.89	9.60	3.37
	5.10	21.7	5.06	4.97	6.05	1.38	1.12	9.83	3.39
"Rock Garden"	0.13	49.3[a]	18.2[b]	10.2	9.27	1.64	1.45	9.80	3.37
	0.33	1.98	0.70	1.84	2.77	0.84	1.54	9.74	3.38
	0.73	2.03	0.71	2.07	3.89	0.92	1.57	9.86	3.34
Average error (%)		6.1	5.9	5.9	6.0	6.0	7.8	2.3	1.2

[a]Data not plotted in Fig. 6.2, as the respective saturation is above 1200%.
[b]Data not plotted in Fig. 6.2, as the respective saturation exceeds 1000%.

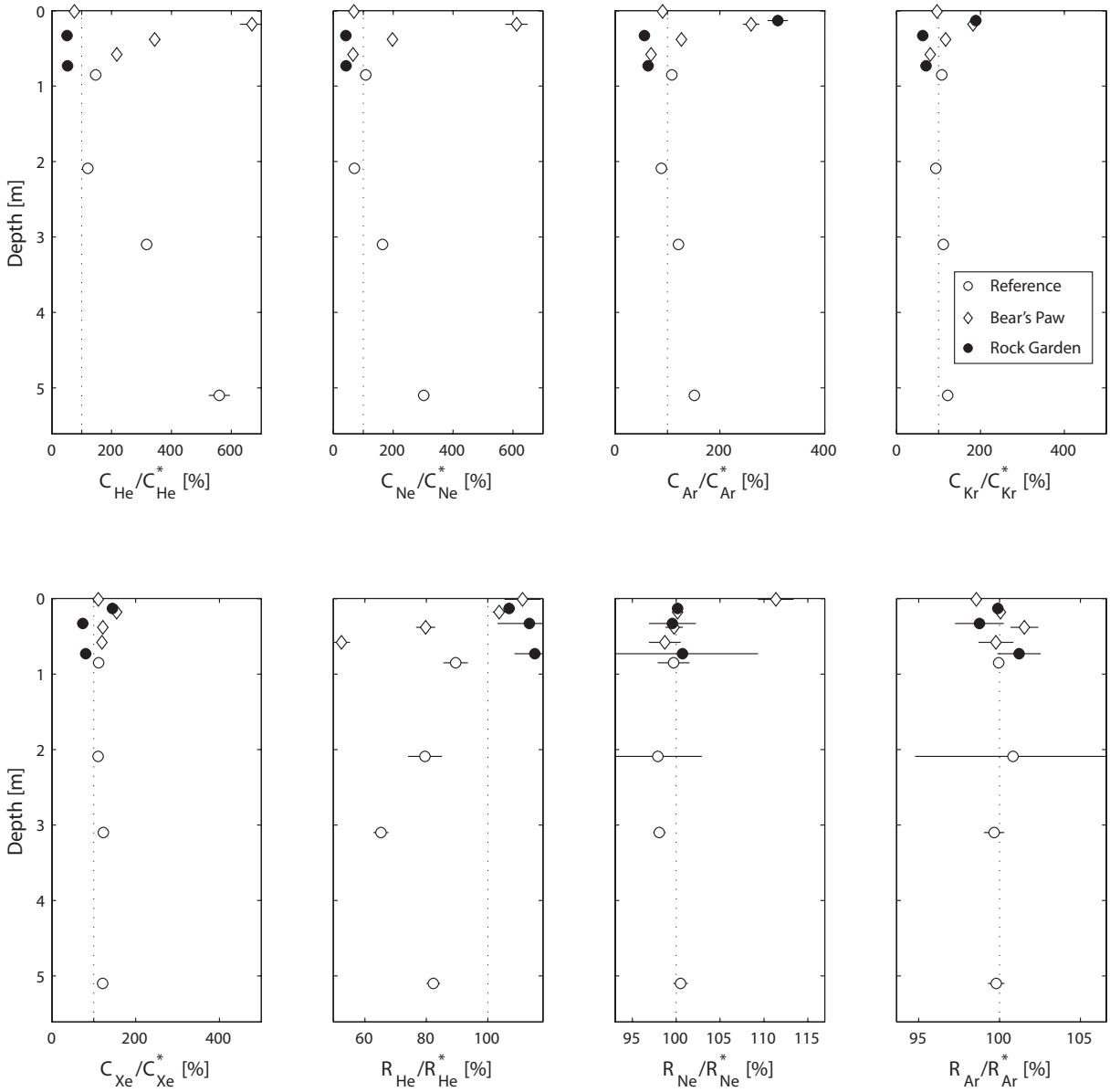

Figure 6.2: Noble-gas saturation profiles for the three cores taken off shore from New Zealand (for T=6℃ and S=35 g/kg, air saturated water is indicated by the dotted line). The white dots and diamonds represent "Reference" and "Bear's Paw", respectively. The black dots indicate the measurements of the sediments samples from "Rock Garden". The isotope ratios are plotted with the light isotopes as numerator (i.e. $^{3}He/^{4}He$, $^{20}Ne/^{22}Ne$ and $^{36}Ar/^{40}Ar$).

incomplete (see Brennwald et al., 2004; Strassmann et al., 2005) as they trap a part of the gases dissolved in the pore water which hampers a complete gas extraction. The observed incomplete extractions, however, will not affect the characterization of He in the sediment column, as the extraction efficiency for light elements is higher because of their larger diffusion coefficient. For these elements the applied extraction method was shown to be robust against degassing problems related to the sediment matrix (Brennwald et al., 2003).

Due to the absence of replicate samples it is not possible to reliably identify as outliers all the samples with concentrations of atmospheric noble gases significantly above or below the expected equilibrium concentrations.

For instance, in the cores from "Reference" and "Bear's Paw" two samples with high supersaturations for all atmospheric noble gases (all above 140% saturation) are present at 0.18 m and 0.13 m depth, respectively. It is possible that the samples were contaminated by air during the sampling, however the $^3He/^4He$ isotope ratios are above the value for ASW ($1.36 \cdot 10^{-6}$) suggesting that at least part of the concentration increase at this depth is a real feature produced by the active seepage (e.g. gas stripping, gas bubbles trapped in the sediment matrix, etc.).

The only sample where contamination is clearly identified belongs to the "Reference" site at 5.10 m depth. All the measured noble-gas concentrations are above 120% saturation and the $^3He/^4He$ isotope ratio is affected by a clear shift towards the value expected for ASW. Therefore the sample seems to be "contaminated" by air during the sampling on the ship. Hence, this sample will be excluded from the characterization of terrigenic He (see below).

As the aim of this work is not focused on the interpretation of the atmospheric noble-gas data, we will not further discuss the respective measured profiles which might be affected by the cold seepage activity as shown for the case of the Black Sea (Holzner et al., 2008).

The three sites show different He concentration and $^3He/^4He$ ratio profiles with depth. At "Reference" and "Bear's Paw" He concentrations increase and the $^3He/^4He$ ratios decrease with depth indicating the accumulation of terrigenic He. As the accumulating He is isotopically heavy ($^3He/^4He <$ ASW), it is most probably of "crustal" origin, i.e. the He isotope signature is characteristical for He being produced in common sedimentary mineral phases ($^3He/^4He$ several times 10^{-8}). At "Rock Garden" the He concentrations hardly increase with depth (note, however, that the maximum depth is only ~ 70 cm). In contrast to the other sites, He is isotopically light and the determined $^3He/^4He$ ratios of $1.5 \cdot 10^{-6}$ are slightly but significantly higher than the atmospheric saturation ratio.

If the observed ^3He enrichment in the sediment pore water of "Rock Garden" is attributed to the decay of ^3H, up to 4 TU (tritium units) would be required to explain the determined high $^3He/^4He$ ratios. Such high ^3H activities for South Pacific water at a depth of $\sim 500 - 1000$ m are not realistic, as ^3H is mostly confined to the surface water layer of the open ocean. The little ^3H data available from the water body indicate that less than 0.4 TU are expected for this depth range in the region of the sampling stations (Talley, 2007). The ^3H activity extrapolated based on this data for the mid-sixties is less than 1.6 TU which is not sufficient to explain the observed ^3He excess. Therefore, the high $^3He/^4He$ ratios at "Rock Garden" are probably the result of ^3He-rich fluids from the Earth's mantle that emanate in response to subduction activity off shore from New

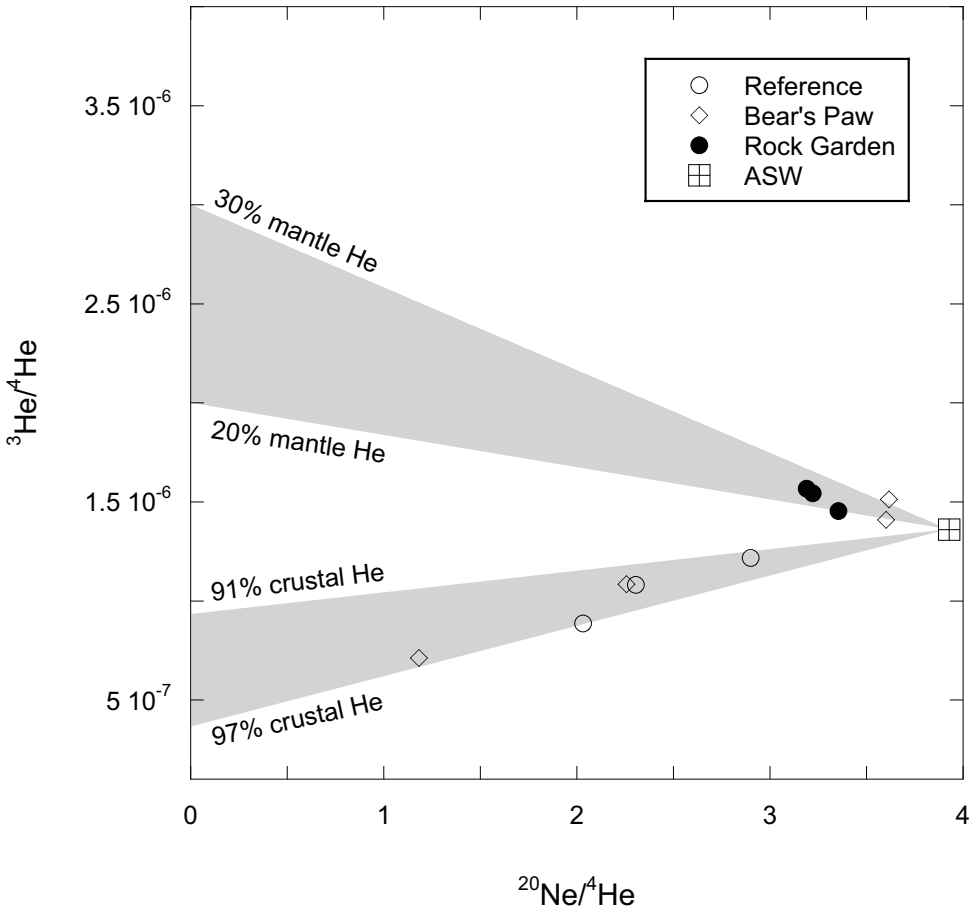

Figure 6.3: Three-isotopes plot of $^3He/^4He$ vs. $^{20}Ne/^4He$. Extrapolation for the Ne-free terrigenic component (i.e. $^{20}Ne = 0$) for each station indicate that He has mainly a crustal origin for cores at "Reference" and "Bear's Paw" while at "Rock Garden" He emanates from a depleted mantle source.

Zealand.

The three-isotopes plot of $^3He/^4He$ vs. $^{20}Ne/^4He$ (Fig. 6.3) shows that the samples of "Reference" and "Bear's Paw" on one hand and the samples from "Rock Garden" on the other hand, fall on different geochemical mixing trends. Terrigenic He in the sediment column at "Reference" and "Bear's Paw" (both in the region of Omakere Ridge) has a $^3He/^4He$ ratio of $\sim 3 - 9 \cdot 10^{-7}$ (back extrapolation of the $^3He/^4He$ signature for the virtually Ne-free He component). At "Rock Garden", in contrast, a significantly larger share of ^{3}He-rich fluids from a depleted mantle source seem to produce the observed high He isotope ratios in the pore waters ($^3He/^4He \sim 2 - 3 \cdot 10^{-6}$). These differences in the $^3He/^4He$ ratio are in line with the tectonical setting of the Hikurangi Margin: near the Pacific-Australian subduction zone preferentially mantle fluids are expected to be released from the sediments into the water body (Hilton et al., 2002). The data also demonstrate that the relative contribution of He released from the sediments differs greatly within 30 km that separates the "forearc" stations of Omakere Ridge (i.e. "Reference" and "Bear's Paw") from the "subduction" station ("Rock Garden").

In light of the He characterization at "Reference" and "Bear's Paw", where more than 90% of terrigenic He is produced in the sediment (or the crust), we conclude that methane at Omakere Ridge is most likely of biological origins, as no mantle-derived fluids strongly affect the He isotope signature in the sediment column. At "Rock Garden" about 20–30% of the emanating He may originate from the deep lithosphere indicating that a notable amount of mantle fluids arise from the nearby subduction zone. Although methane at this sampling station is also for the most part biogenic, the presence of a thermogenic/abiogenic component cannot be excluded, as isotopically light He clearly emanates from the underlying deeper part of the subduction zone. A shift in the δ^{13}C isotope composition in the water column measured by Faure et al. (2009) supports this idea: the δ^{13}C values determined at "Rock Garden" are slightly higher compared to the ones at Omakere Ridge. As methane of thermogenic/abiogenic origins off shore from New Zealand has been shown to have higher δ^{13}C values (from -24.6‰ to -28.9‰, see Botz et al., 2002) we speculate on the basis of our He measurements that the observed shift is produced by the presence of traces of thermogenic/abiogenic methane.

6.5 Conclusions

For the first time noble-gas concentrations and isotope ratios were routinely measured in ocean sediments (core length > 5 m) from the Hikurangi Margin off shore from New Zealand where an active methane seepage is present. The adaptation of the method by Tomonaga et al. (2010) was successful in most cases with the exception of a few samples. For these samples, the presence of residual sediment clusters probably hampered the complete extraction of noble gases dissolved in the pore water. It turned out that the determination of the exact position of the sediment/water interface after centrifugation is crucial to achieve the complete separation of water and sediment phases (see Tomonaga et al., 2010). Hence, for future applications of the method on the same type of sediments, we strongly suggest to use aliquots from the same cores/stations to exactly determine the geometrical position of the sediment/water interface in the centrifugated sediment samples. Such empirical determination of the sediment/water interface will avoid incomplete degassing in response to the presence of sediment clusters within the copper tubes.

The noble-gas results indicate that the He emanation in the region of Omakere Ridge near the coast of New Zealand is mostly of "crustal"/sediment origin whereas at "Rock Garden" a significant part of the present He is of mantle-type. The spatial distribution of the He isotope signature follows the local tectonical setting: in the vicinity of the Pacific-Australian subduction zone more mantle fluids enriched in light He emanate, whereas the near-continent region of Omakere Ridge is characterized by heavy He of "crustal" origin, most probably produced in situ in the sediment column.

The ^{3}He/^{4}He signature at all sampling stations indicates that He is for the most part produced in the sediment column (or in near-surface regions of the crust). Therefore, other fluids emanating from the sediments are most likely to be related to the same shallow geochemical compartments. This is also the case for methane which seems to be of biologic origin and is produced in the uppermost part of the sediments. However, the presence of traces of thermogenic/abiogenic CH_4 cannot be excluded for "Rock Garden", where a significant mantle He component is present.

More detailed sampling is needed in order to understand the effects of the methane

emission on the noble-gas composition in the sediment column and vice versa. From this point of view the use of transects to sample noble-gases in ocean sediments across the Hikurangi Margin should facilitate interpretation of the vertical structure of the measured profiles and yield insight into the relevant solute transport processes in the sediment column.

Chapter 7

Conclusions and outlook

Despite the great potential of rare gases in unconsolidated sediments as an emerging research field of terrestrial noble-gas geochemistry, until now the applications of the developed analytical tools were confined to a few case studies with a limited amount of data. In Lake Issyk-Kul (Kyrgyzstan) an anomaly in the determined noble-gas concentrations profile was interpreted in terms of lake level changes (Brennwald et al., 2004). However, the low resolution of the acquired profile (five samples within $\sim 1.2\,\mathrm{m}$) only allowed the effective diffusivity to be estimated at least two orders of magnitude lower than molecular diffusion in free water. A similar conclusion was drawn for the case of Lake Soppen, where a noble-gas depletion in the sediment column was caused by methane ebullition (Brennwald et al., 2005). In the sediments of Lake Soppen the noble-gas effective diffusivity was also found to be strongly attenuated (even negligible) in order to explain the observed depletion pattern. The work by Strassmann et al. (2005) yielded a first quantitative insight into the attenuation of diffusion in lacustrine sediments using tritium as a tracer. From the numerical modeling of the temporal variation of the tritium concentrations within the sediment column of Lake Zug, the effective diffusivity was determined to be four times smaller than diffusion in bulk water (Strassmann et al., 2005).

In this thesis the analytical methods used to determine noble gases in unconsolidated sediment have been further developed and three case studies were presented. For the first time noble gases were extensively applied as tracers to describe the solute transport in the pore space of lacustrine and ocean sediments. The deviations of the measured noble-gas abundances with respect to the expected atmospheric equilibrium concentrations allowed fluxes and the origin of geogenic fluids to be clearly determined, and structural changes of the pore space to be identified.

Analytical method Although the extrusion method to determine noble gases in the pore waters developed by Brennwald et al. (2003) works in a reliable and robust manner, the demanding analytical procedure requires well-trained experts. With the new centrifugation method the issues affecting the standard extrusion method are successfully bypassed. The sediment matrix is completely separated from the pore water during the degassing phase and the samples can be analyzed like common free water samples. From this it follows that the risk of an incomplete extraction is minimized and therefore the determined noble-gas concentrations can reliably be converted into noble-gas temperatures (as shown for Lake Van). Furthermore, uncontrolled He release from the sediment grains

is principally suppressed (as water and sediment are separated), leading to more reliable results for both He concentrations and isotopic ratios. For the first time the new extraction method also worked successfully for ocean sediments, as shown for the sediments from the Hikurangi Margin off shore from New Zealand. As the separation of pore water and sediment matrix by centrifugation is generally possible, in the near future noble-gas geochemistry in unconsolidated sediments will probably be adopted and applied by other research groups around the world.

He release First experimental results concerning the spatial distribution of terrestrial He emanation on local scales were achieved in the case study on Lake Van. Even accounting for some shortcomings related to the uncontrolled He release from the sediment grains using the standard extrusion method to extract noble gases, the numerous sediment cores sampled for noble-gas analysis and the resultant concentration profiles allowed the He data to be clearly interpreted in terms of terrestrial He release. The He fluxes greatly differ within a distance of a few kilometers, and the spatial distribution of the He release seems to be related to particular geological structures below the sediments.

Transport in sediments The attenuation of diffusivity in the sediment column was experimentally documented for the very different environmental conditions in Lake Van and in the Stockholm Archipelago. In Lake Van, the effective diffusivity in the sediments was found to be about four times lower than molecular diffusion in bulk water. The data from the Stockholm Archipelago suggest that diffusive transport appears to be negligible below the first 40 cm of the sediment, where the sediment texture changes abruptly due to the occurrence of a mass movement. The sediment lamination present in both case studies and the occurrence of a clear disturbance in the core taken from the Stockholm Archipelago, indicate that such horizontal structures may play a role in the attenuation of diffusivity. In the case of the Stockholm Archipelago however, structures residing in the mass movement (e.g. gas bubbles) are likely the main factor responsible for the observed attenuation of effective diffusivity.

Outlook As this thesis represents just one further step towards a wider use of noble gases in unconsolidated sediments from lakes and oceans, different questions still remain open and wait to be answered. A few topics are listed here which may stimulate further research:

- *Vertical structure of terrestrial He emanation*: As already mentioned in Chapter 5, an ICDP project will start in 2010 in Lake Van with the goal to retrieve > 300 m long sediment cores. The results presented in this thesis are bound to the quasi-horizontal dimension as the investigated cores only reached depths of ~ 2 m. However, the transport processes occurring at greater depths in the sediment column are still unknown. Hence, the ICDP drilling in Van is expected to yield more insight into the solute transport in the uppermost few hundred meters of the continents. For instance, the role of the geological setting of the lake basin and/or particular sediment structures that modulate the He release into the water body could be identified and studied.

- *Factors determining the effective diffusivity in sediments*: More sedimentological and physical work is needed in order to mechanistically understand the solute transport in the pore space of unconsolidated sediments. Noble-gas analysis and solute transport modeling in combination with more conventional sedimentological methods have the potential to broaden our current understanding of solute transport in sediments. We suggested completing these studies with techniques able to depict the geometry of the pore space on a microscopical scale (such as X-ray tomography).

- *Past ocean circulation*: In the past, analytical difficulties hampered a reliable determination of noble-gas abundances in ocean sediments. The case study in New Zealand shows that noble gases in ocean sediments can now be successfully analyzed and hence noble gases can be used to determine past ocean circulation by reconstructing palaeosalinity and palaeotemperature.

- *In situ sampling in aquifers*: Groundwater sampling techniques mainly rely on pumping water from (screened) piezometers. De facto the applied high pumping rates foster preferential flow paths through the aquifer leading to sampling artifacts due to the induced water mixing, i.e. the acquired samples may not belong to the local natural groundwater flow regime. This is a problematic aspect which significantly affects state-of-the-art numerical transport models in aquifers. Coring techniques are commonly used to study geological structures underground and to install observation wells in aquifers. Therefore, the same (adapted) methods to sample and analyze noble gases in unconsolidated sediments of lakes and oceans can be applied to determine the local noble-gas concentrations in "aquifer cores".

- *Gas exchange in the human body*: Looking beyond the geochemical boundaries, noble gases in blood may be a very interesting tool to analyze gas exchange in the human body. As the spectrum of the physical properties of noble gases is quite wide, they can be used as proxies to study the behavior of gas species with similar atomic mass. For instance Ar concentrations may give quantitative insight into oxygen saturation changes in blood and on the efficiency of pulmonary gas exchange. First laboratory tests show that the method by Brennwald et al. (2003) and the new centrifugation method can be applied to measure noble-gas concentrations and isotope ratios in (human) blood samples. The preliminary results for Kr and Xe are in line with former studies (Isbister et al., 1965; Kitani, 1972; Goto et al., 1998) and show that heavy noble gases are enriched in the red blood cell phase. However, the previous studies are mainly based on the partition coefficient between plasma and red blood cells in artificial gas equilibration experiments. The direct determination of noble gases in blood is expected to yield insight into the air/fluid partitioning in the lungs and blood under real natural physiological conditions

These are just a few suggestions, but the wide and diverse application of noble-gas geochemistry in unconsolidated sediments shows how much potential has yet to be released by future projects.

Bibliography

Aeschbach-Hertig, W. (1994). *Helium und Tritium als Tracer für physikalische Prozesse in Seen*. Diss. ETH Nr. 10714.

Aeschbach-Hertig, W., Baur, H., Hofer, M., Kipfer, R., and West, A. (1991). Mantle helium in Lake Van and Lake Nemrut, Eastern Turkey. *Terra abstracts*, 3(1):492–493.

Aeschbach-Hertig, W., Hofer, M., Kipfer, R., Imboden, D. M., and Wieler, R. (1999a). Accumulation of mantle gases in a permanently stratified volcanic lake (Lac Pavin, France). *Geochim. Cosmochim. Acta*, 63(19-20):3357–3372.

Aeschbach-Hertig, W., Hofer, M., Schmid, M., Kipfer, R., and Imboden, D. M. (2002). The physical structure and dynamics of a deep, meromictic crater lake (Lac Pavin, France). *Hydrobiologia*, 487:111–136.

Aeschbach-Hertig, W., Kipfer, R., Hofer, M., Imboden, D. M., and Baur, H. (1996a). Density-driven exchange between the basins of Lake Lucerne (Switzerland) traced with the ^{3}H-^{3}He method. *Limnol. Oceanogr.*, 41(4):707–721.

Aeschbach-Hertig, W., Kipfer, R., Hofer, M., Imboden, D. M., Wieler, R., and Signer, P. (1996b). Quantification of gas fluxes from the subcontinental mantle: The example of Laacher See, a maar lake in Germany. *Geochim. Cosmochim. Acta*, 60(1):31–41.

Aeschbach-Hertig, W., Peeters, F., Beyerle, U., and Kipfer, R. (1999b). Interpretation of dissolved atmospheric noble gases in natural waters. *Water Resour. Res.*, 35(9):2779–2792.

Aeschbach-Hertig, W., Peeters, F., Beyerle, U., and Kipfer, R. (2000). Palaeotemperature reconstruction from noble gases in ground water taking into account equilibration with entrapped air. *Nature*, 405:1040–1044.

Andrews, J. N., Goldbrunner, J. E., Darling, W. G., Hooker, P. J., Wilson, G. B., Youngman, M. J., Eichinger, L., Rauert, W., and Stichler, W. (1985). A radiochemical, hydrochemical and dissolved gas study of groundwaters in the Molasse basin of Upper Austria. *Earth Planet. Sci. Lett.*, 73(2-4):317–332.

Appleby, P. G. (2001). Chronostratigraphic techniques in recent sediments. In Last, W. M. and Smol, J., editors, *Tracking Environmental Change Using Lake Sediments. Volume 1: Basin Analysis, Coring, and Chronological Techniques*, pages 171–201. Kluwer Academic Publishers, Dordrecht, The Netherlands.

Appleby, P. G. and Oldfield, F. (1978). The calculation of lead-210 dates assuming a constant rate of supply of unsupported ^{210}Pb to the sediment. *CATENA*, 5(1):1–8.

Ballentine, C. J., Burgess, R., and Marty, B. (2002). Tracing fluid origin, transport and interaction in the crust. In Porcelli, D., Ballentine, C., and Wieler, R., editors, *Noble Gases in Geochemistry and Cosmochemistry*, volume 47 of *Rev. Mineral. Geochem.* Mineralogical Society of America, Geochemical Society.

Ballentine, C. J. and Burnard, P. G. (2002). Production, release and transport of noble gases in the continental crust. In Porcelli, D., Ballentine, C., and Wieler, R., editors, *Noble Gases in Geochemistry and Cosmochemistry*, volume 47 of *Rev. Mineral. Geochem.* Mineralogical Society of America, Geochemical Society.

Ballentine, C. J. and Hall, C. M. (1999). Determining paleotemperature and other variables by using an error-weighted, nonlinear inversion of noble gas concentrations in water. *Geochim. Cosmochim. Acta*, 63(16):2315–2336.

Ballentine, C. J., Schoell, M., Coleman, D., and Cain, B. A. (2001). 300-Myr-old magmatic CO_2 in natural gas reservoirs of the west Texas Permian basin. *Nature*, 409:327–331.

Barnes, R. O. (1979). Operation of the IPOD in situ pore water sampler. In Sibuet, J. and Ryan, W., editors, *Initial reports of the Deep Sea Drilling Project*, volume 47, part 2, pages 19–22. DSDP, Washington (U.S. Govt. Printing Office).

Barnes, R. O. and Bieri, R. H. (1976). Helium Flux through Marine Sediments of the Northern Pacific Ocean. *Earth Planet. Sci. Lett.*, 28:331–336.

Baur, H. (1999). A noble-gas mass spectrometer compressor source with two orders of magnitude improvement in sensitivity. In *American Geophysical Union, Fall Meeting*, volume 80 of *EOS, Trans. Am. Geophys. Union*, page F1118, San Francisco. American Geophysical Union.

Bayer, R., Schlosser, P., Bnisch, G., Rupp, H., Zaucker, F., and Zimmek, G. (1989). Performance and Blank Components of a Mass Spectrometric System for Routine Measurement of Helium Isotopes and Tritium by the ^{3}He Ingrowth Method. Sitzungsberichte der Heidelberger Akademie der Wissenschaften Mathemathisch-naturwissenschaftliche Klasse 5, Springer-Verlag.

Berner, R. (1975). Diagenetic models of dissolved species in the interstitial waters of compacting sediments. *Am. J. Sci.*, 275:88–96.

Beyerle, U., Aeschbach-Hertig, W., Hofer, M., Imboden, D. M., Baur, H., and Kipfer, R. (1999). Infiltration of river water to a shallow aquifer investigated with ^{3}H/^{3}He, noble gases and CFCs. *J. Hydrol.*, 220(3-4):169–185.

Beyerle, U., Aeschbach-Hertig, W., Imboden, D. M., Baur, H., Graf, T., and Kipfer, R. (2000). A mass spectrometric system for the analysis of noble gases and tritium from water samples. *Env. Sci. Technol.*, 34:2042–2050.

Beyerle, U., Purtschert, R., Aeschbach-Hertig, W., Imboden, D. M., Loosli, H. H., Wieler, R., and Kipfer, R. (1998). Climate and groundwater recharge during the last glaciation in an ice-covered region. *Science*, 282:731–734.

Beyerle, U., Redi, J., Leuenberger, M., Aeschbach-Hertig, W., Peeters, F., Kipfer, R., and Dodo, A. (2003). Evidence for periods of wetter and cooler climate in the Sahel between 6 and 40 kyr BP derived from groundwater. *Geophys. Res. Lett.*, 30(4):1173.

Botz, R., Wehner, H., Schmitt, M., J., W. T., Schmidt, M., and Stoffers, P. (2002). Thermogenic hydrocarbons from the offshore Calypso hydrothermal field, Bay of Plenty, New Zealand. *Chem. Geol.*, 186:235–248.

Boudreau, B. P. (1986). Mathematics of tracer mixing in sediments. *Am. J. Sci.*, 286:161–238.

Brennwald, M. S. (2004). *The Use of Noble Gases in Lake Sediment Pore Water as Environmental Tracers*. Diss. ETH Nr. 15629, ETH Zürich.

Brennwald, M. S., Hofer, M., Peeters, F., Aeschbach-Hertig, W., Strassmann, K., Kipfer, R., and Imboden, D. M. (2003). Analysis of dissolved noble gases in the pore water of lacustrine sediments. *Limnol. Oceanogr.: Methods*, 1:51–62.

Brennwald, M. S., Imboden, D. M., and Kipfer, R. (2005). Release of gas bubbles from lake sediment traced by noble gas isotopes in the sediment pore water. *Earth Planet. Sci. Lett.*, 235(1-2):31–44.

Brennwald, M. S., Peeters, F., Imboden, D. M., Giralt, S., Hofer, M., Livingstone, D. M., Klump, S., Strassmann, K., and Kipfer, R. (2004). Atmospheric noble gases in lake sediment pore water as proxies for environmental change. *Geophys. Res. Lett.*, 31(4):L04202.

Castro, M. C., Goblet, P., Ledoux, E., Violette, S., and de Marsily, G. (1998a). Noble gases as natural tracers of water circulation in the Paris Basin, 2. Calibration of a groundwater flow model using noble gas isotope data. *Water Resour. Res.*, 34(10):2467–2483.

Castro, M. C., Jambon, A., de Marsily, G., and Schlosser, P. (1998b). Noble gases as natural tracers of water circulation in the Paris Basin, 1. Measurements and discussion of their origin and mechanisms of vertical transport in the basin. *Water Resour. Res.*, 34(10):2443–2466.

Chaduteau, C., Fourré, E., Jean-Baptiste, P., Dapoigny, A., Baumier, D., and Charlou, J.-L. (2007). A new method for quantitative analysis of helium isotopes in sediment pore-waters. *Limnol. Oceanogr.: Methods*, 5:425–432.

Chahin, M. (2001). *The Kingdom of Armenia: A history*. Curzon Press, 2nd rev. edition. ISBN 0-7007-1452-9.

Clarke, W. B., Jenkins, W. J., and Top, Z. (1976). Determination of tritium by mass spectrometric measurement of ^{3}He. *Int. J. appl. Radiat. Isotopes*, 27:515–522.

Clever, H. L. (1979). *Krypton, xenon and radon - gas solubilities*, volume 2 of *Solubility data series*. Pergamon Press, Oxford.

Collier, R. W., Dymond, J., and McManus, J. (1991). Studies of hydrothermal processes in Crater Lake, OR. Report 90-7:1:201, College of Oceanography, Oregon State University.

Craig, H., Clarke, W. B., and Beg, M. A. (1975). Excess ^{3}He in deep water on the East Pacific Rise. *Earth Planet. Sci. Lett.*, 26(2):125–132.

Craig, H. and Lal, D. (1961). The production rate of natural tritium. *Tellus*, 13(1):85–105.

Craig, H. and Weiss, R. F. (1971). Dissolved gas saturation anomalies and excess helium in the ocean. *Earth Planet. Sci. Lett.*, 10(3):289–296.

Şaroğlu, F., Emre, O., and Kuşçu, I. (1992). Active Fault Map of Turkey.

Degens, E. T., Wong, H. K., and Kempe, S. (1984). A geological Study of Lake Van, Eastern Turkey. *Geol. Rundsch.*, 73(2):701–734.

Demirel-Schlueter, F., Krastel, S., Niessen, F., Demirbag, E., Imren, C., Toker, M., Litt, T., and Sturm, M. (2005). Seismic Pre-Site Survey for a potential new ICDP site PaleoVan - at Lake Van, Turkey. In *Geophys. Res. Abstracts*, volume 7.

Dyck, W. and Da Silva, F. (1981). The Use of Ping-Pong Balls and Latex Tubing for Sampling the Helium Content of Lake Sediments. *J. Geochem. Explor.*, 14:41–48.

Faure, K., Greinert, J., Pecher, I. A., Graham, I. J., Massoth, G. J., de Ronde, C. E. J., Wright, I. C., Baker, E. T., and Olson, E. J. (2006). Methane seepage and its relation to slumping and gas hydrate at the Hikurangi margin, New Zealand. *N. Z. J. Geol. Geophys.*, 49(5):503–516.

Faure, K., Greinert, J., Schneider von Deimling, J., McGinnis, D., Kipfer, R., and Linke, P. (2009). Free and dissolved methane in the water column and the sea surface: Geochemical and hydroacoustic evidence of bubble transport. *Mar. Geol.*, submitted.

Fritz, S. C. (1996). Paleolimnological Records of Climatic Change in North America. *Limnol. Oceanogr.*, 41(5):882–889.

Goto, T., Suwa, K., Uezono, S., Ichinose, F., Uchiyama, M., and Morita, S. (1998). The blood-gas partition coefficient of xenon may be lower than generally accepted. *Br. J. Anaesth.*, 80:255–256.

Hilton, D. R., Fischer, T. P., and Marty, B. (2002). Noble Gases and Volatile Recycling at Subduction Zones. In Porcelli, D., Ballentine, C., and Wieler, R., editors, *Noble Gases in Geochemistry and Cosmochemistry*, volume 47 of *Rev. Mineral. Geochem.*, pages 319–370. Mineralogical Society of America, Geochemical Society.

Hohmann, R., Hofer, M., Kipfer, R., Peeters, F., and Imboden, D. M. (1998). Distribution of helium and tritium in Lake Baikal. *J. Geophys. Res.*, 103(C6):12823–12838.

Holocher, J., Peeters, F., Aeschbach-Hertig, W., Kinzelbach, W., and Kipfer, R. (2003). Kinetic Model of Gas Bubble Dissolution in Groundwater and Its Implications for the Dissolved Gas Composition. *Env. Sci. Technol.*, 37:1337–1343.

Holzner, C. P., McGinnis, D. F., Schubert, C. J., Kipfer, R., and Imboden, D. M. (2008). Noble gas anomalies related to high-intensity methane gas seeps in the Black Sea. *Earth Planet. Sci. Lett.*, 265(3-4):396–409.

IAEA/WMO (2006). Global network of isotopes in precipitation. The GNIP database. URL `http://isohis.iaea.org`.

Igarashi, G., Ozima, M., Ishibashi, J., Gamo, T., Sakai, H., Nojiri, Y., and Kawai, T. (1992). Mantle helium flux from the bottom of Lake Mashu, Japan. *Earth Planet. Sci. Lett.*, 108(1-3):11–18.

Imboden, D. M. (1975). Interstitial transport of solutes in non-steady state accumulating and compacting sediments. *Earth Planet. Sci. Lett.*, 27:221–228.

Ingram, R. G. S., Hisckok, K. M., and F., D. P. (2007). Noblegas excess air applied to distinguish groundwater recharge conditions. *Environ. Sci. Technol.*, 2007(41):1949–1955.

Isbister, W. H., Schofield, P. F., and Torrance, H. B. (1965). Measurement of the Solubility of Xenon-133 in Blood and Human Brain. *Phys. Med. Biol.*, 10(2):243–250.

Jähne, B., Heinz, G., and Dietrich, W. (1987). Measurement of the diffusion coefficients of sparingly soluble gases in water. *J. Geophys. Res.*, 92(C10):10767–10776.

Jenkins, W. J. (1998). Studying subtropical thermocline ventilation and circulation using tritium and ^{3}He. *J. Geophys. Res.*, 103(C8):15817–15831.

Kaden, H., Peeters, F., Kipfer, R., and Tomonaga, Y. (2006). Mischungsprozesse im Van See / Türkei. In *Spring meeting of the German Physical Society*.

Kaden, H., Peeters, F., Lorke, A., Kipfer, R., Brennwald, M., and Tomonaga, Y. (2005). Mixing processes in Lake Van (Turkey). In Folkard, A. M. and Jones, I., editors, *9th European Workshop on Physical Processes in Natural Waters*, Lancaster.

Kaden, H., Peeters, F., Lorke, A., Kipfer, R., Tomonaga, Y., and Karabiyikoğlu, M. (2010). The impact of lake level change on deep-water renewal and oxic conditions in deep saline Lake Van, Turkey. *Water Resour. Res.*

Kadıoğlu, M., Şen, Z., and Batur, E. (1997). The greatest soda-water lake in the world and how it is influenced by climate change. *Ann. Geophysicae*, 15:1489–1497.

Kempe, S., Kazermierczak, J., Landmann, G., Konuk, T., Reimer, A., and Lipp, A. (1991). Largest known microbialites discovered in Lake Van, Turkey. *Nature*, 349:605–608.

Kılınçaslan, T. (2000). The rising water level in Lake Van: environmental features of the Van basin which increase the destructive effect of the disaster. *Water Sci. Technol.*, 42(1-2):173–177.

Kipfer, R., Aeschbach-Hertig, W., Baur, H., Hofer, M., Imboden, D. M., and Signer, P. (1994). Injection of mantle type helium into Lake Van (Turkey): the clue for quantifying deep water renewal. *Earth Planet. Sci. Lett.*, 125(1-4):357–370.

Kipfer, R., Aeschbach-Hertig, W., Peeters, F., and Stute, M. (2002). Noble gases in lakes and ground waters. In Porcelli, D., Ballentine, C., and Wieler, R., editors, *Noble Gases in Geochemistry and Cosmochemistry*, volume 47 of *Rev. Mineral. Geochem.*, pages 615–700. Mineralogical Society of America, Geochemical Society.

Kitani, K. (1972). Solubility Coefficients of ^{85}Krypton and ^{133}Xenon in Water, Saline, Lipids, and Blood. *Scand. J. clin. Lab. Invest.*, 29(2):176–172.

Klump, S., Cirpka, O. A., Surbeck, H., and Kipfer, R. (2008a). Experimental and numerical studies on excess-air formation in quasi-saturated porous media. *Water Resour. Res.*, 44(5).

Klump, S., Grundl, T., Purtschert, R., and Kipfer, R. (2008b). Pleistocene groundwater dynamics in Wisconsin derived from noble gas, ^{14}C and stable isotope data. *Geology*, 36:395–398.

Klump, S., Tomonaga, Y., Kienzler, P., Kinzelbach, W., Baumann, T., Imboden, D., and Kipfer, R. (2007). Field experiments yield new insights into gas exchange and excess air formation in natural porous media. *Geochim. Cosmochim. Acta*, 71:1385–1397.

Landmann, G., Reimer, A., Lemcke, G., and Kempe, S. (1996). Dating Late Glacial abrupt climate changes in the 14,570 yr long continuous varve record of Lake Van, Turkey. *Palaeogeogr. Palaeocl.*, 122(1-4):107–118.

Lang, D. M. (1980). *Armenia: Cradle of Civilization*. George Allen & Unwin, London, 3rd edition.

Lemcke, G. (1996). *Paläoklimarekonstruktion am Van See*. PhD thesis, Swiss Federal Insitute of Science and Technology. Diss. ETH Nr. 11786.

Lerman, A., Imboden, D. M., and Gat, J. R. (1995). *Physics and chemistry of lakes*. Springer, Berlin, 2nd edition.

Linke, P., Sommer, S., Rovelli, L., and McGinnis, D. F. (2009). Physical limitations of dissolved methane fluxes: The role of bottom-boundary layer processes. *Mar. Geol.* doi:10.1016/j.margeo.2009.03.020.

Litt, T., Krastel, S., Sturm, M., Kipfer, R., Orcen, S., Heumann, G., Franz, S. O., Ulgen, U. B., and Niessen, F. (2009). 'PALEOVAN', International Continental Scientific Drilling Program (ICDP): site survey results and perspectives. *Quaternary Sci. Rev.*, 28(15-16):1555–1567.

Lucas, L. L. and Unterweger, M. P. (2000). Comprehensive review and critical evaluation of the half-life of tritium. *J. Res. Natl. Inst. Stand. Technol.*, 105(4):541–549.

Maerki, M., Wehrli, B., Dinkel, C., and Mller, B. (2004). The influence of tortuosity on molecular diffusion in freshwater sediments of high porosity. *Geochim. Cosmochim. Acta*, 68(7):1519–1528.

Mamyrin, B. A. and Tolstikhin, I. N. (1984). *Helium isotopes in nature*, volume 3 of *Developments in Geochemistry*. Elsevier, Amsterdam, Oxford, New York, Tokyo, 1 edition.

Martel, D. J., Deak, J., Horvath, F., O'Nions, R. K., Oxburgh, E. R., Stegena, L., and Stute, M. (1989). Leakage of Helium from the Pannonian Basin. *Nature*, 342:908–912.

Marty, B., Dewonck, S., and France-Laord, C. (2003). Geochemical evidence for efficient aquifer isolation over geological timeframes. *Nature*, 425:53–58.

Marty, B., Torgersen, T., Meynier, V., O'Nions, R. K., and De Marsily, G. (1993). Helium isotope fluxes and groundwater ages in the Dogger Aquifer, Paris Basin. *Water Resour. Res.*, 29(4):1025–1035.

Meili, M., Jonsson, P., and Carman, R. (2000). PCB Levels in Laminated Coastal Sediments of the Baltic Sea along Gradients of Eutrophication Revealed by Stable Isotopes (δ^{15}N and δ^{13}C). *Ambio*, 29(4-5):282–287.

Mills, R. (1973). Self-diffusion in normal and heavy water in the range 1-45. *J. Phys. Chem.*, 77(5):685–688.

Morrison, P. and Pine, J. (1955). Radiogenic origin of the helium isotopes in rock. *Ann. NY Acad. Sci.*, 62:69–92.

Naudts, L., Greinert, J., Poort, J., Belza, J., Vangampelaere, E., Boone, D., Linke, P., Henriet, J.-P., and De Batist, M. (2009). Active venting sites on the gas-hydrate-bearing Hikurangi Margin, off New Zealand: Diffusive versus bubble-released methane. *Mar. Geol.* doi:10.1016/j.margeo.2009.08.002.

O'Nions, R. K. and Oxburgh, E. R. (1983). Heat and helium in the earth. *Nature*, 306:429–431.

Oxburgh, E. R. and O'Nions, R. K. (1987). Helium loss, tectonics, and the terrestrial heat budget. *Science*, 237:1583–1588.

Oxburgh, E. R., O'Nions, R. K., and Hill, R. I. (1986). Helium isotopes in sedimentary basins. *Nature*, 324:632–635.

Ozima, M. and Podosek, F. A. (1983). *Noble gas geochemistry*. Cambridge Univ. Press, Cambridge, London, New York.

Ozima, M. and Podosek, F. A. (2002). *Noble gas geochemistry, second edition*. Cambridge University Press, Cambridge, 2 edition.

Peeters, F., Kipfer, R., Achermann, D., Hofer, M., Aeschbach-Hertig, W., Beyerle, U., Imboden, D. M., Rozanski, K., and Fröhlich, K. (2000). Analysis of deep-water exchange in the Caspian Sea based on environmental tracers. *Deep-Sea Res. I*, 47(4):621–654.

Peeters, F., Kipfer, R., Hohmann, R., Hofer, M., Imboden, D. M., Kodenev, G. G., and Khozder, T. (1997). Modelling transport rates in Lake Baikal: gas exchange and deep water renewal. *Env. Sci. Technol.*, 31(10):2973–2982.

Pennington, W., Tutin, T. G., Cambray, R. S., and Fisher, E. M. (1973). Observations on Lake Sediments using Fallout ^{137}Cs as a Tracer. *Nature*, 242(5396):324–326. doi:10.1038/242324a0.

Persson, J. and Jonsson, P. (2000). Historical Development of Laminated Sediments an Approach to Detect Soft Sediment Ecosystem Changes in the Baltic Sea. *Mar. Poll. Bull.*, 40(2):122–134.

Pinti, D. L. and Marty, B. (1995). Noble gases in crude oils from the Paris Basin, France: Implications for the origin of fluids and constraints on oil-water-gas interactions. *Geochim. Cosmochim. Acta*, 59(16):3389–3404.

Pinti, D. L., Marty, B., and Andrews, J. N. (1997). Atmosphere-derived noble gas evidence for the preservation of ancient waters in sedimentary basins. *Geology*, 25(2):111–114.

Pitre, F. and Pinti, D. L. (2010). Noble gas enrichments in porewater of estuarine sediments and their effect on the estimation of net denitrification rates. *Gechim. Cosmochim. Acta*, 74:531–539.

Podosek, F. A., Bernatowicz, T. J., and Kramer, F. E. (1981). Adsorption of xenon and krypton on shales. *Geochim. Cosmochim. Acta*, 45(12):2401–2415.

Podosek, F. A., Honda, M., and Ozima, M. (1980). Sedimentary noble gases. *Geochim. Cosmochim. Acta*, 44:1875–1884.

Previté-Orton, C. W. (1971). *The Shorter Cambridge Medieval History*. Cambridge University Press, Cambridge. ISBN 0-521-05993-3.

Rayleigh, J. (1896). Theoretical Considerations respecting the Separation of Gases by Diffusion and similar Processes. *Phil. Mag.*, 42:493–498.

Reimer, A., Landmann, G., and Kempe, S. (2008). Lake Van, Eastern Anatolia, Hydrochemistry and History. *Aquat. Geochem.*, 15:195–222.

Ritchie, J. C., McHenry, J. R., and Gill, A. C. (1973). Dating recent reservoir sediments. *Limnol. Oceanogr.*, 18:254–263.

Roether, W. (1989). On oceanic boundary conditions for tritium, on tritiugenic ^{3}He, and on the tritium-^{3}He age concept. In Anderson, D. L. T. and Willebrand, J., editors, *Oceanic circulation models: Combing data and dynamics*, pages 377–407. Kluwer Academic Press.

Salvini, M. (1995). *Geschichte und Kultur der Urartäer*. Wissenschaftliche Buchgesellschaft, Darmstadt. ISBN 3-534-01870-2.

Salvini, M. (2005). Some considerations on Van Kalesi. In Çilingiroğlu, A. and Darbyshire, G., editors, *Anatolian Iron Ages 5: Proceedings of the 5th Anatolian Iron Ages Colloquium Held at Van, 6-10 August 2001*, pages 145–156, Ankara. British Institute of Archaeology.

Sano, Y., Kusakabe, M., Hirabayashi, J., Nojiri, Y., Shinohara, H., Njine, T., and Tanyileke, G. (1990). Helium and carbon fluxes in Lake Nyos, Cameroon: Constraint on next gas burst. *Earth Planet. Sci. Lett.*, 99(4):303–314.

Sano, Y. and Wakita, H. (1987). Helium Isotope Evidence for Magmatic Gases in Lake Nyos, Cameroon. *Geophys. Res. Lett.*, 14(10):1039–1041.

Sano, Y., Wakita, H., and Huang, C.-W. (1986). Helium flux in a continental land area estimated from $^3He/^4He$ ratio in northern Taiwan. *Nature*, 323:55–57.

Schlosser, P., Bullister, J. B., and Bayer, R. (1991). Studies of deep water formation and circulation in the Weddell Sea using natural and anthropogenic tracers. *Mar. Chem.*, 35:97122.

Schlosser, P. and Winckler, G. (2002). Noble gases in the ocean and ocean floor. In Porcelli, D., Ballentine, C., and Wieler, R., editors, *Noble Gases in Geochemistry and Cosmochemistry*, volume 46 of *Rev. Mineral. Geochem.* Mineralogical Society of America, Geochemical Society.

Schubert, C. J., Durisch-Kaiser, E., Klauser, L., Wehrli, B., Holzner, C. P., Kipfer, R., Schmale, O., Greinert, J., and Kuypers, M. (2006). Recent studies on sources and sinks of methane in the Black Sea. In Neretin, L., Jørgensen, B., and Murray, J. W., editors, *Past and Present Water Column Anoxia*, Nato Science Series: Earth and Environmental Sciences, pages 419–441. Kluwer-Springer.

Schwarzenbach, R. P., Gschwend, P. M., and Imboden, D. M. (2003). *Environmental Organic Chemistry*. John Wiley & Sons, Inc., New York, 2 edition.

Seyir Hidrografi ve Oşinografi Dairesi (1990). Bathymetry of Lake Van.

Sommer, S., Linke, P., Pfannkuche, O., Niemann, H., and Treude, T. (2009). Benthic respiration in a seep habitat dominated by dense beds of ampharetid polychaetes at the Hikurangi Margin (New Zealand). *Mar. Geol.* doi:10.1016/j.margeo.2009.06.003.

Stephenson, M., Schwartz, W. J., Melnyk, T. W., and Motycka, M. F. (1994). Measurement of advective water velocity in lake sediment using natural helium gradients. *J. Hydrol.*, 154:63–84.

Stiller, M., Carmi, I., and Mnnich, K. (1975). Water Transport through Lake Kinneret Sediments Traced by Tritium. *Earth Planet. Sci. Lett.*, 25:297–304.

Strassmann, K., Brennwald, M., Peeters, F., and Kipfer, R. (2005). Dissolved Noble Gases in Porewater of Lacustrine Sediments as Palaeolimnological Proxies. *Geochim. Cosmochim. Acta*, 69(7):1665–1674.

Stute, M., Forster, M., Frischkorn, H., Serejo, A., Clark, J. F., Schlosser, P., Broecker, W. S., and Bonani, G. (1995). Cooling of tropical Brazil (5 ℃) during the Last Glacial Maximum. *Science*, 269:379–383.

Stute, M. and Schlosser, P. (2000). Atmospheric noble gases. In Cook, P. and Herczeg, A. L., editors, *Environmental tracers in subsurface hydrology*, pages 349–377. Kluwer Academic Publishers, Boston.

Stute, M., Schlosser, P., Clark, J. F., and Broecker, W. S. (1992). Paleotemperatures in the Southwestern United States derived from noble gases in ground water. *Science*, 256:1000–1003.

Stute, M. and Talma, A. S. (1998). Glacial temperatures and moisture transport regimes reconstructed from noble gases and delta ^{18}O, Stampriet aquifer, Namibia. In *Isotope techniques in the study of environmental change*, pages 307–318, Vienna, Austria. IAEA-SM-349.

Talley, L. (2007). *Hydrographic Atlas of the World Ocean Circulation Experiment (WOCE). Volume 2: Pacific Ocean*. International WOCE Project Office, Southampton, U.K. ISBN 0-904175-54-5.

Thorpe, S. A. (1984). The Role of Bubbles Produced by Breaking Waves in Supersaturating the Near-surface Ocean Mixing Layer with Oxygen. *Ann. Geophys.*, 2(1):53–56.

Tolstikhin, I., Lehmann, B. E., Loosli, H. H., and Gautschi, A. (1996). Helium and argon isotopes in rocks, minerals, and related groundwaters: A case study in northern Switzerland. *Geochim. Cosmochim. Acta*, 60(9):1497–1514.

Tolstikhin, I. N. and Kamenskiy, I. L. (1969). Determination of ground-water ages by the T-^{3}He method. *Geochem. Int.*, 6:810–811.

Tomonaga, Y., Brennwald, M. S., and Kipfer, R. (2010). An improved method for the analysis of dissolved noble gases in the pore water of unconsolidated sediments. *Limnol. Oceanogr.: Methods*, submitted.

Torgersen, T. and Clarke, W. B. (1985). Helium accumulation in groundwater, I: An evaluation of sources and the continental flux of crustal ^{4}He in the Great Artesian Basin, Australia. *Geochim. Cosmochim. Acta*, 49(5):1211–1218.

Torgersen, T., Clarke, W. B., and Jenkins, W. J. (1979). The tritium/helium-3 method in hydrology. In IAEA, editor, *Isotope Hydrology 1978*, pages 917–930, Vienna. IAEA.

Torgersen, T., Top, Z., Clarke, W. B., Jenkins, W. J., and Broecker, W. (1977). A new method for physical limnology - tritium-helium-3 ages - results for Lakes Erie, Huron and Ontario. *Limnol. Oceanogr.*, 22(2):181–193.

Unterweger, M. P., Coursey, B. M., Schima, F. J., and Mann, W. B. (1980). Preparation and Calibration of the 1978 National Bureau of Standards Tritiated-water Standards. *Int. J. appl. Radiat. Isot.*, 31:611–614.

Weiss, R. F. (1970). Helium isotope effect in solution in water and seawater. *Science*, 168:247–248.

Weiss, R. F. (1971a). The effect of salinity on the solubility of argon in seawater. *Deep-Sea Res.*, 18:225–230.

Weiss, R. F. (1971b). Solubility of helium and neon in water and seawater. *J. Chem. Eng. Data*, 16(2):235–241.

Weiss, R. F., Carmack, E. C., and Koropalov, V. M. (1991). Deep-water renewal and biological production in Lake Baikal. *Nature*, 349:665–669.

Weiss, R. F. and Kyser, T. K. (1978). Solubility of krypton in water and seawater. *J. Chem. Eng. Data*, 23(1):69–72.

Weiss, W., Bullacher, J., and Roether, W. (1979). Evidence of pulsed discharges of tritium from nuclear energy installations in central european precipitation. In IAEA, editor, *Behaviour of tritium in the environment*, Proceedings Series, pages 17–30, San Francisco, 16-20 Oct. 1978. IAEA.

Weyhenmeyer, C. E., Burns, S. J., Waber, H. N., Aeschbach-Hertig, W., Kipfer, R., Loosli, H. H., and Matter, A. (2000). Cool glacial temperatures and changes in moisture source recorded in Oman groundwaters. *Science*, 287(5454):842–845.

Wick, L., Lemcke, G., and Sturm, M. (2003). Evidence for Lateglacial and Holocene climatic change and human impact in eastern Anatolia: high-resolution pollen, charcoal, isotopic and geochemical records from the laminated sediments of Lake Van, Turkey. *Holocene*, 13(5):665–675.

Zhou, Z., Ballentine, C. J., Kipfer, R., Schoell, M., and Thibodeaux, S. (2005). Noble gas tracing of groundwater/coalbed methane interaction in the San Juan Basin, USA. *Gechim. Cosmochim. Acta*, 69(23):5413–5428.

Zhu, C. and Kipfer (2010). Noble gas signatures of high recharge pulses and migrating jet stream in Late Pleistocene over Black Mesa, Arizona, USA. *Geology*, 38:83–86. in press.